NUMERICAL ANALYSIS IN THE DETECTION OF ABNORMAL UPTAKE OF RADIONUCLIDE BY THE BRAIN

by

John L. Woolley, M.Sc., M.Inst.P.

Thesis submitted for the degree of Doctor of Philosophy

in the University of Aston in Birmingham

March, 1977

The Midland Centre for Neurosurgery and Neurology

ABSTRACT

Radionuclide brain imaging is a well established diagnostic investigation, and electronic data processing is often used to improve the information yielded. Two methods of data analysis have been researched. The first used statistical techniques to analyse images of the distribution of a radionuclide in the brain to detect areas where the uptake pattern differed from the expected value, indicating disease. The normal uptake pattern, and the normal variability of this pattern in a population, was established by combining proven normal patterns into a composite. Novel methods of normalising individual patient data were developed, and these methods revealed previously unreported features of the radionuclide scan in certain pathological conditions which could be useful as diagnostic indicators. It was also found that the normalised patterns could be used in the automatic screening of large series of patient data to search for specific features within scans. This latter technique was used in the evaluation of the efficiencies of two choroid plexus blocking agents. The results of the statistical analysis showed that the computer assessment was closely comparable in diagnostic accuracy to an experienced radiologist.

The second method of analysis used the computer in conjunction with a commercially available scanner to produce transverse axial images of a radionuclide distribution in the brain. Substantial modifications to both scanner and data processor were made, and new electronic circuitry was developed. A pilot study using programs developed elsewhere was conducted and this showed the potential value of the method. New programs were then developed suitable for routine use and intended

to maximise the speed of the reconstruction and to minimise the size of the computer required. These programs were used in a clinical trial involving approximately 100 cases. The results obtained are discussed and compared with the results obtained with a similar technique using an X-ray scanner.

Acknowledgements

It is a pleasure to acknowledge the following:

The staff of the Radioisotope department, the Midland Centre for Neurosurgery and Neurology, for their help throughout this project.

Former colleagues, especially Dr. J.H.W.Pexman, Mrs J.Norton and Mrs S.Venkatesh who have helped at various stages of the project.

Mr. M.Ahmon,for building the data logging system.

Mr. B.N.Williams,for help with the clinical case histories.

Dr. W.I.Keyes, for making available his Section Scan program for use in the pilot study.

Mrs M. Purvis and Mrs R. Johal,for secretarial assistance.

Professor T. Mulvey,for his interest and encouragement.

The former Birmingham Regional Hospital Board,for a grant to permit the construction of the data logging system.

Above all, I would like to thank Dr. P.E.Francois for his advice and patience, and for the many interesting discussions we have had.

CONTENTS

		Page
Abstract		(ii)
Acknowledgements		(iv)
Table of figures		(x)
CHAPTER 1	Radionuclide imaging	
	1.1 Introduction	2
	1.2 Factors governing choice of isotope	5
	1.2.1 Choice of radiopharmaceutical for brain scanning	8
	1.3 Instruments for radioisotope imaging	9
	1.3.1 Radiation detectors	10
	1.4 Radioisotope scanners	11
	1.4.1 Collimators for radioisotope scanners	12
	1.5 Gamma cameras	14
	1.5.1 Recent improvements in Anger camera performance.	18
	1.6 Tomographic imaging systems	20
	1.7 Scanner display systems	23
	1.7.1 Reprocessing of scanner output data	25
	1.7.2 Quantitative analysis of scanner output data	26
CHAPTER 2	The data logging system	
	2.1 Design of digital data logging systems	30
	2.2 Requirements and precision of data	30
	2.3 Design of the optimum data logging system	32
	2.3.1 Data logger constuctional details	35
	2.3.2 Mechanical modifications to the scanner	38

Page

CHAPTER 2 (cont'd)

2.3.3 Testing the data logging system 40

2.3.4 Modification of the data logging system 42

CHAPTER 3 The choice of a suitable data processor and development of data entry programs

3.1 The data processing problem 50

3.1.1 Batch processing computers 50

3.1.2 Small dedicated computers 51

3.2 The Nuclear Data 50/50 MED system 53

3.2.1 System hardware 53

3.3 Data input program 56

CHAPTER 4 Normalisation of patient scan data

4.1 Analysis of count rate patterns 62

4.1.1 Normalising the anatomical features of the individual patient scan 63

4.1.2 Normalisation of count rate data 64

4.2 Data processing of scan image files 65

4.2.1 Initial checks to determine suitability of data for analysis 68

4.2.2 The count-rate histogram 69

4.3 Normalisation of spatial coordinate data 73

4.4 Use of normalised scan data to establish patterns of isotope uptake in the choroid plexus region 74

4.4.1 Objective assessment of choroid plexus activity by area of interest analysis 76

Page

CHAPTER 5 The derivation and use of composite normal scan images

5.1 Computation of the composite normal scan 81

5.1.1 The variance of composite normal scan data 84

5.2 Comparison of individual patient scan data with composite normal patterns 86

5.2.1 A check on the validity of the composite normal pattern variance 88

5.3 Criteria for abnormality 88

5.4 Results of a trial based on 50 individual patient scan data 89

5.4.1 Correlation between views 95

5.4.2 Analysis of the trial results 96

CHAPTER 6 Transverse axial radionuclide tomography

6.1 Medical radiographic imaging techniques 100

6.1.1 Contrast radiography 101

6.1.2 Conventional X-ray tomography 102

6.1.3 Tomographic isotope examinations 102

6.2 Development of a system for routine transverse axial isotope tomography 104

6.2.1 The J&P Engineering Ltd MS 430 scanner 106

6.2.2 Design and construction of the scanner/computer interface 108

6.2.3 Display of computer processed results on the scanner display circuits 116

6.3 The suitability of the detector system for transverse axial reconstruction techniques 117

Page

CHAPTER 6 (cont'd)

6.3.1 Mechanical characteristics of the detector system 120

6.4 Image reconstruction methods 123

6.5 Successive approximation reconstruction methods 125

6.5.1 Algebraic reconstruction technique 127

6.5.2 Simultaneous iterative reconstruction technique 130

6.6 Methods using the Fourier transformation 130

6.6.1 The 'convolution' method 133

CHAPTER 7 A pilot study of radionuclide tomography

7.1 A pilot study of transverse axial isotope imaging 137

7.2 The reconstruction algorithm 137

7.3 Implementation of the algorithm 138

7.3.1 Check on the alignment of the data 139

7.3.2 Modification of the data profiles 140

7.3.3 Back projection of the modified profiles 140

7.4 Additional software necessary to implement Aberdeen University programs 142

7.4.1 Input procedures 142

7.4.2 Output procedures 144

7.5 The computer program 145

7.6 Design of a phantom to test the section scan method 146

7.6.1 Results obtained with Aston University Phantom 146

7.7 Patient investigations 149

Page

CHAPTER 8 Further development of the tomographic imaging method

8.1 Development of the section scan method 156

8.2 Hardware development 156

8.2.1 Dataway terminating module circuit description 158

8.3 Software development 162

8.3.1 Alignment of the data 163

8.3.2 Data input procedures 164

8.3.3 Data storage and display 165

8.4 Clinical results 168

8.4.1 Quality and accuracy of section scanning 168

8.4.2 Effect of site 170

8.4.3 Shape of lesions as a diagnostic indicator 173

8.5 Imaging of CSF pathways 176

8.5.1 Case studies using indium-111 DTPA 180

CHAPTER 9 Review of methods and conclusions

9.1 The changing pattern of encephalography 188

9.1.1 Invasive methods of investigation 188

9.1.2 Non-invasive methods of investigation 189

9.2 The accuracy of TCAT scanning as compared to isotope scanning 191

9.3 The value of analysing radionuclide scan images by reference to standardised normal patterns 192

9.4 The value of radionuclide section scanning as a complementary investigation to TCAT scanning 194

9.5 The value of radionuclide section scanning in general 195

REFERENCES 197

APPENDIX 209

Table of figures

		Page
CHAPTER 1		
Figure 1.1	The radioisotope imaging process	4
Figure 1.2	Some properties of radioisotopes used in brain imaging	7
Figure 1.3	A focussed collimator for a rectilinear scanner	13
Figure 1.4	Line source response function for a 109 hole focussed collimator	15
Figure 1.5	The Anger camera (general arrangement)	16
CHAPTER 2		
Figure 2.1	Line source response function for Picker V Magnascanner, 85 hole collimator	31
Figure 2.2	Block diagram of data logging system	37
Figure 2.3	Magnascanner drive mechanisms	39
Figure 2.4	Circuit of Scanner Control Module	43
Figure 2.5	Print control module command sequence	45
Figure 2.6	Scanner Control Module- output codes	47
CHAPTER 3		
Figure 3.1	Advantages and disadvantages of batch processing computer versus dedicated systems	52
Figure 3.2	Block diagram showing main components of data processing system	54
CHAPTER 4		
Figure 4.1	Count rate histogram. Lateral view. No abnormality detected	66
Figure 4.2	Count rate histogram. Lateral view. Large malignant tumour	67
Figure 4.3	Count rate histogram. Lateral view. Extensive sub-dural haematoma	71

Page

Figure 4.4 Count rate histogram. Lateral view. Paget's disease of skull. 72

Figure 4.5 Computer generated scan image showing areas of interest used in the evaluation of choroid plexus activity 77

CHAPTER 5

Figure 5.1 Results of comparing the reporting accuracy of an experienced observer with the computer result 90

Figure 5.2 Number of cells at different levels of significance which fulfil the criteria for abnormality 92

Figure 5.3 Visually abnormal case which fails to meet the criteria for abnormality 94

CHAPTER 6

Figure 6.1 Narrow beam transmission of X-rays 100

Figure 6.2 The mechanism of conventional X-ray tomography 103

Figure 6.3 Method of transverse axial isotope tomography proposed by Kuhl and Edwards (1963) 105

Figure 6.4 The J & P MS 430 scanner 107

Figure 6.5 Block diagram of scanner/computer interface 109

Figure 6.6 Input circuits of 50 MHz analogue-digital converter 111

Figure 6.7 Tank used for plotting collimator characteristics 119

Figure 6.8 Isocount contours for detection system with collimator separation of 32 cm 121

Figure 6.9 Arrangement for locating centre of rotation of detector system 122

Figure 6.10 Profiles obtained by scanning an object containing two active areas 124

Figure 6.11 Back projection of four profiles 126

Page

Figure 6.12 Algebraic Reconstruction Technique 128

Figure 6.13 Example of the use of the Simultaneous Iterative Reconstruction Technique 131

Figure 6.14 The convolution method 134

CHAPTER 7

Figure 7.1 Rotation of cartesian coodinate system 141

Figure 7.2 University of Aston phantom 147

Figure 7.3 Scans of phantom fitted with central and off-axis tubes, with and without aluminium shell 148

Figure 7.4 Scans of phantom fitted with transverse axial and off axis tubes, with and without aluminium shell 150

Figure 7.5 Two normal section scans 152

Figure 7.6 Two section scans demonstrating malignant tumours 153

CHAPTER 8

Figure 8.1 Buffered memory register signals during a typical peripheral transfer operation 157

Figure 8.2 J & P designed dataway terminating module 159

Figure 8.3 Redesigned dataway terminating module including computer control circuitry 161

Figure 8.4 Case studies (a) parafalx meningioma (b) acoustic neurinomata 171

Figure 8.5 Case studies. Peripheral astrocytoma 172

Figure 8.6 Case study. Parasagittal angioma-comparison of vertex and section scans 174

Figure 8.7 Case studies (a) basal meningioma (b) recurrent meningioma 175

Figure 8.8 A case of infarction 177

Page

Figure 8.9 Case study. Two areas of infarction 178

Figure 8.10 Case study. Subdural haematoma 179

Figure 8.11 Case study. A child with a mild hydrocephalus 181

Figure 8.12 Case study. A patient with raised intracranial pressure following brucella meningitis 183

Figure 8.13 Case study. A patient with Dandy-Walker cyst. X-ray ventriculogram 184

Figure 8.14 Case study. A patient with Dandy-Walker cyst. Indium 111 DTPA ventriculogram 185

CHAPTER 1

Radionuclide imaging

1.1 Introduction

Radiation physics and medical science have enjoyed a long and fruitful association. Rontgen (1896) in his original publication concerning his work on x-rays mentioned the fact that the bones of the hand could be photographed using the newly discovered radiation. Industry and medical science were quick to sense the significance of Rontgen's observations and within a few months the F.J. Pearson Manufacturing Company of St. Louis advertised "a portable x-ray apparatus for physicians, professors, photographers and students for the price of $15 net delivered in the United States with full guarantee".

The announcement of the discovery of radium by Curie and Debierne (1910) was also quickly taken up by the medical profession. The biological effects of x-radiation had been recognised for some time and use had been made of x-rays in the treatment of some skin disorders. The more penetrating radiation from radium suggested the possibility of treating deep seated tumours. Thus began the twin sciences of radio-diagnosis and radio-therapy.

The applications of radioisotopes to medical diagnosis began much later. Before the advent of the nuclear reactor, apart from the radioactive elements radon and various isotopes of radium, the only available radioisotopes were those produced in small quantities by cyclotrons. Nevertheless the potential value of these applications was recognised and as early as 1936 thyroid iodine uptake studies were carried out by administering a small amount of cyclotron produced iodine ^{131} to a subject and then holding a Geiger counter tube directly over the thyroid gland to detect the location of the isotope.

The situation changed completely with the coming of the nuclear reactor. A great many potentially useful radioactive isotopes can be

recovered from waste products or produced in the nuclear reactor. Some of the new radioisotopes have brought about radical extensions to the earlier forms of radiotherapy. In place of a few curies of radium, at one time the most active single source, sources of 5,000 curies or more of cobalt 60 now provide intense beams of highly energetic gamma rays for both medical and industrial uses. Internal irradiation of specific tissues may now be carried out by such radioisotopes as ^{131}I, ^{32}P and ^{189}Au. It is however, as biological tracers that radioisotopes have found their most significant use in the field of medicine. Because most of the biologically important elements can be produced in radioactive form with convenient half life periods, radioisotopes such as ^{3}H, ^{24}Na, ^{32}P, ^{42}K, ^{59}Fe ^{131}I and others can be used for such typical purposes as the investigation of problems of blood and electrolyte volumes, the location of particular tissues, the differentiation of tumorous and normal tissues and the fate and function of the elements and compounds in the body.

Improvements in instrumentation during the early 1950's enabled full use to be made of these newly available radioisotopes. The first major improvement was the development of the scintillation counter which greatly reduced the dose of tracer material required. Later came the development of radioisotope scanners and cameras, highly developed electronic devices which enable one to visualise the distribution of radioactive substances within the living body thereby assessing the size, shape, position and function of organs and locating lesions in them.

Different types of scanners vary in their construction and operation. However, they are alike in the employment of certain essential parts, a gamma detector, a collimating system, electronic amplification, discrimination, count rate determination and some means of visual representation.

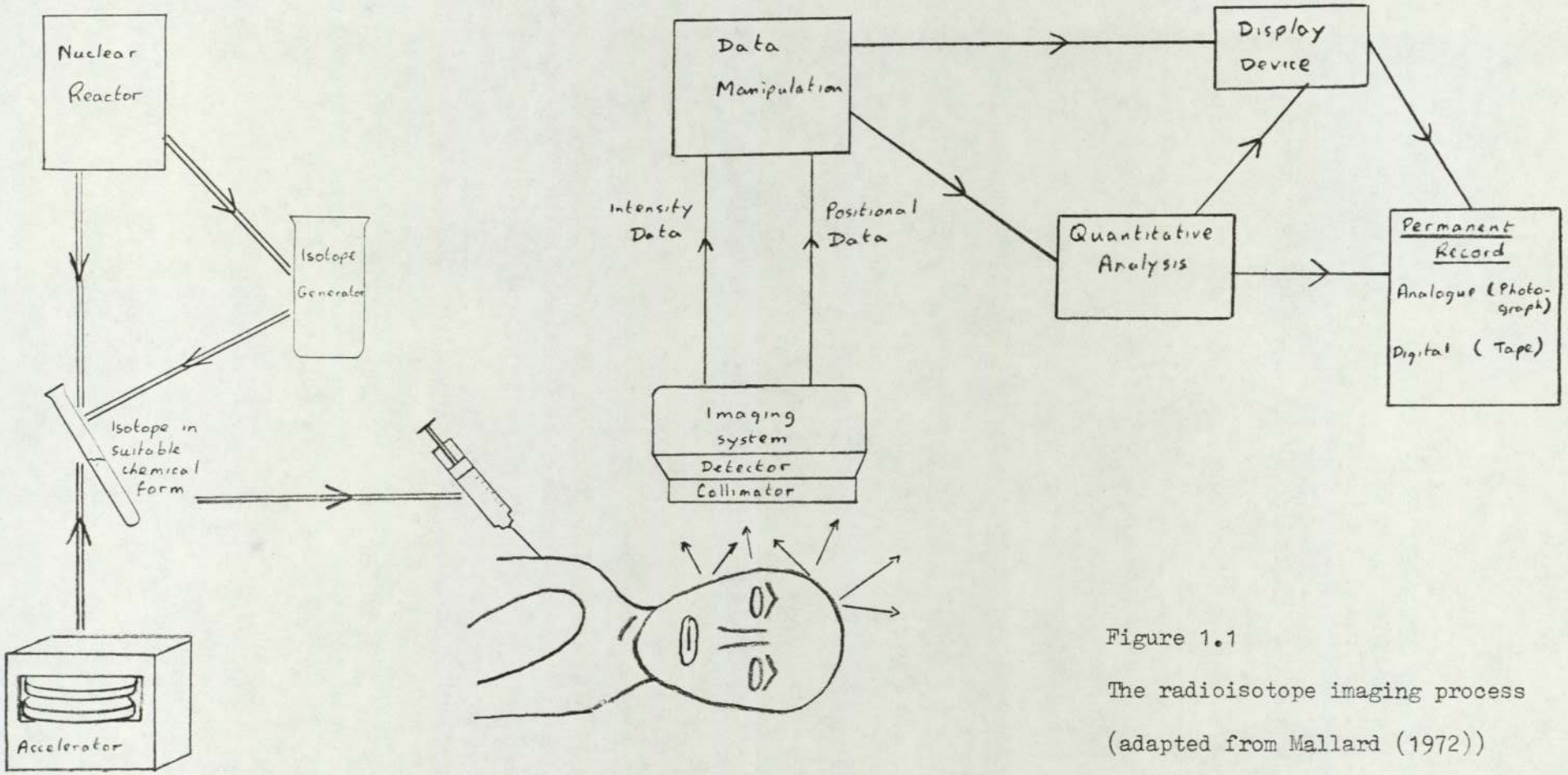

Figure 1.1

The radioisotope imaging process

(adapted from Mallard (1972))

The block diagram fig. 1.1. shows the main components of a practical system for medical radioisotope scanning. All aspects of this system have been subjects of intensive research for the past 20 years and this research will now be briefly be surveyed.

1.2 Factors governing choice of isotope

Any use of radioisotopes in human beings is subject to very strict controls. In this country any proposed use of isotopes in vivo must be licenced by the Medical Research Council. The fundamental problem, as outlined in an essay by Stanbury (1970), is to select a dose of radioisotope which is sufficiently large to give the investigator the answers to his inquiries, without endangering the patient or his progeny. Although much work has been done on the effects of radiation on the human organism, the long term effects are still largely unknown. Hence extreme caution must be exercised, and the radiation dose received by the patient is usually a limiting factor in any investigation.

The advantages of using isotopes with short half lives have been pointed out by many authors among them Scheer (1969) and Wolf and Kronert (1969). Use of a short lived isotope will permit a larger activity to be given with a consequent improvement in the information content of the scan. The radiological dose received by the patient is no greater, and may be less, than that received if longer lived isotopes are used. This does not mean, however, that only those isotopes with a short physical half life may be used. Many substances are rapidly excreted from the body, and the "biological half life" may be much shorter than the physical half life. Examples are in the use of inert gases such as ^{133}Xe or ^{85}Kr in the study of the blood flow in the brain. Although the two isotopes have half lives of 5.3 days and 10.6 years respectively their "biological half life" is in the order of seconds only as the gases

are almost completely eliminated in a single passage through the lungs.

The type and quality of the radiation must also be considered. Generally speaking, only gamma emitters are suitable, as only gamma rays are sufficiently penetrating to be detected outside the body. For examinations of the brain, it was suggested by Husak (1969) that a gamma energy in the range 100 kev to 400 kev was most suitable as the absorption in the skull rises steeply below 100 kev (Oldendorf and Lisaka (1969). Ideally, the isotope should emit only gamma radiation, as any beta emission would contribute to the radiological dose received by the patient without yielding useful information about the isotope distribution.

It may be difficult to arrange for a regular supply of sufficient short lived radioisotopes. This may often be overcome by use of an isotope "generator" in which the clinically useful short half life isotope may be produced and separated from a longer lived parent isotope.

A number of generator systems were described by Richards (1960) and others have been described by Nagai and Watari (1968) Bedrossian et.al (1968) and Yano and Anger (1964). Generator systems that are now commercially available include indium-113m from tin-113, iodine-132 from tellurium-132, strontium-87m from yttrium-87, technetium-99m from molybdenum-99 and gallium-68 from germanium-68.

Fig. 1.2, based on the work of Van Eck (1968) with some additions summarises the properties of isotopes which have been successfully used in brain scanning. The isotope most widely used for brain imaging is ^{99m}Tc. This isotope possesses almost ideal radiation properties, and possesses other important virtues in that it is chemically reactive (hence forming stable compounds) and is reasonably cheap.

Radio-isotope	Radiation β	Radiation γ	Gamma ray energy used for scanning (keV)	Physical half-life	Acceptable Dose (mCi)	Optimum duration between injection and examination	Radiation dose (rad) Whole Body	Radiation dose (rad) Critical Organ
^{197}Hg		+	77	2.7 days	0.5	3-6 h	0.1	kidneys 4-13
^{203}Hg	+	+	279	46.5 days	0.5	3-6 h	0.2	kidneys 35-165
^{131}I	+	+	364	8 days	0.5	24 h	1.0	thyroid (blocked) 12-18, blood 3-15
^{99m}Tc		+	140	6 h	10	30-60 mins	0.1	thyroid 1-4
^{113}In	(+)	+	392	1.7 h	66	20-30 mins	0.06	kidney 0.6
^{169}Yb		+	177) 198)	32 days	10	20-30 mins	0.2	bladder 3.0
^{67}Ga		+	185) 296)	78 h	2	48 h	.64	liver 3.4

Figure 1.2 Some properties of isotopes used in brain imaging

1.2.1 Choice of Radiopharmaceutical for Brain Scanning

Having chosen the particular radioisotope required for an investigation, this must then be incorporated into a suitable molecule for administration to the patient. The substance injected should obviously have no harmful side effects and must also possess the property of selective concentration in the organ or tumour one wishes to detect. The term target/non-target ratio is used, and this must be as large as possible. Experimental studies have shown that ^{206}Bi-citrate gives the highest ratios (75-100:1)(Werff,1966) and more commonly used radioisotopes give give much lower values - an average of 12:1 for Na $^{99m}TcO_4$ and Na ^{131}I (Matthews and Mallard,1965), 28:1 for ^{203}Hg chlormerodrin (Dereymaker,1967) 29:1 for ^{113m}In - DTPA (diethyl triamine pentaacetic acid) (O'Mara,1969). The results reported by various workers in this field do not always correspond, nor are the implications always clear.

It is important to note that a target / non-target ratio of, say, 10:1 does not imply that a ten-fold increase in count rate will be recorded over the site of an abnormality. Because of the shape of the abnormality and the characteristics of the collimator used, radiation will, in general, be accepted from a volume of non-target tissue which is relatively much larger than the volume of target tissue contained within it. Mallard (1972) has shown that with a radioactive object 1 cm thick placed at a depth of 12 cm in a water filled phantom containing isotope of one-eighth the concentration in the target object, an increase in counting rate of only 10% was obtained over the target, compared with non-target areas.

The values for target / non-target ratios obtained experimentally with a wide variety of pharmaceuticals suggest that the mechanism involved in concentrating isotope into diseased or damaged regions of the brain is a non-specific one, and research on the properties of the blood/

brain barrier reported by Holman (1972) tends to support this view. The interesting results obtained with ^{206}Bi - citrate suggests that a more active transport mechanism may apply in this case. Trials with a ^{99m}Tc labelled citrate complex have been interesting, but have so far failed to provide convincing evidence of the superiority of this pharmaceutical.

1.3 Instruments for Radioisotope Imaging

The function of any radioisotope imaging system is to provide an image of the distribution of radioactivity in the part of the body under examination, most usually in the form of a two dimensional intensity distribution plotted onto paper or film. The imaging device must therefore provide both spatial information and intensity information. Two main classes of instruments have been developed to fulfil this function. They differ in the means by which the spatial information is generated, which may be obtained in either a serial or parallel manner.

Those instruments in which spatial information is obtained in a serial manner are known as rectilinear scanners. The radiation detector is used to measure a count rate in a small volume of the organ under investigation, and spatial information is obtained by relative movement of the detector and the organ, usually in a rectilinear manner. These instruments are described in more detail in section 1.4. The other class of instruments use detected events to form positional information, and the position of each event is plotted on the output device. Information on the concentration of radioactivity in different parts of the organ is obtained in the final displayed output by observing the manner in which the plotted points group together. Such devices are usually referred to as gamma cameras. They are discussed further in section 1.5.

1.3.1 Radiation Detectors

The use of scintillation detectors, especially sodium iodide crystals for imaging systems is now almost universal. Other devices that have been described include solid state semiconductor systems, using either lithium drifted germanium detectors described by Hoffer, Beck and Charleston (1971) or lithium drifted silicon detectors as used by Detko (1969). The advantage of this type of detector over the sodium iodide type lies in its extremely good energy resolution, which with suitable pulse height selection can virtually eliminate the loss of image contrast due to Compton scattering. The disadvantages lie in its limited sensitivity and the problem of operating the detector at liquid nitrogen temperatures. The device described by Detko would be suitable for the construction of a gamma camera, being based on a semi-conductor matrix. Charge pulses from ionising radiations would be localised by a row and column addressing system.

Another unusual device is the spark imaging camera described by Horwitz et.al. (1967) and Lansiart and Kellershohn (1966). These devices are very simple, but have a relatively low detection efficiency. Horwitz has compared the spark imaging camera results to those obtained by a conventional scanner in 75 studies of the thyroid, and claims a much higher resolution with the former device (Horwitz, Lofstron and Forsith (1966)).

Other detection methods which have been proposed or constructed include multiwire proportional chambers, described by Kaplan et. al (1973), Chu (1976) and others and stimulated positron emission devices, described by Drukier (1976). Some of these types of radiation detector, especially the semiconductor types show promise, and may be used in future nuclear medicine instruments.

1.4 Radioisotope Scanners

The first instruments designed for radioisotope imaging were developed in 1950 by two groups working in London and California. The methods used were described by Cassen et. al. (1951) and Mayneord et. al. (1951). Briefly, these early instruments consisted of a small, collimated scintillation detector which could be moved in a raster over the organ of interest. Counts were recorded by a tapper bar making dots on a piece of paper. The dot density was proportional to the amount of radioactivity detected.

The basic principles of these early machines can still be recognised in the latest types of scanners, although many improvements have been made. Modern scanners normally use sodium iodide crystals of between 3" and 8" diameter for improved sensitivity, and some use multiple crystals. An early example of a multi-crystal scanner was described by Hindel et. al. (1967). Use of large crystals requires sophisticated collimation, and multi-hole focussing collimators are normally employed. Pulse-height analysis is used to discriminate against scattered radiation and hence to improve contrast in scans of deeply lying structures. The simple tapper bar display system has been improved by the introduction of systems using multi-coloured ribbons, originally described by Mallard and Peachey (1959) in which the radiation intensity is indicated by both dot density and also the colour of the dots. Alternative forms of display include the photoscan display, originally described by Kuhl et.al. (1956)in which the intensity (or more usually the frequency) of a flashing light source is modulated by the ratemeter output to produce a latent image on a sheet of X-ray film. Development of the film produces an image in which the distribution of radioactivity is indicated by shades of grey.

Some of these improvements in moving detector instruments will

be described in more detail in later sections.

1.4.1 Collimators for radioisotope scanners

The design of the collimator is a key factor in determining the performance of any radionuclide imaging device. Modern scanners invariably use multi-holed focussing collimators, and design of such collimators is a complex task.

A multi-holed, focussing collimator suitable for a radioisotope scanner is shown diagrammatically in fig. 1.3.

This arrangement multiples the number of gamma ray photons allowed to pass through the collimator, by N, the number of holes. However, the radius of the field of view in the focal plane, R, remains the same as that of any one of the holes. As a result, sensitivity is improved, whilst in the focal plane, at least, the spatial resolution of the small single hole is preserved.

A typical example of a focussed collimator used clinically would be about 10 cms. in length, and have the focal point placed about 10 cms. beyond its inlet face. The holes are usually circular or hexagonal in cross section, and arranged in a hexagonal array. Hexagonal holes usually provide a sensitivity about 10% higher than circular holes for the same resolution, but penetration of the septa separating the holes is a little greater, and resolution varies slightly in different directions (Mallard, 1972).

Any collimator represents a compromise between resolution and sensitivity. In order to achieve as faithful a reproduction as possible of the isotope distribution, the resolution (often expressed as the full width at half maximum of the system response to a point source) should be good, but in order to achieve this, the sensitivity will be reduced. Since, for a large organ such as the brain, there is a lower practical

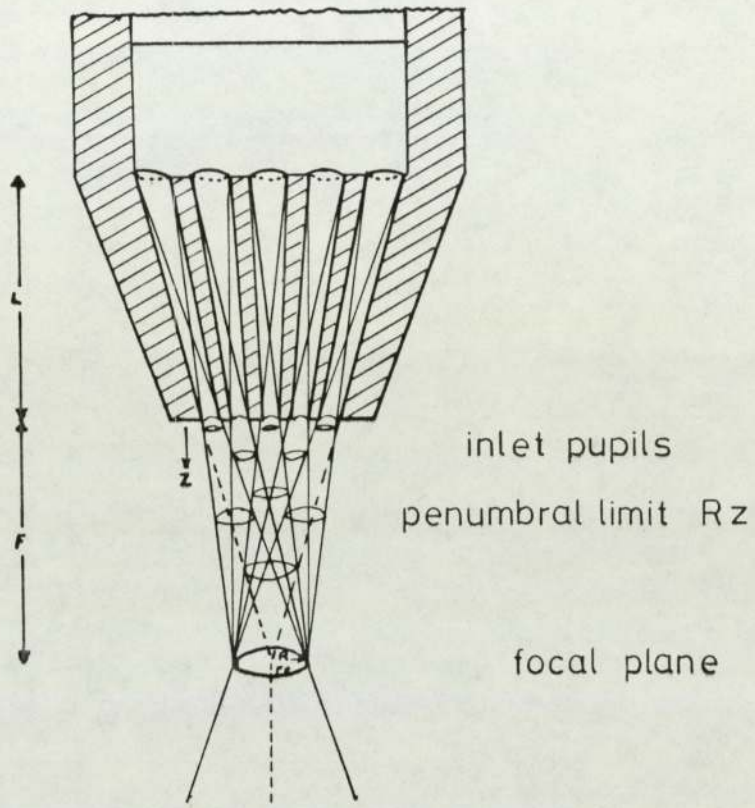

Fig. 1.3 A cross-section of a focussed collimator of length L, with focal point Fp at a distance F from the inlet face of the collimator. The inlet pupils and detector pupils of the holes are shown. The field of view in the focal plane, of radius R, is seen to be the complete overlap of each field of view of each individual hole; in all other planes they do not completely overlap and the resulting field of view is contained within the penumbral limit which is shown.

(from Mallard, J.R. (1972))

limit to the scan speed of about 2 cm/sec., the sensitivity must be good in order to provide a counting rate over a tumour which is statistically significantly higher than that of the background. This problem has been examined in some detail by Westerman, Sharma and Fowler (1968). It had been shown earlier, by Dewey and Sinclair (1961) that for sources greater in size than the full width half maximum (i.e., "resolution") of the collimator, the isotope distribution is reproduced reasonably faithfully. Sources smaller than this produce an image of approximately the size of the point source response image.

The collimator designer has to consider not only the lateral response of the collimator, but also the longitudinal response. Generally speaking, the longitudinal response becomes less uniform as the detector size is increased, and this factor is crucial in determining the size of the crystal employed.

A typical series of line source response functions, measured by the author, is given in fig. 1.4.

1.5. Gamma Cameras

Gamma cameras are instruments in which a visual representation of a radioisotope distribution can be achieved without relative movement of the source and detector. A gamma camera consists essentially of a large-area radiation detector with a collimator or other device to produce a radiation image on the detector. A suitable form of amplification with a gain in the range 10^5-10^7 is required to enable the detector signals to drive the display, and a data transfer component must transfer the signals from the radiation detector to the display system (fig. 1.1).Unlike the moving detector devices, the data transfer system has to transfer the positional information as well as the gamma-ray intensity information. In the ideal device intensity is distributed from point to point in the

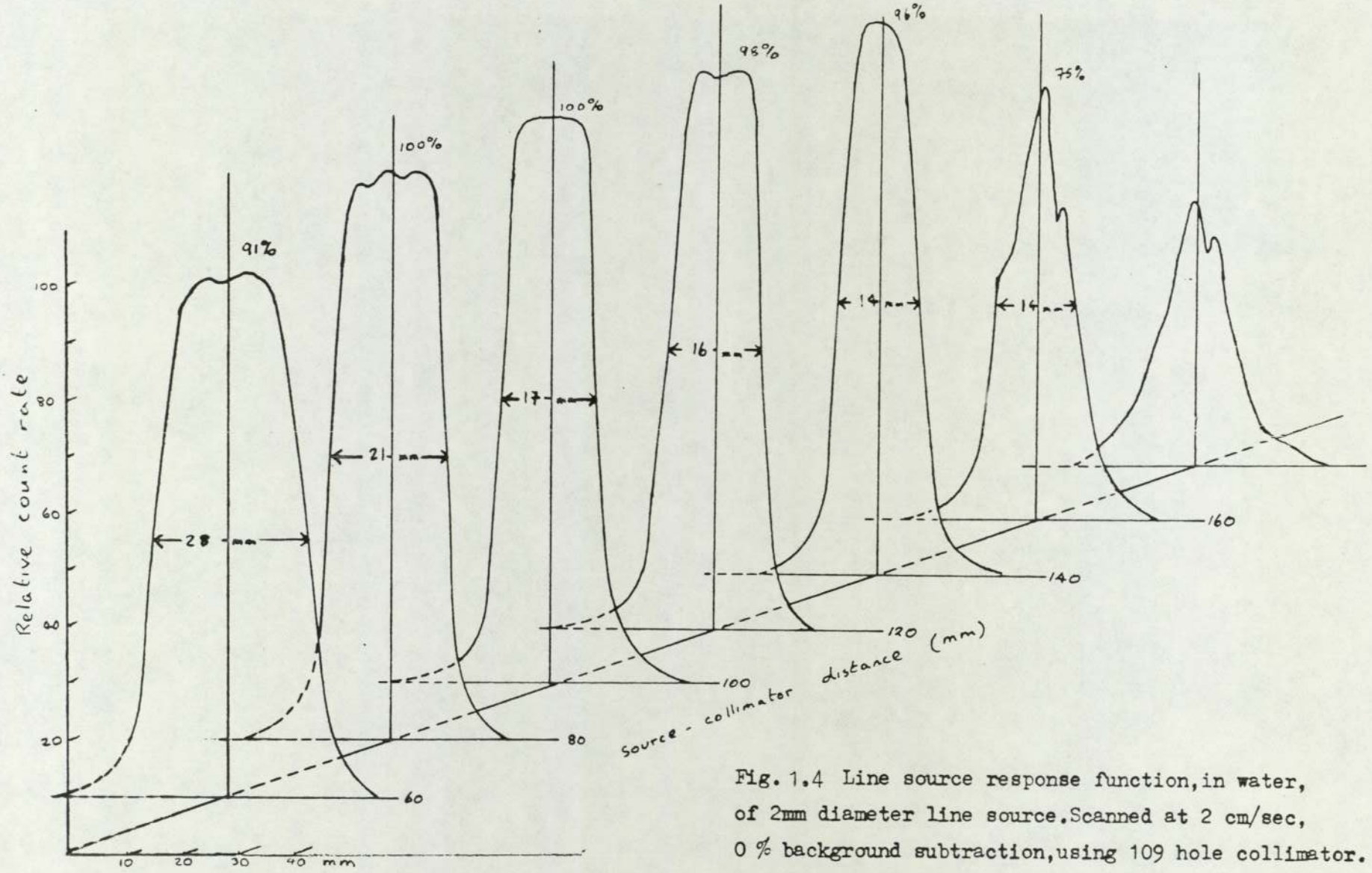

Fig. 1.4 Line source response function, in water, of 2mm diameter line source. Scanned at 2 cm/sec, 0 % background subtraction, using 109 hole collimator.

same way as in the radioactive source: in practice, distortions of intensity and geometry occur.

Because of the large area radiation detector, which gives good sensitivity, and the gamma cameras ability to view the organ as a whole, rather than a little at a time, shorter exposure times become possible and dynamic processes can be studied.

The most commonly used type of gamma camera is that originally developed by Anger (1958,1963) and usually referred to as the Anger Camera. The general arrangement of this type of instrument is shown in fig. 1.5. The radiation detector is a single thallium activated sodium iodide crystal, a typical size being 12 inches diameter x $\frac{1}{2}$ inch thick.

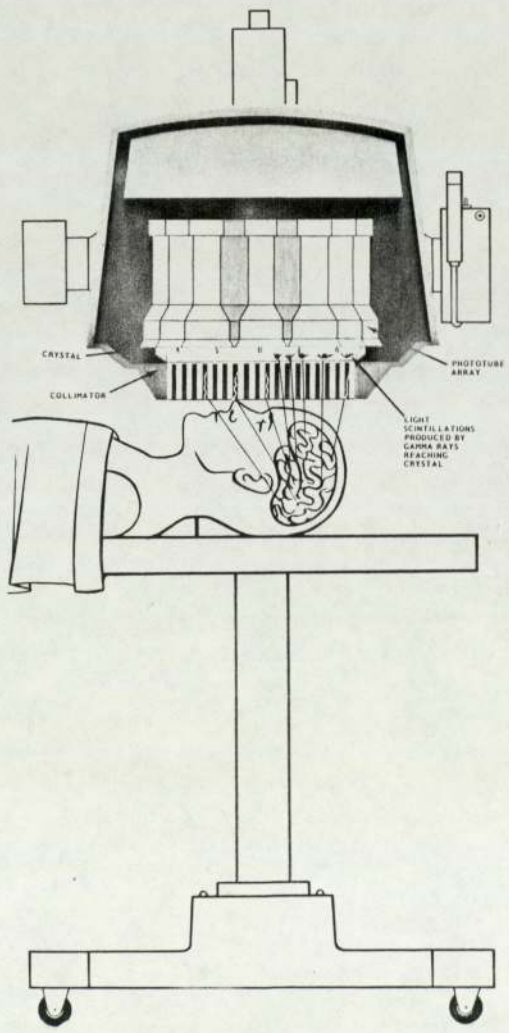

Figure 1.5
The Anger camera
(general arrangement)

The scintillations in the crystal are viewed by a number of photomultiplier tubes in a close packed hexagonal array. These are optically coupled to the crystal. The design of the 'light pipe' is important, and has been discussed by Mueller et.al. (1965). Most instruments produced prior to 1973 employed 19 photomultipliers, but more modern high resolution cameras now commonly have 37.

Gamma cameras are inherently unstable devices. They are based on a number of individual photomultipliers which are essentially amplifiers with a gain of 10^6 and no feedback. The outputs of the tubes have to be carefully adjusted to ensure uniformity over the area of the detector and to minimise spatial distortion. This problem has been examined in some detail by Todd-Pokropek (1976). With most commercially available devices it is found that after a few weeks of operation the uniformity remains within $\pm$ 10% over the field of view and adjustments to the gain of individual tubes are only occasionally necessary.

The information derived from the Anger Camera system is conventionally displayed on an oscilloscope, which is viewed over a period of time by an open shutter camera.

The Anger camera is the most widely used type of stationary detector device, but two other systems have been produced commercially.

The digital autofluoroscope was originally developed by Bender and Blau (1962, 1964). A commercially available machine has been described by Fitzer (1967). The detector of this instrument consists of a rectangular matrix of small crystals, each one behind the hole of a multi-hole collimator. Quite thick crystals may be used, giving a higher sensitivity and a better performance with high gamma energy isotopes than is possible with the $\frac{1}{2}$ inch thick crystal of the Anger camera.

The data transfer system comprises two light pipes optically

coupled to each crystal. Twenty-one light pipes, from each crystal in a row, go to one photomultiplier, and fourteen light pipes, from each crystal in a column, go to another. Simultaneous pulses in any two photomultipliers identify the crystal in which the event occurred. This system of addressing obviously lends itself to digital processing techniques, and the device is invariably operated on-line to a magnetic core memory. Aspects of the data processing system have been discussed by Spergel (1966) and Bender, Blau and Sigmund (1966).

A number of interesting gamma camera systems using image intensifier tubes have been described. Image intensifiers are electron-optical devices used for low intensity light and X-ray applications. Gamma cameras based on these devices were originally proposed by Kellershohn and Pellerin (1955) and apparatus of this type has been described by Ter-Pogossian and Eichling (1964), Kellershohn and Lansiart (1967) and Mallard and Wilks (1969). More recently a gamma camera using an image intensifier tube has been described by Mulder and Pauwels (1976). This latter device is interesting in that it appears to combine features of both image intensifier gamma cameras and Anger cameras and seems to offer very high resolution and a reasonable sensitivity.

1.5.1 Recent improvements in Anger camera performance

Until the early 1970s, most radionuclide imaging systems in routine use in the United Kingdom were of the rectilinear scanner type. Anger cameras, though they had been commercially available for an equal length of time had not been widely adopted, despite their advantages of speed and their ability to perform dynamic studies. This was principally because the resolution of the earlier generation of Anger camera, especially at a depth of 8-10 cms, was not as good as that of a well

designed rectilinear scanner with an appropriate collimator. More recently, however, a dramatic improvement in Anger camera performance especially in resolution, has been achieved and most new isotope imaging systems now ordered are of this type.

The improvement in Anger camera performance was brought about in part as a consequence of the necessity to redesign systems to optimise performance at the relatively low gamma ray energy of technetium-99m. The isotopes most widely used previously generally had gamma ray energies in the range 200-500 keV, and for such medium to high energy gamma radiation the overall resolution of the system was largely determined by the resolution of the collimators, as discussed by Anger (1967). Gamma camera collimators are usually parallel holed, and medium to high energy collimators are normally,of necessity, constructed with fairly thick septa to avoid excessive septal penetration. To maintain a reasonable sensitivity a relatively small number of relatively large holes are required. Typical values are about 2,000 holes of about 5mm diameter in a collimator with a useful field of view of 25 cm diameter.

The use of lower energy isotopes allowed the use of much thinner septa, and high resolution collimators containing as many as 20,000 holes of about 2mm diameter were designed. The overall system resolution was now largely determined by the 'intrinsic' resolution of the Anger camera, that is, the accuracy with which the position of a scintillation event in the crystal could be computed. The type of arithmetic performed by the 'analogue computer' network of the camera is important not only in terms of defining the intrinsic resolution, but also in specifying coordinate linearity and uniformity of regional response.

Modifications to Anger's original position computer were suggested by Mallard and Myers (1963), Baker and Scrimager (1967), Svedberg (1968) Tanaka, Hiramoto and Nohara (1970) and others. These improvements in the position arithmetic were incorporated into commercially available Anger cameras built after 1970, and resulted in a considerable improvement in performance. One such instrument was evaluated by the author (Pexman and Woolley, 1974) and was found to have a performance equal to that of a rectilinear scanner, even for deeply lying lesions in the brain.

Further improvements in performance have mainly been brought about by the use of a larger number of smaller diameter photomultiplier tubes. Most commercially available Anger cameras now use 37 two inch diameter photomultipliers, compared to the 19 three inch diameter tubes used on most pre-1973 cameras. This trend is likely to continue. One system uses no fewer than 91 photomultipliers.

1.6 Tomographic imaging systems

The use of high performance isotope imaging equipment, in the hands of skilled operators and using the best available isotopes and pharmaceuticals results in the detection of a large proportion of focal lesions in the organs investigated. In the case of the brain, most authors report a detection rate of 80-85% although this may be higher for certain types of lesion. The 15-20% of focal lesions not detected are either very small (below 1 cm diameter) or are located close to the base of the brain or in the posterior fossa where superficial concentrations of radioactivity frequently mask the presence of abnormal concentrations within the brain. It seems likely, therefore, that a significant improvement in the results of radionuclide imaging could be obtained if a means could be developed to separate superficial radioactivity from more deeply lying activity, that is, to image clearly

the isotope distribution in a layer at some specified depth in an organ.

A number of methods have been devised to perform this type of imaging. The method is refered to as layer scanning or tomography. Most systems that have been described in the literature use a computer to reconstruct the sectional images, though this is not always necessary.

Many methods use an Anger camera as the imaging element in the system, and rely on special collimation coupled with movement of the collimator or the collimator/camera assembly to give depth dependant information. The multiplane tomographic scanner described by Anger (1969) used a small gamma camera fitted with a multihole focussing collimator, and scanned over the subject in a rectilinear raster. A computer was used to give reconstructed images at depths of 1,2,3,4,5 and 6 inches from the collimator face.

Another approach was described by Freedman (1970,1972). He used a standard Anger camera fitted with a special collimator containing 1,500 parallel holes each inclined at 20° to the vertical. During the examination, the collimator rotated through 360° in increments of 30°. At each collimator position, an image of the organ was acquired which was stored for processing in a digital computer. An image could, in principle, be reconstructed for any specified depth in the range of 1-12 cm from the collimator face.

A rather similar approach was used by Muehllehner (1971) except that a synchronised circular motion of the patient couch was used in addition to the collimator rotation. This method overcame the problem of decreasing field of view with increasing depth which was inherent in Freedman's method, and allowed the use of analogue rather than digital processing methods.

A less conventional, but potentially very attractive method of performing tomography replaces the conventional collimator of the

gamma camera with a Fresnel zone plate. The image is not directly discernable, and resembles an optical hologram even though the process of image formation is somewhat different. As with the hologram, the coded image contains three dimensional information and may be decoded to form an image in any chosen plane within the object. This method has been described by Barrett et. al. (1972) among others.

All these instruments perform longitudinal tomography, that is, the images are formed in a plane parallel to the body axis, as is also the case with conventional isotope images. None of these methods actually removes any overlying or underlying activity from the readout. The process is rather one of defocussing, in that overlying or underlying structure is not imaged clearly in the plane of interest. Not infrequently, however, such defocussing can generate artefacts in the plane of interest from adjacent structures.

The problems inherent in longitudinal tomography have led some workers to attempt the alternative approach of transverse axial tomography. In this method a ring of detectors surrounding the body is used, or a detector system is rotated around the body. The plane of interest is a cross section of the body, perpendicular to the axis of the body. Only activity in the plane of interest is detected, thus avoiding the problem of artefacts arising from adjacent sections.

An instrument to perform this type of examination was first described by Kuhl and Edwards (1963). The approach appeared to be a very promising one, especially as the type of instrument described could also be used for conventional radionuclide scanning. A means of implementing this method of tomography using commercially available equipment has been developed, and is described in chapters 6-8 of this thesis.

1.7 Scanner display systems

Some of the forms of data presentation from isotope scanners have already been mentioned. The three methods most commonly employed are photoscanning, in which the intensity of radiation detected at any point is represented by the degree of blackening of the corresponding point on a photographic film, tapper display, in which the isotope distribution is represented by the spatial distribution of ink spots on a piece of paper, and colour tapper displays in which the isotope distribution is represented both by spatial distribution of dots, and their colour. Most commercial scanners provide two of these three outputs as standard.

Various refinements of these systems have been proposed. Desgrez et al. (1968) have described a system of colour recording which appears to overcome the problem of the finite time constant of more conventional colour recording systems. Another method for recording colour displays using photographic colour paper has been described by Morrison et al. (1968). It is claimed that 'in the occasional case, the authors feel that it has been possible to derive more information from the colour scan than from the photoscan.' This seems a modest claim to make for a system that would cost many times more, in materials, than either the colour dot scan or the photoscan.

Mantel, Cook and Ruskin (1967) described an attempt to improve the black and white dot scan merely by reducing the size of the output display. Other authors including Teddenham (1957), Morgan (1966) and Mishkin et al. (1970) have suggested that, in photographic displays at least, reduction in size of the display improves the rate of detection of abnormalities.

A fairly widely used method of attempting to improve the conventional forms of display is the use of statistical averaging, usually referred to as 'smoothing' or 'data blending.' There appear to be good

reasons for this form of presentation, as the image transfer system does not image a point source as a point, but as an approximately Gaussian distribution. It would therefore seem logical to arrange for the light spot exposing the film to have a similar distribution. Onai et al. (1967) and Christie et al. (1966) have described suitable methods. There has been a good deal of controversy about this procedure, and theoretical studies carried out by Freedman, Wolberg and Johnson (1968) seem to show that the absolute information content of the conventional photoscan throughout the diagnostic clinical range is higher than that of the data - blended format. Kuhl (1972) came to a similar conclusion from experimental evidence, although Atkins, Hauser and Richards (1968), whilst accepting that some loss of contrast does occur, thought that the data blended output has certain advantages. The limited experience in this area of the author confirms Atkins' finding that where counting statistics are good, the data blended output is useful in that shapes of objects are better delineated. The disadvantages were also apparent in that where counting statistics are poor, (as occurs over the cerebral hemispheres for a normal brain scan) a mottling effect occurs. This was referred to by Kuhl as 'quantum mottle' and can conceal low uptake lesions, or actually result in a false positive report. An important point is that the interpretation of isotope scans is inevitably somewhat subjective, and that those outputs which theoretically offer the greatest information content are not necessarily the most helpful.

A number of studies, notably by Mallard (1967), Damascelli et al. (1967), and Heiss et al. (1969) have analysed the efficiency of the various conventional forms of output. A general conclusion which may be drawn from these reports is that the conventional forms of output are fairly efficient, although the settings of the controls are critical if the maximum diagnostic information is to be extracted. More unusual forms of output might be helpful in certain borderline or equivocal cases. There

is thus an argument for the reprocessing of certain scans to improve their clarity where the original scan failed to yield the required information.

1.7.1 Reprocessing of scanner output data

The starting point for the image enhancement process is usually the original photoscan transparency. As discussed by Ben-Porath et al.(1966)and Mante,Allen and Verdon (1968) a high contrast print from this can often yield information which was not apparent in the original.

A more popular approach,described by Harris et al. (1966), Charleston et al (1967) and others, is to convert the density levels of the original black and white photograph into colour levels, often employing a flying spot scanner and a colour T.V. system fitted with suitable filter circuits. These systems can certainly enhance the contrast of the original photoscan, but they must be used with extreme caution, as the colours, in general, are not related in any known way to the count rate of the original scan. In particular, the boundary between different colours tends to assume great significance to the observer, but this may not have the same significance when the original count rate data are considered.

The fundamental fallacies of the above approach have been pointed out by Chaapel and Sprau (1967) who noted that (a) all the information is not necessarily in the photoscan to begin with, and (b) that it is possible to enhance a 'molehill' into a 'mountain', i.e., one might delve into the statistically insignificant. A more fundamental means of extracting the necessary information is therefore required.

Magnetic tape recorders have been and are widely used for recording scan data. These are useful in that if the settings of the scanner display controls have been incorrect, a record on tape can be played back to give a better display.Such a system was described by Corry (1966) and

a number of commercial systems are now available. These systems are useful as a safeguard against instrument failure and human error, but do not in themselves contribute to an improvement in scanner display systems. Workers have tended to turn increasingly to computer data processing methods in an attempt to improve display of information.

1.7.2 Quantitative analysis of scanner output data

Any assessment of the efficiency of a particular display system requires some estimate of the detection capabilities of the eye and brain of the observer, that is, the magnitude of the change in count rate that is required before a change would be perceived.

It was shown by Dewey and Sinclair (1961) that if R_T and R_{NT} are the count rates when the collimator is placed over the target and non-target areas respectively, and if t is the time for which counts are accumulated, then the difference in the recorded count rate will be n times the standard deviation of the difference estimated from the observed counts where

$$n = \frac{(R_T - R_{NT})t}{\sqrt{(R_T + R_{NT})t}} \qquad \ldots\ (1.1)$$

This expression assumes that the observer compares the target area with an adjacent or surrounding non-target area of similar size. This may not, in fact, be the case. Mallard and Corfield (1969) have suggested that the eye compares the target area with an extended surrounding area.

Dewey and Sinclair suggested that tmours would be recognised if $n \geq 3$. Most other workers disagree with this value and it was, in fact chosen rather arbitrarily as a basis for the intercomparison of

collimators rather than from experimental evidence of what observers could actually perceive in a display.

Rose (1957) found that an area of increased dot density would not be perceived unless $n \geq 5$ and Vernon (1968) using computer generated dot distributions found that at a value of $n = 6.4$, 50% of observers saw a circular area of increased dot density, irrespective of the background count rate.

The experimental results obtained by Mallard and Wilks (1968) confirmed that for a cathode ray tube display (as used with a gamma camera) the visual threshold was $n = 5$, calculated as above. However they found that for colour tapper displays and monochrome photographic recording, the visual threshold was lower. Using the latter display systems, a change in count rate of 10% could be visualised irrespective of the background count rate. This improved result is no doubt due to the contrast enhancement possible with these methods of display.

Using the count rates obtained for a typical brain scan using technetium-99m, and assuming a target area of $6cm^2$ with typical scan speed and line spacing values, a 10% change in count rate corresponds to $n = 3$. A three standard deviation threshold has statistical significance for a target area of this size, as was shown by Haybittle (1966). There is a 92% probability that such a change would be genuine rather than merely due to statistical variation.

It is encouraging to the observer to know that the display system in use is capable, under ideal conditions, of demonstrating all statistically significant changes, but it is unrealistic to assume that ideal conditions will always apply. The observer is

frequently confronted with the problem of deciding if an apparent increase in uptake, perhaps in a small or irregular region, is genuine or not. It seems likely that numerical analysis could yield objective information on which such a decision could be based.

The methods described by Popham, Bull and Emery (1970) and Dowsett and Perry (1970) appeared particularly promising, as the counts in each area of the scan are compared with the expected result derived from an analysis of proven normal case material. The development of such a method of analysis is described in chapters 3-5 of this thesis.

CHAPTER 2

The Data Logging System

2.1 Design of Digital Data Logging systems

In order to carry out quantitative data analysis of radionuclide scan data some means of transfering information from the imaging device to a suitable computer must be devised. In the case of gamma cameras, on-line operation is almost essential, as the data are generated in a random manner and the coordinates of each event have to be recorded. With a rectilinear scanner however, data are output serially and a relatively cheap dedicated data logger can be devised which will record information in a form suitable for computer input.

Modern scanners, which usually employ digital methods of information processing,can very readily be adapted to output data in a form suitable for computer input, either on-line or off-line. Positional information on these machines may be derived from the pulses used to drive the stepping motors which are now almost universally used to drive the detector and display systems.

There are still a number of the earlier types of isotope scanners in routine use, of which the Picker Magnascanner is perhaps the commonest example. The design philosophy and detailed construction of a data logger for such an instrument will now be described.

2.2 Requirements and precision of data

The essential requirement of a data logging system is a means of recording count rate and positional data in computer compatible form.

The full width half maximum of the line source response curve of the Picker Magnascanner V fitted with a 5 inch focal length,low energy 85 hole collimator is approximately 10mm in the focal plane (see fig. 2.1). As Dewey (1961) has shown,only sources with a size larger than this will be imaged reasonably faithfully. In practical terms, the smallest tumour one expects to find is in the region of 1.5 cm diameter.

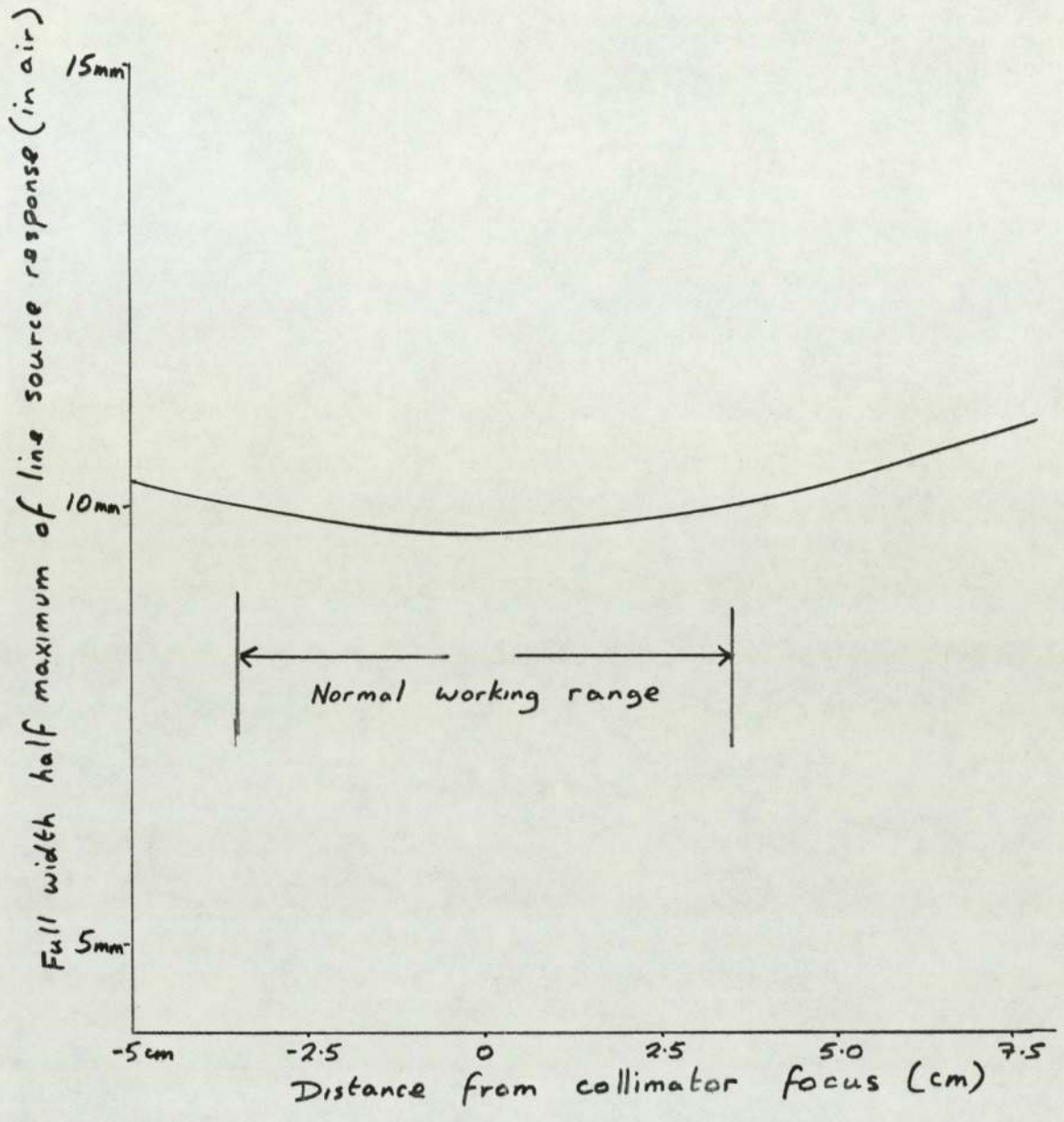

Figure 2.1 Source distance vs Full Width Half Maximum of Line Source response curve for Picker V Magna-Scanner fitted with 5 inch focal length, 85 hole collimator.

Smith and Lowe (1967) described a system in which individual scintillation pulses are recorded on magnetic tape. This system appears costly and complicated, and for such an inherently low resolution device there seems little justification for recording individual events. The "cell" size, i.e. the area over which counts are collected, must clearly be smaller than the full width half maximum: a size of about 4 mm. square would seem to be a suitable choice.

A typical scan speed for an examination of the brain would be about 2 cm/sec. It is therefore necessary to sample and output the data about 5 times per second. The maximum counting rate for a brain scan under normal conditions is about 100 K counts/min. The number of counts recorded in a time of 0.2 seconds is therefore not likely to exceed 300. Only three counting decades are required.

Positional information must also, in general, be recorded. By whatever means this information is derived, one assumes that an accuracy of 0.1% might be required. This again requires three decades of data output. Because of the rectilinear nature of the scan, it should only be necessary to output the Y position at the beginning of each new line.

If the information is to be printed in decimal or binary-coded decimal form, each cell of information requires six data characters and two or three editing characters. Additional data words and editing characters would occur at the beginning and end of a line. The required data output rate is therefore approximately 45 characters per second.

2.3 Design Of The Optimum Data Logging System

The choice of a suitable recording medium must be made at an early stage. A data transfer rate of 45 characters per second can easily be handled by a paper tape system. Both punched paper tape and computer compatible magnetic tape are equally suitable for computer input; it is

very hard to see the justification for the statment made by Dyer, McClain and Satterfield, (1970) which reads,

"..... it is advantageous to make the primary record on magnetic tape since in this case there need be no re-recording or data translation before the material is read into the computer. With punched paper tape, on the other hand, such processing is usually necessary."

In the construction of data logging systems scintillation pulses are often taken directly from the output of the pulse height analysers on the scanner. Some data manipulation is necessary before information is recorded; there are two approaches:-

(a) accumulation of counts up to a preset value

(b) accumulation of counts for a preset time or distance.

The first approach has the virtue of simplicity, as greater use can be made of the scanner internal circuits. Scaling down circuits ('dot-factor' controls) are provided in the tapper display system. The approach is usually to record the position of the probe at the moment a pulse representing a certain number of counts occurs. Such a system was described by Kemplay (1968); a similar system has been proposed by Pizer and Vetter (1969).

Kemplay described two methods for the derivation of positional information. The first used optical shaft encoders and the second design used potentiometers linked to Analogue to Digital Converters (ADC's). There is little difference in accuracy between the two, though the ADC system yielded positional as opposed to incremental data.

Although the methods described by Kemplay for the recording of positional data were accurate, the method of accumulating counts up to a preset value suffered from certain inaccuracies. As pointed out by Lying and Soderborg (1971) the relationship between dots and counts is not

necessarily linear and this must be allowed for. Additionally, errors occur at cell boundaries, since one dot represents a number of randomly occurring events and there is no way of recording how many of the preset number of counts occurred in the cell under consideration and how many in the previous cell. The present author did not consider this approach to be a particularly promising one.

The system described by Dowsett and Ritchie (1971) was based on method (b) and integrated the counts over a certain length of travel of the scanning head. They attached a slotted bar to the scanner arm, and used a photocell to measure the light transmitted through the slots from a light source on the opposite side. This very simple system produced pulses which defined the limits of the cells and initated the print out of counting information from a buffered scalar.

Integrating the counts over a certain length of travel is the method of choice for modern scanners employing stepping motors. The electronics of such systems can be made to be very cheap and simple, as discussed by Hardwick and Wilks (1972)

A slightly different approach is that described by Clifton et al.(1968) This was based on a computer compatible magnetic tape system, and was intended as a general purpose data acquisition system. An application to the Picker Magnascanner was described. Clifton points out that as the velocity of the scanning head could not be assumed to be constant, it was necessary to record both time and distance travelled in order to measure accurately the count rate in cells of a given size. The system used optical shaft encoders generating 500 pulses per revolution of the scanner head drive shaft, and an accurate 1 kHz clock to give timing information.

The optimum data logging system would have the following desirable features:-

(i) The system would require minimal alteration to the electronic or mechanical systems of the scanner as it is still necessary to obtain and output results using the conventional output circuits.

(ii) The output from the data logging system must be directly compatible with the computer. Videotape or cartridge magnetic tape systems are therefore not, in general, admissable.

(iii) The system should record actual counts from the output of the scanner pulse height analyser, perhaps integrated over a given time or distance. Systems using scale down circuits (Kemplay (1968)) or binary data compression (Dyer et al. (1970)) do not yield the necessary quantitative data. By whatever means the pulses are integrated, it is necessary to output both time and distance information to allow for non-uniform velocity of the scanning head (Clifton et al. (1968)).

(iv) The outputs from the scalars and the position sensors must be buffered, so that information is not lost during the finite period required to output the information.

2.3.1 Data logger constructional details

The required data output rate has already been discussed; a speed of about 45 characters per second is adequate. Paper tape was therefore chosen as an output medium, as paper tape punches with speeds of over 100 characters per second are readily available at modest cost. Computer compatible magnetic tape systems are considerably faster, but cost at least four times as much.

It would have been possible to develop the necessary counting and electronic drive circuits as a special system using discrete components. It was felt, however, that a modular approach would be more appropriate to minimise the time required to develop the interface and to improve the flexibility of the design. The system was therefore

based on a range of commercially available Nuclear Instrument Modules. The interface as originally conceived is shown in fig. 2.2.

The system is controlled by the timer, which is variable over the range .01 to 10 seconds. When a timing pulse is received, information in the 15 MHz scalar is transferred to a buffer module and simultaneously the voltages derived from helical potentiometers fitted to the scanning arm are digitised and held in the buffers of the Analogue to Digital Convertor. The print control module then assumes control and outputs the information in the appropriate computer code onto 8 track paper tape. This cycle is completed before the next timing signal is received.

The punch used was a 110 character per second punch, which was geared down to 63 characters per second maximum speed. This was done primarily to improve the reliability of the system, as paper tape punches wear rapidly when idling - i.e., when in motion, but not punching data. With a character output speed of 45 characters per second, idling time was reduced by 75% with the lower gearing. The high speed is still available if required.

The choice of helical potentiometers and analogue to digital conversion as opposed to the simpler and cheaper Optical Shaft Encoder (OSE) system was made for two reasons. Firstly, it was felt that the OSE system which gives incremental data by reference to photo-electrically derived pulses would be more susceptible to random electronic noise from the relays and motors of the scanner. The effect of pick up of such noise would completely ruin the precision of the data output.

Secondly, it is necessary to enter onto the data tape positions of certain anatomical reference points. The OSE system is not in general capable of doing this as it measures, not position, but only increments of position. It was therefore decided that a system based upon helical

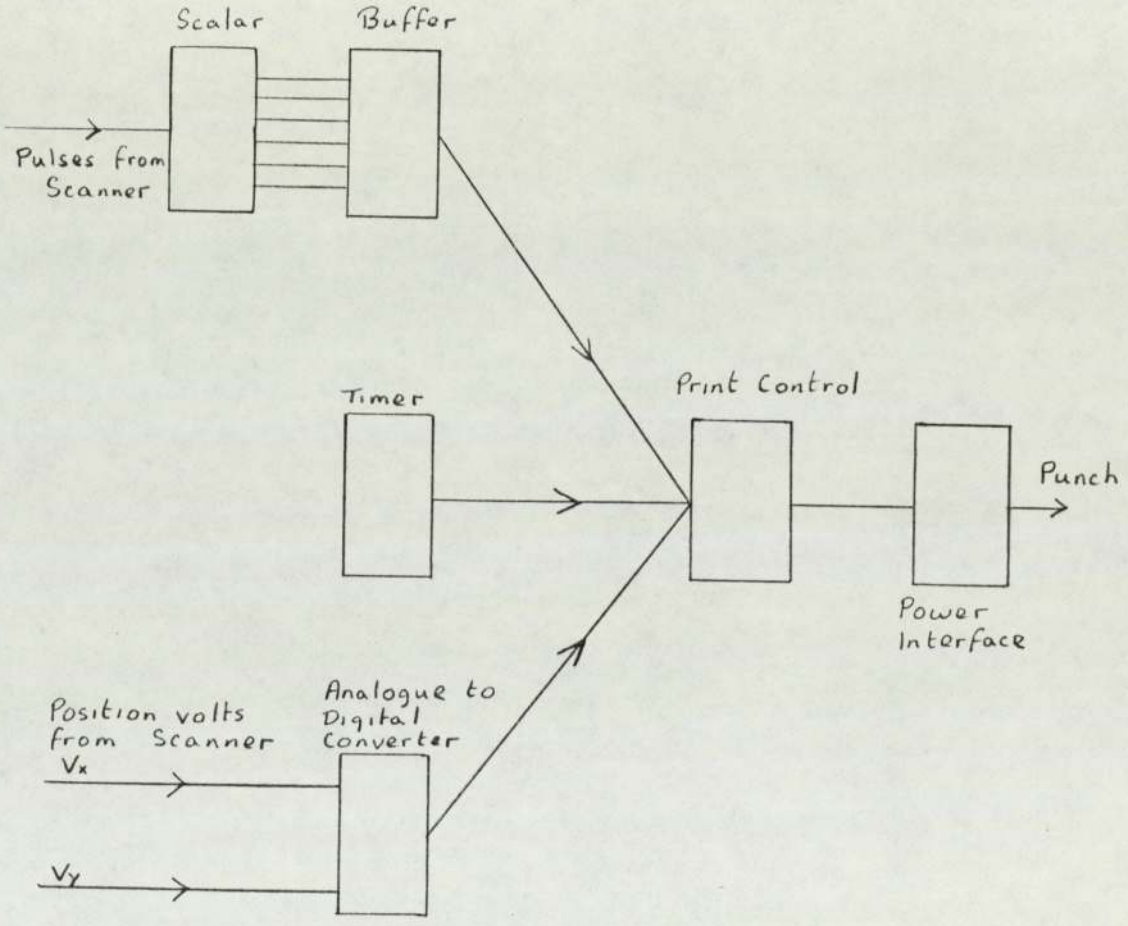

Figure 2.2 Block diagram of data logging system

potentiometers mechanically linked to the scanning arm and producing voltages directly proportional to the position of the probe within the scanning field was a more versatile approach.

2.3.2 Mechanical Modifications To The Scanner

The layout of the mechanical systems of the scanner are illustrated in fig 2.3. The arm carrying the scanner head (A) is mounted on rollers (B) on a movable carriage (41/42). The carriage is mounted on rollers (E) running on steel rails (F) set at right angles to the scanning arm. This arrangement gives the two perpendicular motions required for the scan raster.

The scanning arm is driven by a motor (G) through a gearbox and gear train. The gear wheel (H) drives a shaft on which is mounted a pinion; the latter drives the scanning arm through a rack mounted underneath.

The carriage itself is driven by a leadscrew (I) which meshes with a rack fixed to the umderside of the carriage. The shaft (I) is driven by a stepping motor (not shown) which controls the line spacing.

A potentiometer giving voltage readings along the line (the X signal) was mounted on the carriage in position J, and was driven through a collar attached to the boss of the gear H.

To the scanner main frame member K was fixed a 17 inch long rack. This was used to drive a pinion fixed to the shaft of a second potentiometer which was used to derive the Y signal. The latter potentiometer was mounted on the back of the carriage frame. The voltages applied across the potentiometers were derived from the +6V supply of the instrument bin.

Pulses representing detected photons were taken directly from the output of the scanner pulse-height analyser. A spare socket providing a - $\frac{1}{4}$ V pulse was used. As the scalars of the data logging system

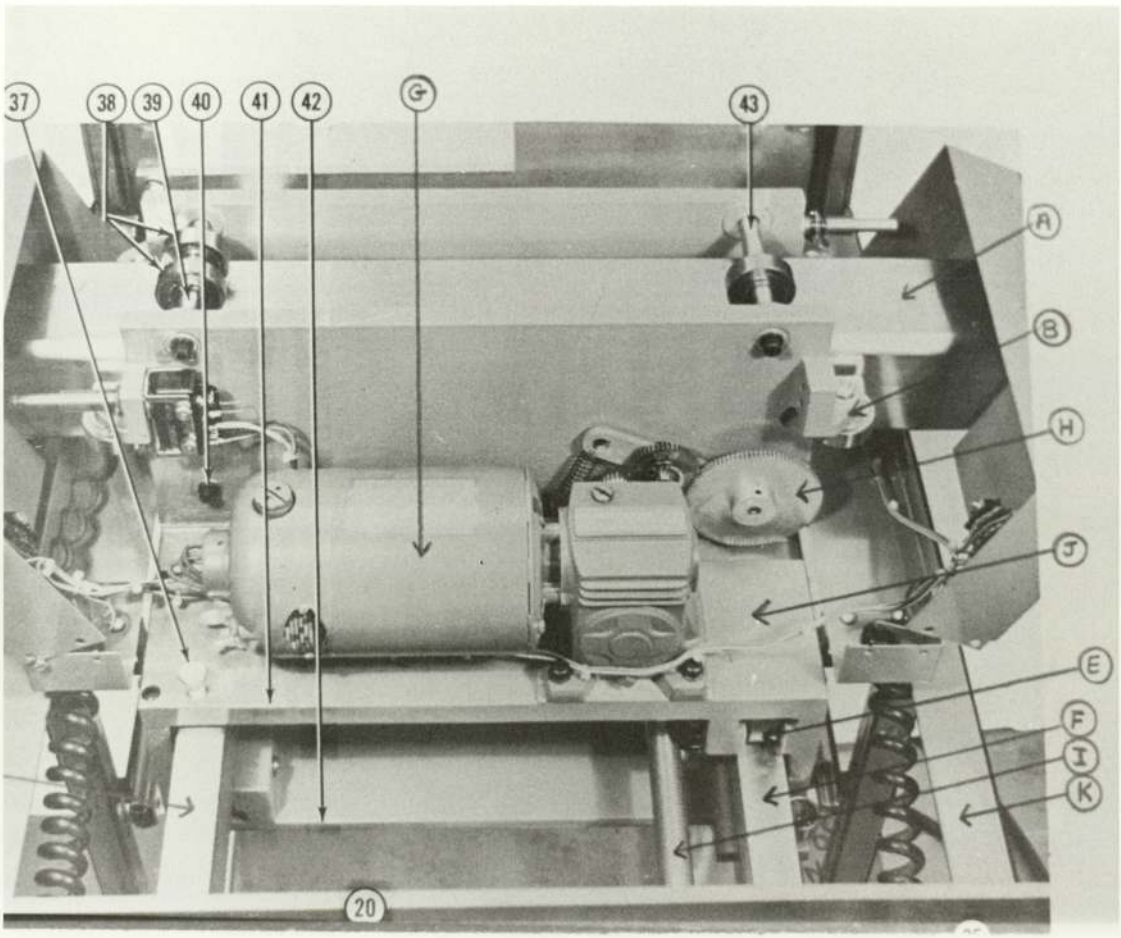

Figure 2.3 Magnascanner drive mechanisms

A - Scanning arm

B - Roller

E - Carriage rollers

F - Carriage rails

G - Scanning motor

H - Gearwheel and drive shaft

I - Carriage lead screw

J - Mounting point for potentiometer

K - Scanner main frame member

41,42 - Carriage upper and lower castings

required a + 10 V pulse for operation a linear amplifier with a gain of - 40 was oonstructed. This was built into a single width module and plugged into a spare station in the data logging system instrument rack.

The data logging system as originally constructed required no modifications of or additions to the electronic systems of the scanner.

2.3.3 Testing The Data Logging System

The data logging system as originally constructed was used to obtain count rate data on a small number of patients. A number of serious operational and electronic defects were found.

It was discovered that the print controller was not able to drive the system at speeds above 25 characters per second. The print controller was a standard module with the capacity to output data from up to ten input channels. Only three of these channels were in use, but all ten were routinely addressed by the controller. When any channel was found not to be present the print controller, which was strobed by a signal generated by the motor of the tape punch had to wait for the latter to complete another revolution before the next channel could be addressed. Thus in each data output cycle, a considerable amount of time was lost. This fault was corrected by the manufacturers of the electronic systems by the introduction of a purely electronic switching circuit. The modified system was capable of a maximum output rate of 62 characters per second, very close indeed to the tape punch maximum of 63 characters per second.

Operation of the original system required much manual intervention. For each projection, the name of the projection had to be written on the tape and the co-ordinates of certain anatomical points had to be read off from the scalars and then written onto the tape for subsequent punching.

This was time consuming. Furthermore, any errors or omissions would invalidate the information for the entire projection.

The data logging system had to be started, stopped and reset by hand and the patient data tapes were so long that a new 1,000 foot roll of paper tape was required for each patient. In fact, only 34% of the information on the tape was useful, as in each print cycle, three decades of the standard 6 decade counting scalar never contained useful information and the Y channel of the ADC system did not change value during the scanning of a single line. Information was recorded during the fast return of the scanner arm, but it was not intended to use this information. It was clear that the system would have to be modified and the following features incorporated.

1. Additional editing codes should be introduced which could be used to refer to particular projections or anatomical points. These editing codes and any necessary additional data should be automatically punched onto the tape by the operation of a push button or switch.

2. The system should be started, stopped and reset automatically by normal operation of the scanner controls.

3. Output of data should be suppressed during the flyback of the scanner arm.

4. The Y channel of the ADC should be read and punched at the start of each line only.

5. Only 3 decades of the 6 decade counting scalar should be punched.

Analysis of the problem showed that only very minor modifications to the standard modules were required and that these additional features could be incorporated into the system by construction of a scanner control

module which would plug into a spare station in the NIM bin. These modifications to the system will now be described.

2.3.4 Modification Of The Data Logging System

The data highway and print control module of the original system was designed to handle data in binary coded decimal (BCD) form. It was noted that if this could be modified to accept pure binary data, the handling of numeric data would not be altered, but six additional codes corresponding to binary numbers 1010 to 1111 would be obtained. Study of the circuits of the print control module showed that the only modification required was the substitution of a SN 7442 N integrated circuit (BCD to decimal decoder) by a SN 74180 N integrated circuit. The latter is a parity generator.

The buffer module was modified by the introduction of a front panel switch, which in one position interrupted the circuit through one NAND gate, effectively converting this module to a 3 decade buffer. The full 6 decades are still available if required.

The circuit of the Scanner Control Module is shown in fig. 2.4. Input A takes a signal from the circuit supplying the armature of the scanning motor, and B takes a signal from the circuit supplying the line spacing motor. If the armature voltage is positive (i.e. the scanner is scanning a line) and the line spacing motor is off, G1.2 is enabled, and the output of this gate changes from High to Low. This transition triggers the monostable SN 74121 and also enables gate G1.4. The latter will now change state whenever a timing pulse is received from the timer module via pin 36 on the data highway, and will initiate a print out cycle. On the flyback when the armature voltage is negative G1.2 and hence G1.4 are disabled, and timing signals are not transmitted.

The pulse produced by the monostable causes the J-K flip flop FF 4.2 to change state. This disables gates G6, G7.1 and G8.1. Transition

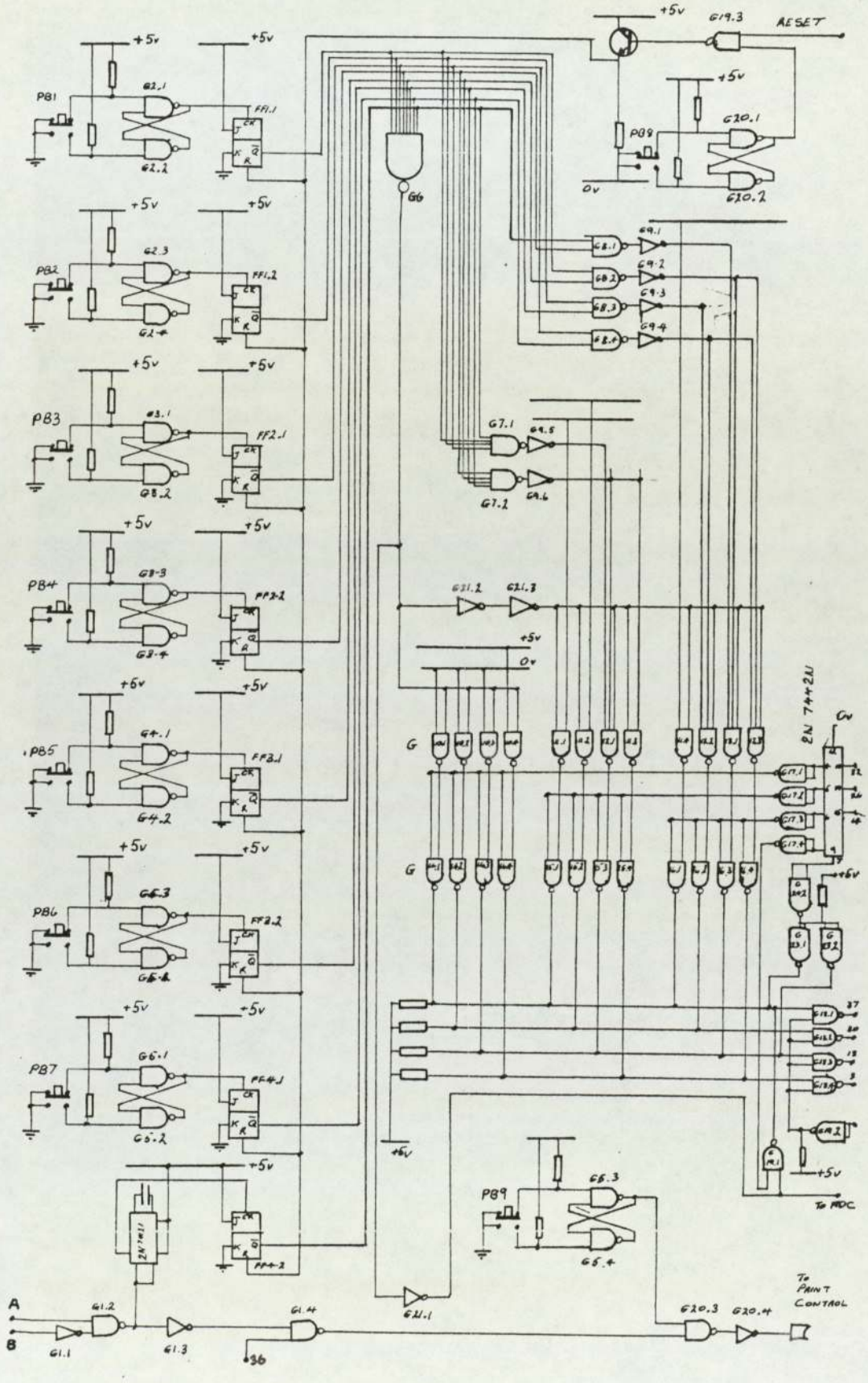

Figure 2.4 Circuit of Scanner Control Module

of G6 enables gates G10 to G13 and the outputs of these gating circuits then rest in states 0001, 0101 and 0101. These are the complements of the binary numbers 1110, 1010 and 1010. The number 1110 indicates that in this printing cycle, data will be a mixture of alphanumeric and numeric data. If any printing cycle does not contain this symbol as the first data 'word' the computer will assume that the output consists only of numerical data.

The second data word 1010 indicates that two ADC channels are to be printed. The third data word 1010 coming in this position is a beginning of line symbol.

The disabling of G6 also causes one input of G19.1 to go low. The significance of this will be seen later. The general way in which data are transferred between modules must now be considered.

Seven bussed wires are connected to all the stations in the NIM bin. Pins 3, 14, 18, 26, 30, 32 and 37 are used. An additional Module Address wire from each module is connected to the Print Control Module via the dataway system.

Any individual module is addressed by the print controller by changing the logic state of the module address wire from 1 to 0. A 'prefix command' is then given to the module, which replies with a 4 bit function code, giving the print controller information about the forthcoming data transfer. The data transfer then takes place under the control of the Print Control Module, and, finally the Print Control Module gives a 'suffix command' and receives a reply. Fig. 2.5 details the coding.

In the particular case of the Scanner Control Module under the conditions described above, the sequence is as follows. The receipt of a 0 on the module address wire disables G19.2 thus enabling gates G18. Receipt of the prefix command 111 (binary 7) disables G17.4 causing one

Module Address	32 26 14 Command Code	37 30 18 3 Reply Code Or Data	Action
1			No module address, no action
0	1 1 1		Module addressed "Prefix Command"
0		x x (B) (A)	x x 2 bits of function code. If both 0, three decades otherwise six decades (A) at logic 0 indicates "data present" (B) at logic 0 indicates command from controller - keep highway clear
	0 0 0 0 0 1 0 1 0 0 1 1 1 0 0 1 0 1	x x x x x x x x x x x x x x x x x x x x x x x x	Most significant data 24 bits of data for six decade module. Least significant data
0	1 1 0		"Suffix command"
0		x x x (C)	x three bits of function code.(C) at logic 1 indicates response to command from controller. (C) at logic 0 indicates data was presented from module.

Figure 2.5 Print Control Module command sequence

input of G19.1 to go high. As the other input of this gate is low because of the disabling of gate G6 and the inversion of G21.1 gate G19.1 remains disabled. Therefore the reply code of this module in this case is 0000.

This code is interpreted by the print control module as representing a 3 decade scalar containing data. A 1 in the first 3 bits indicates a 6 decade scalar, and a 1 in the 4th bit indicates 'data not present.' The print controller then responds with code 011 (binary 3). This enables gates G14 allowing the code previously stored here to be transferred. Data transfers via gates G15 and G16 follow, the command codes being 100 and 101 respectively. Finally the suffix command 110 is presented and the module replies with code 0000. The last 0 indicates that data was presented from the module. The print control module then addresses the next module, and the module address wire of the Scanner Control Module resumes its normal 1 state. At the end of the printout cycle, when all modules have been printed, a reset pulse is received which resets all flip flops. Resetting FF4.2 enables G6. It should be noted that if G6 is enabled (the normal condition with no flip flops enabled) one input of G19.1 goes high, and receipt of a 0 on the module address enables G19.1. Under these circumstances, the module replies to the prefix command with code 0001 indicating that no data are present. On receipt of this code, the Print Control Module addresses the next module. This process has been described in detail because a similar process takes place in connection with the Y channel of the ADC. This is only printed if G6 is disabled, i.e., at the beginning of a line and in circumstances in which the push buttons are used.

The push buttons are used in the setting up of the equipment to scan a particular projection. Four buttons, PB4 to PB7 provide

Code	Interpretation	
1 1 1 0 1 0 1 0 1 0 1 0	Beginning of line symbol	Both x and y ADC Channels read; Data noted on input to computer
1 1 1 0 1 0 1 0 1 0 1 1	Left external auditory meatus	
1 1 1 0 1 0 1 0 1 1 0 0	Right external auditory meatus	
1 1 1 0 1 0 1 0 1 1 0 1	Nasion	
1 1 1 0 1 0 1 1 1 0 1 0	Left lateral projection	Both x and y ADC Channels read, but data ignored by computer
1 1 1 0 1 0 1 1 1 0 1 1	Right lateral projection	
1 1 1 0 1 0 1 1 1 1 0 0	Antero-posterior projection	
1 1 1 0 1 0 1 1 1 1 0 1	Postero-anterior projection	

Figure 2.6 Scanner Control Module - output codes

codes which are interpreted as the four most commonly used projections, i.e. antero-posterior, left lateral, right lateral and postero-anterior. Buttons PB1 to PB3 refer to the three anatomical points that are normally used i.e., left external auditory meatus, right external auditory meatus, and nasion. At least two of these must be referred to in each projection in order to provide a baseline for the scan. The action of all these seven push buttons is similar. The pulse from the push button triggers a bistable latch, consisting of two interconnected NAND gates. This provides a clean pulse which causes the appropriate J-K flip flop to change state. At the same time a lamp contained within the push button lights up. The driving circuit is not shown on fig. 2.4 but it is switched by the Q output of the flip flop. A visual check is then made to ensure that the correct button has been depressed. If not, the instruction may be cancelled by depressing PB8. If the correct button has been selected, pressing button PB9 will initiate a printing cycle, irrespective of the states of gates G1.2 and G1.4.

In the case of buttons PB4 and PB7, although both X and Y ADC channels will be punched, the code will indicate to the computer that these data should be ignored. Fig. 2.6 gives the output codes from the Scanner Control Module.

It will be obvious that many other codes could be generated, if required. These could be used in conjunction with equipment to monitor and correct for movement of the patient, thus enabling the computer to reconstruct an acceptable quality scan from data obtained on a restless patient.

The availability of the Scanner Control Module makes the operation of the data logging system very simple, and very little operator intervention is required.

CHAPTER 3

The choice of a suitable data processor and the development of data entry programs

3.1 The Data Processing Problem

There are two main ways of approaching the problem of processing the data provided by data logging devices such as that previously described. One is to use a large batch processing computer, which will almost invariably be located at a site remote from that at which the experiment is performed. The other is to use a small computer, largely or entirely dedicated to the work, located in the department. Both systems have their advantages and disadvantages.

3.1.1 Batch Processing Computers

These are invariably large machines, which can be programmed with high level languages, such as ALGOL and FORTRAN, and have a variety of input and output devices. Input can be accepted in most of the commonly used forms, but there is usually a "preferred" form, either punched paper tape or cards. Output is usually on the line-printer, but output on cards or punched paper tape is also possible.

Processing is carried out in batches, i.e., programs using the same language and same input medium are collected together, and run in the same batch. The turnaround time of such a system cannot therefore be less than the order of hours, even though the individual program may take only a few minutes or even seconds to run. For short programs using the "preferred" form of input and output, the turnaround time may be as little as three hours. For longer programs, or programs utilising the more unusual forms of input or output, 24 hours delay is more usual.

The batch processing computers at both Universities in Birmingham have punched cards as the preferred input medium, and programs punched on paper tape, or having data punched on paper tape, are subject to delay. Whilst it would certainly be possible to use these machines for the project, and their large storage capacity and use of high level languages make their use superficially attractive, there are certain practical difficulties which would limit the clinical usefulness of the system.

3.1.2 Small Dedicated Computers

The most obvious limitations of these small machines are their limited core memory size and their rather slow input and output devices. It is possible to use high level languages, but is usually necessary to place fairly severe restrictions on some of the features of these languages. For many purposes, especially where unusual forms of input and output are required, the use of high level language is inappropriate, and a machine oriented language must be used.

In very general terms, a program written in a machine oriented language will take longer to develop, but the resulting program will probably make more economical use of the available core memory, and will run somewhat faster than the equivalent program written in a high level language.

In spite of the rather tedious work of developing the necessary software for a small dedicated computer, it has certain quite significant advantages. The most obvious advantage is that it is immediately available, or available at short notice. With such a system, interactive data processing is possible, in which the operator or the radiologist can process or display the information in different ways, and can use his judgement to assess intermediate results. With such an arrangement, it is certain that data processing would be used in the assessment of a much broader spectrum of patients than a system which required transport of data to a distant computer for processing.

The main advantages and disadvantages of the two approaches to the data processing problem are summarised in fig. 3.1. The advantages of the small dedicated computer and the availability of such a system made this the method of choice. The data processor used for the work is described below.

	Batch-processing computer	Dedicated computer
Input medium :-	Paper tape ;cards	Paper tape
Output medium :-	Line printer (Cards and paper-tape possible)	Oscilloscope;Special displays;Teletype
Storage capacity	Large	Very limited
Programming languages	High level languages (FORTRAN, ALGOL etc)	FORTRAN possible, Machine oriented languages more usual
Availability/turn round time	Short notice Turn round time up to 24 hours	Immediate: User/ machine interactive processing possible
Effect of errors on input paper tape	Program failure	Can be corrected by operator

Figure 3.1 Advantages and disadvantages of batch processing computers versus dedicated systems

3.2 The Nuclear Data 50/50 MED System

This instrument is intended primarily for processing data from gamma camera systems, but can equally well be used for data from rectilinear scanners. An unusual feature of the machine is that it has two separate memories. The computer section has a basic memory of 4K 12 bit words which can be expanded to 8K words. There is a separate memory in the analyser section, consisting of 4K 24 bit words, which is normally used as if it consisted of 8K 12 bit words. For the latter purpose, the lower order 12 bits are considered to be separate from the upper order 12 bits; these are referred to as 'lower' and 'upper' analyser memory respectively. Most input and output devices are interfaced directly to the latter memory, and this section is used mainly for data acquisition and display. Switches are provided on the front panel of the analyser unit which permits the user to control the functions of acquisition and display off-line from the computer. All these functions can also be controlled by the computer. Having a choice of operational system is frequently an advantage when a number of instruments are interfaced to the system.

3.2.1 System Hardware

The block diagram (Fig. 3.2) shows the main components of the data processing system, as interfaced to two scanners.

The computer has a teletype and a fast paper tape reader interfaced to it. The teletype is most commonly used to control the operation of the computer. It can also be used to print out data from the computer, and to read and punch data on paper tape at a speed of 10 characters per second. The fast paper tape reader is used to read program or data tapes into the computer at a speed of 300 characters per second. This device is used to read paper tapes produced by the data logging system of the Picker Scanner.

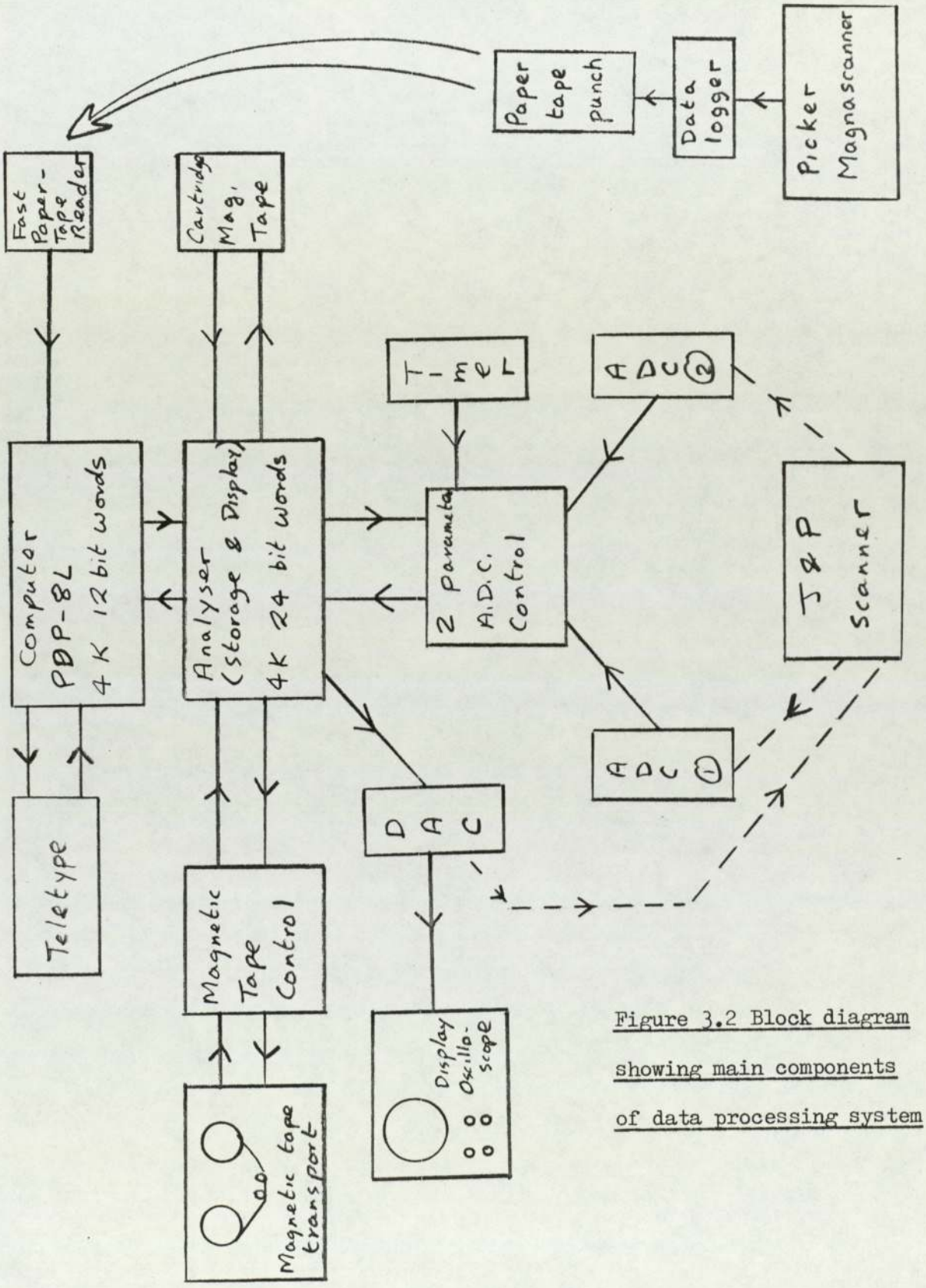

Figure 3.2 Block diagram showing main components of data processing system

The computer is interfaced to the Analyser unit, and may be operated either on-line or off-line to this device.

Input to the analyser unit is via a two channel analogue to digital conversion system. This arrangement is intended for the analysis of X and Y coordinate information from a gamma camera. It is also possible to use this system to input information from a rectilinear scanner, provided that information is presented from the scanner in an appropriate form. The method used in the case of the J & P scanner is described in section 6.2.2.

Output from the analyser unit is to a 5" oscilloscope, via a Digital to Analogue conversion system. Hardware controls allow the information to be displayed in a number of different ways, and this is a very useful feature.

A second analogue output channel may be obtained by operating the J & P Scanner on-line to the analyser section. The scanner is set up to scan in the normal way, but count rate information is derived, not from the detectors, but from the analyser memory. This is a rather slow, but high quality output mode, and will find wide application.

The analyser unit has two magnetic tape backing store systems. One is a 7 track computer compatible tape deck, which may be used for storage of either program or data. This operates on a time sharing basis with the analyser unit, and can transfer blocks of data very rapidly. A complete tape has a storage capacity of 1.6×10^7 bits of information. The other magnetic tape system is a cartridge tape device. This operates more slowly than the 7 track system and has a much more limited storage capacity. Its main use in the present project has been as a 'scratch pad' memory used for the storage of tables and intermediate values. The relatively short access time of the cartridge tape recorder makes it useful in this application.

All of the devices described above are available to the computer, when this is operated on-line to the analyser unit. Many of the peripherals, including the magnetic tape units, may also be operated independantly of the computer under manual control.

3.3 Data input programs

Use has been made of some software subroutines supplied as part of the standard package. These deal mainly with input and output of alphanumeric information and a floating point arithmetic package. The data input procedure is described below in broad outline. Reference should be made to the flow diagrams given in the appendix.

After starting the computer manually, the program goes into a loop, in which the computer awaits a keyboard instruction. The entry of data is initiated by typing the characters 'HE' followed by the key ALT. The computer echoes 'LLO' and then proceeds to wind on the seven track magnetic tape to the end of the last legal record, and to clear the first 64 channels of the storage and display unit memory in preparation for writing the patient identification data. These identification data are only written once, for each patient. All views on the same patient are labelled with the same identifier, apart from certain characters that identify the view and the type of information.

After clearing the registers, the computer types "NAME and NUMBER" at which point the patient details are entered, then types "MACHINE?" If the Picker Magnascanner is used data are entered off line using the fast paper tape reader. If the J & P Scanner is used data are entered on-line, through the analyser section. Having specified which machine is to be used, the computer clears the memory bank of the analyser (with the exception of the first 64 channels) in preparation for entering the data. The machine then types "P.TAPE GO?" and awaits a response before proceeding with the reading in the data. If the response is in the negative a subroutine will be entered which permits data to be read from the magnetic tape.

If the response is positive, the computer expects input to be via the high-speed paper tape reader, and will modify two instructions in the floating point input program to allow this method of data input to be used.

Having received the appropriate command, the fast paper tape reader reads blank tape until the first character is encounted. The computer expects this to be the character '>' or binary 1111 in 4 track character code as output by the scanner control module. If this is not the first character encountered the computer prints the illegal character, and continues its search for > . Any character on the tape before > will be printed to help in identifying the fault.

The character following > will be either ; (binary 1101) or : (binary 1100). The character ; specifies that the character string is the name of a projection . Character : is used for identifying a particular anatomical point or a beginning of line symbol. The scanner operator is expected to identify the projection being scanned before entering data on the location of the anatomical points. Failure to do so will cause an error condition, although it is possible by operator intervention in the processing to overide this.

After the computer has read the character ';', the next character is decoded to identify the projection, either antero-posterior, postero-anterior, left lateral or right lateral. This is typed out on the teletype. The computer also opens a number of registers, depending upon the particular anatomical points which have to be entered for each projections. For example if a left lateral projection is being scanned the computer expects data for the left external auditory meatus, and the nasion. Only these two registers will be opened. As the data for the location of the anatomical points are entered the computer checks that the points have been correctly specified.

After reading in the character string which identifies the projection being scanned, the tape is searched for the end of data block symbol. Although coordinate data will be punched on the tape following the projection identifier these are meaningless and will be ignored by the computer.

The character strings which identify the various anatomical points, together with the x and y coordinates of these points are read next. The coordinates are stored in predetermined locations in the lower data frame first profile. (As the memory contents are usually displayed as a 64 x 64 matrix, a 'row' of 64 locations is usually referred to as a 'profile'). The name of the point and the x and y coordinates are typed by the computer.

After the anatomical point data have been read from the tape the next character string should be the beginning of line symbol. When this is encountered for the first time on the tape the computer checks that all the necessary basic data have been entered. If they have the computer proceeds to read the tape. If not, the computer prints out "Insufficient Data" and terminates the program.

Assuming that all the initial data have been correctly entered the computer reads the data tape until blank tape is encountered, which indicates the end of the data for that projection.

Data are entered in blocks. Each block contains a number representing an x coordinate, followed by a space and a second number representing count rate. The computer checks that each block is correctly formatted and contains no illegal characters before storing the information in the appropriate memory locations. If an error is found, an error number is printed and the computer stops to allow the operator to take corrective action.

Storage of the data starts in the third profile. When the beginning of line symbol is encountered, the profile counter is incremented and the resulting binary number is multiplied by 2^6 to form the starting address of the next line of data. The y coordinate appears only in the beginning-of-line data block. This is stored in the first profile of upper memory. Counts are stored in addresses 128-4095 of lower memory, and x coordinate data in addresses 128-4095 of upper memory.

After entering the data from paper tape, the computer types M.T. STORE? If the ALT key is pressed (equivalent to a 'Yes' reply) the computer checks that the tape is correctly positioned, and verifies the record number of the last record. It then prints out, for example TAG = 46 GO TO. The tag referred to is the record number of the new record. If this is correct, pressing the ALT key will write the data stored in memory onto magnetic tape. If the record number is not the desired record, the correct number can be entered, and after finding the specified record on the tape, data stored in the memory will be written onto the tape to replace the previously existing record.

After writing the record onto magnetic tape the computer prints out "PRINT?" This allows the record to be printed out on the teletype, a rather lengthy procedure. If printing is required, the sequence is initiated by typing ALT. The computer then prints "FRAME". Lower or upper memory can be printed out by typing 1 or 2 respectively. If ALT is typed, both frames are printed out. Now the computer prints LIMITS X = Y = and the appropriate print limits can be entered, terminating the number each time by typing ALT. The computer then proceeds to type out the required data. As the line length on the teletype is insufficient to print out a complete profile, the profile is typed in sections consisting of sixteen cells, plus an extra cell which appears also on the next section, to assist in lining up the sections after printing. Each section is headed by the patient identifier, followed by SECTION N to identify the section.

After completing the printout sequence, the computer types "PROCESS?" This forms a link with later sections of the program which enable processing to be carried out on data held in the memory. The normal reply to this is 'No' and the computer then writes an extra record onto the magnetic tape. This allows space for processed information to be stored on tape, if required, at a later stage.

The computer then prints "NEXT VIEW?" If a positive reply is received, indicating that more views for the same patient are to be entered, the program returns to the paper tape input procedure and prints out "P.TAPE GO?" If the reply is in the negative, an asterisk is printed, and the program must be re-entered by typing 'HELLO'.

An example of a complete data entry sequence of instructions is given below. Underlined characters are those entered manually. The symbols + and = represent 'Yes' (or 'ALT') and 'No' responses and do not appear on the printout.

```
*

HE + LLO
NAME SMITH, JOHN +          NUMBER 74/1234 +
MACHINE PI + CKER
P.TAPE GO? +

M.T. STORE? + YES
TAG = 46 GO TO +
PRINT? =
PROCESS? =
NEXT VIEW? =

*
```

It is necessary to store a considerable number of records in this way, in order to establish a data base to permit the development of methods for scan normalisation and data analysis. These developments will be described in the next chapter.

CHAPTER 4

Normalisation of patient scan data

4.1. Analysis of Count Rate Patterns

One objective of data analysis of count rate patterns is to attempt to define a "normal" pattern of uptake against which any individual patient scan can be compared in the search for abnormal regions of uptake. Previous work along these lines has been described by Popham et.al. (1970), Dowsett and Perry (1970) and Griver et.al. (1976).

The usual way in which to attempt the derivation of a "standard" pattern of uptake is to take a number of individual patient scans which are judged to be visually normal, and in which subsequent investigation has shown that no focal lesion exists. These normal scans are combined to form a standard scan.

Patient to patient variation is of two types. There is the normal statistical variation of the count rate within the scan caused by the random nature of the radioisotope decay processes. There can also be expected to be patient-to-patient variation due to differences in normal anatomy and physiology. If a large number of patient scans are averaged the statistical variation due to radiation emission can be expected to cancel out. That due to patient-to-patient anatomical variation will remain.

Before individual patient scans can be combined into a 'standard' scan, they must usually be normalised in some way. There are two aspects of this:-

(a) Sorting of individual patient data into groups having similar head size and shape.

(b) "Normalising" the count rates to conform to some specified standard.

4.1.1. Normalising The Anatomical Features Of The Individual Patient Scan

The most obvious feature on a normal brain scan obtained with sodium pertechnetate is the skull outline. It is therefore natural to group together patient scans with similarly sized skull outlines, and this is the approach adopted by previous workers. The disadvantage of this approach is that it places a very severe restriction on the number of scans that can be combined into a standard, as it necessarily implies that a number of standard scans will be required. The number of proven normal scans is in any case rather small, as isotope brain scanning is frequently undertaken as an out-patient procedure, and those out-patients which have a visually normal scan are often not investigated further. Within this group, a small number will be false-negatives. It is usual, therefore, to include in the analysis only those patients having normal scans which have been shown, on further and often exhaustive investigation, to have conditions which could not be expected to show focal concentrations of isotope.

Because of the relative paucity of proven normal material, it was decided to attempt to combine all proven normal scans into a single standard scan. For this approach to be successful, all skull outlines must be made to conform to a specified standard. Some modification of the spatial co-ordinate data of individual scans is required, but this should in no way alter the internal consistency of the information, so no information of diagnostic significance will be lost, other than the ability to take absolute measurements of distances or size of features within the scan. As an "average" shape is used as the standard, and the variation in size and shape of adult heads is quite small, any expansion or contraction in the spatial coordinates is modest.

Although this technique does not appear to have been used previously in regard to radioisotope images of the brain, a parallel technique has been described by du Boulay (1973) in which skull radiographs were projected optically onto a standard outline.

The normalisation of head sizes to conform to a single standard can be expected to have other advantages. Regions of anatomical interest can be defined by a single set of coordinates, so automatic searches of the data could be conducted to identify, for example, all lesions falling within the territory of a particular cerebral artery. One application of this technique will be described later.

4.1.2. Normalisation of Count Rate Data

Most previous attempts at the production of a composite "standard" scan have adjusted the total number of counts recorded during a brain scan to a certain value by multiplying the counts in each cell by an appropriate factor. This procedure is reasonably valid for a ^{197}Hg scan, but a number of problems arise when sodium pertechnetate is used.

Normal brain does not take up the pertechnetate ion. The countrates recorded over normal brain tissue are relatively low, and arise from activity remaining in circulation, and activity in vascular structures such as the scalp. On most brain scans, vascular structures exterior to the skull are visible, notably structures below the base of the brain, and these structures contain a high proportion of the total counts recorded. If an abnormality occurs within the brain, especially a large tumour or infarct, high counting rates are recorded and again a significant proportion of the total counts may be recorded over the area of the abnormality. Attempts to scale the total counts to a specified number may then only serve to reduce the counts over the normal

brain to a lower than normal value, and so reduce the amount by which the count rate over the abnormality differs from the count rate over the equivalent area on the standard scan.

In an attempt to overcome these problems, it was decided to 'normalise' the count rate pattern by reference to the areas of normal brain tissue. It is extremely unusual for the area of an abnormality to be greater than the integrated area of normal brain tissue. If the count rates recorded in each cell are sorted into groups depending upon the count rate value, a histogram can be produced, and it can be expected that the relatively low count rate values due to the relatively large areas of normal brain will predominate. Such a count rate histogram is given in fig. 4.1 for a brain scan which was judged to be visually normal, and in fig. 4.2 for a scan which contained a large abnormality. In both cases, there is a peak at low count rates, representing count rates recorded over areas of normal brain tissue. Histograms of this type are useful in normalising count rate values, and have some other interesting features which it may be possible to exploit.

4.2. Data Processing of Scan Image Files

Data files are stored on 7 track magnetic tape by the data input programs. In order to process particular scan images, the appropriate files are read from magnetic tape by a READ Command typed on the teletype keyboard. The computer response to this is to read the file number of the record at which the magnetic tape is currently positioned, type this on the teletype and to ask which file number is required. The required file number is entered by the operator, unless the current file number is the one required, in which case the ALT key is pressed. The computer then searches the tape for the appropriate file, and when

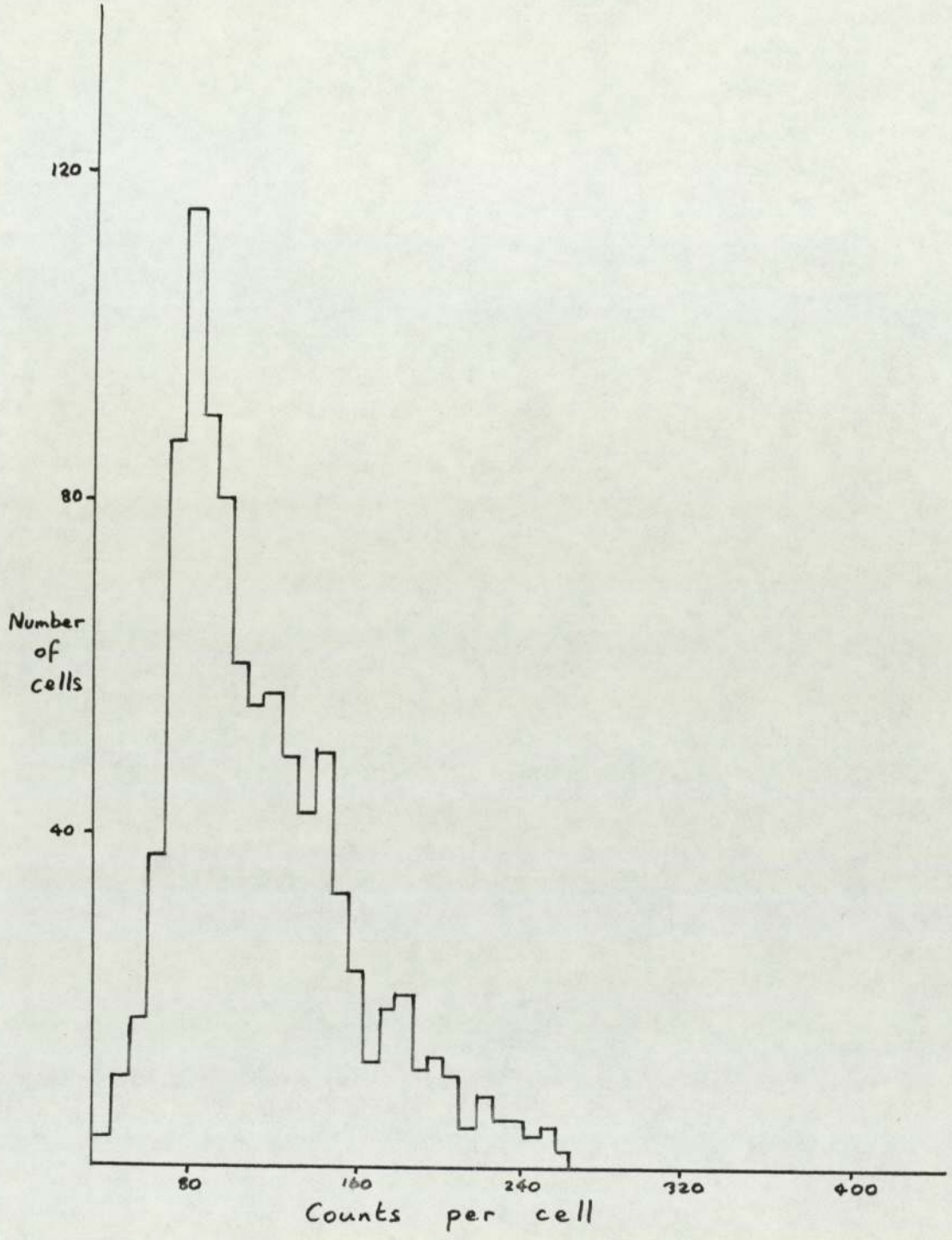

Figure 4.1 Count rate histogram. Lateral view. No abnormality detected.

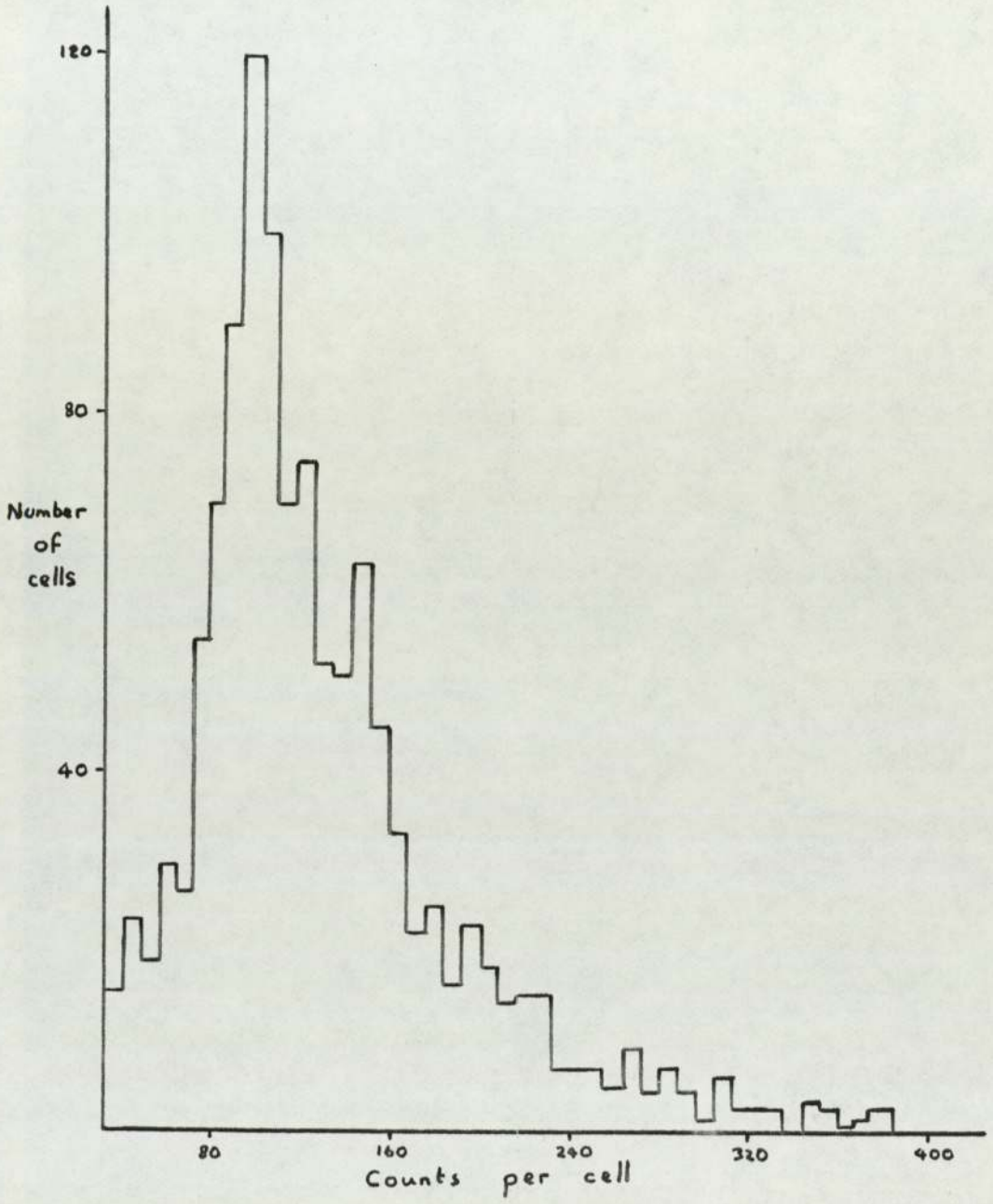

Figure 4.2 Count rate histogram. Lateral view. Large malignant tumour.

this is found, types the file number followed by the patient's name, reference number, and the type of projection. The programs used to perform this operation are slightly modified versions of the standard Nuclear Data programs supplied with the system. The computer then prints an asterisk to indicate that it is awaiting further instructions. The data analysis and normalisation program is started by means of the operator entered command GO (ALT) typed on the keyboard.

4.2.1. Initial Checks To Determine Suitability Of Data For Analysis

Data having been entered into the storage and display unit by the READ command, the computer reads the X and Y coordinates of the anatomical reference points, and the name of the projection. If the projection is antero-posterior (A.P.), three sets of anatomical point data are read in, these being the position of the nasion and the left and right external auditory meati (EAM's). For any other projection only two of these anatomical points will be visible and hence only two sets of anatomical point coordinates will be read in.

The Y values are first examined to see if any serious rotation of the projection is present. The two Y values (or the Y values for the EAM's in the case of the A.P. projection) are examined to see if they agree to within $\pm$ the average cell size. In the case of the lateral projections, the Y values must agree to within $\pm \frac{1}{2}$ cell size, only one of the anatomical points lies on the skull outline, and the other (the EAM) lies roughly in the centre of the skull diameter. If these conditions are not satisfied, the computer prints out "ROTATION" followed by the sense and the amount of the discrepancy between the Y values, It is possible to recover from this error condition by rotating the data in the frame by the appropriate amount about the EAM in the case of the lateral views, and about the midpoint of the line joining the EAM's in the case of the sagittal views.

The computer then checks to see that the profile containing the radiological base line is present in the data. If not (i.e. the scan has been started too high) the computer prints out BASELINE - N, where N is the number of units by which the Y values of the first scan line lie above the radiological base line.

Having made these basic checks using the anatomical point data, the computer checks the X data stored in frame 2. Reading along the line, X data should steadily increase. In fact, because of a synchronisation problem of the data logging system, occasional X values are erroneous. These are corrected, normally, by interpolation between the two adjacent values. However, where an error occurs at the beginning or end of the line, the correct X value is obtained by extrapolation.

4.2.2. The Count-Rate Histogram

After correcting the count rates in each cell for non-uniform scan speed, the populations of cells in successive count rate intervals of eight were determined. From these data, histograms could be plotted. As expected, these showed a peak in the low count region, as the area of normal brain tissue, exhibiting relatively low count rates, should predominate. Even where a large abnormality exists remarkably little difference is noted. Although quite a high proportion of the total counts will be concentrated into such an area, the number of cells involved will be quite small. For example, an abnormal area 4 cms in diameter will only contain about 6% of the total number of cells within the scan. Large focal abnormalities do not therefore distort the histogram to an appreciable extent, although the 'tail' of the histogram in the high count region may be extended.

On plotting out a number of histograms for both normal and

abnormal cases, a small number of cases were found in which the count rate histogram differed strikingly from the normal pattern. Two examples of count rate histograms derived from lateral projections are given in fig. 4.3. and 4.4.

Fig. 4.3 is a histogram of a patient with a large subdural haematoma. This is normally recognised by a marked assymettry on the A.P. and P.A. projections, but usually little or no focal concentration of isotope is noted on the lateral views. The count rate histogram does show, however that the count rate pattern may be grossly abnormal in the lateral projection in such a case. The controls of the scanner are normally set so that the background cut-off to the display circuits is such that only count rates higher than the average found on a manual search over normally 'cold' areas of the brain are displayed. If a large, but non-focal abnormality exists (such as a subdural haematoma in lateral projection) this will not normally be imaged.

Fig. 4.4. is a case of extensive Pagets disease of the skull. Once again, the lesion gives a relatively high count over a large area of the scan, and the histogram is broad and diffuse.

The height of the histogram peak was calculated for 120 patients. Only five exhibited a count rate peak less than 70 cells in height on both lateral projections. Of these five, two were cases of subdural haematoma, and one of extensive Paget's disease of the skull. There were five cases of subdural haematoma where the peak was greater than 70 cells on at least one lateral projection. The finding of a low maximum in the count rate histogram of a patient scan obviously has some significance in supporting a diagnosis of subdural haematoma or extensive skull disease. It is possible that a more detailed analysis of the histogram patterns would be rewarding this respect.

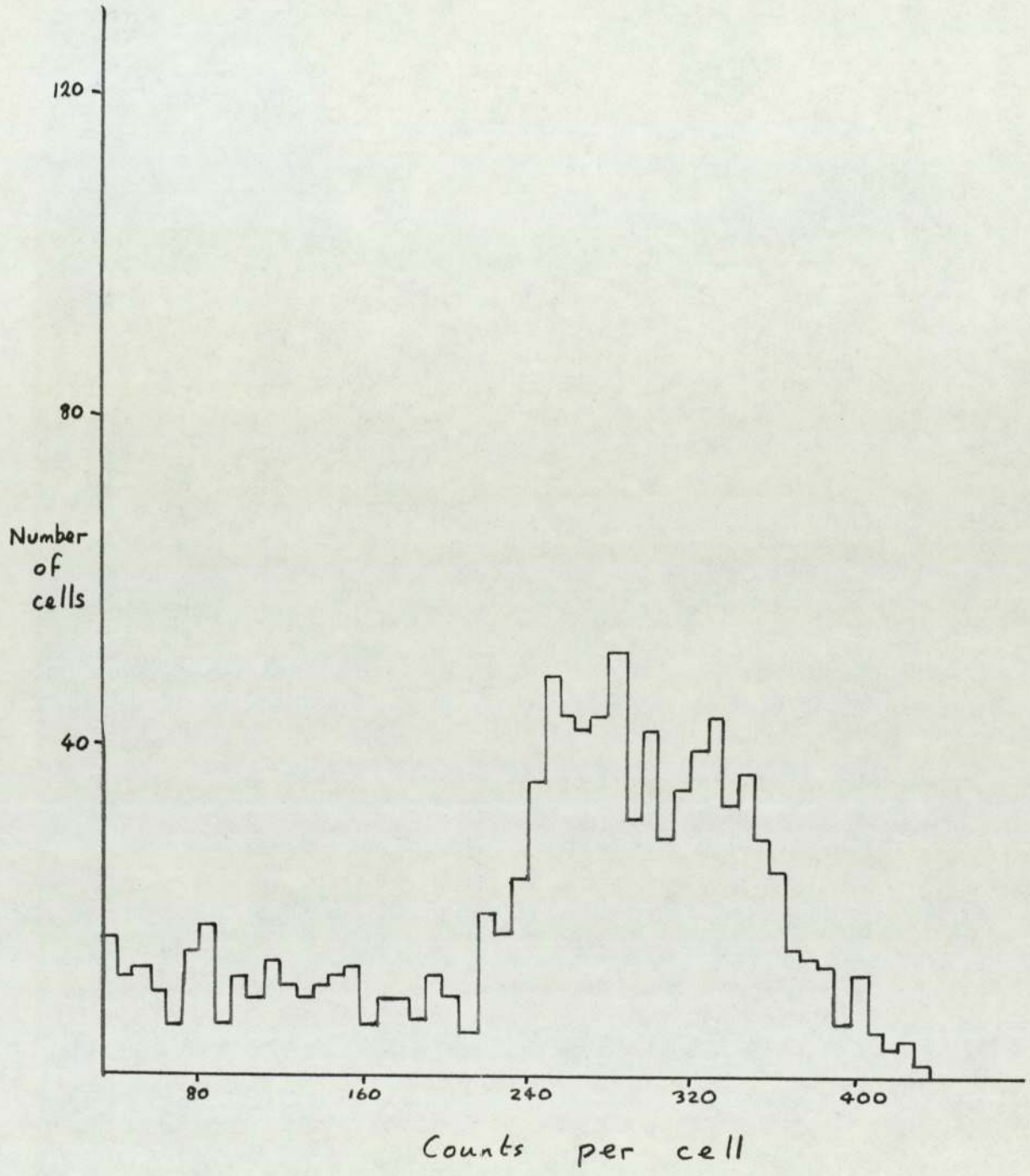

Figure 4.3 Count rate histogram. Lateral view. Extensive subdural haematoma.

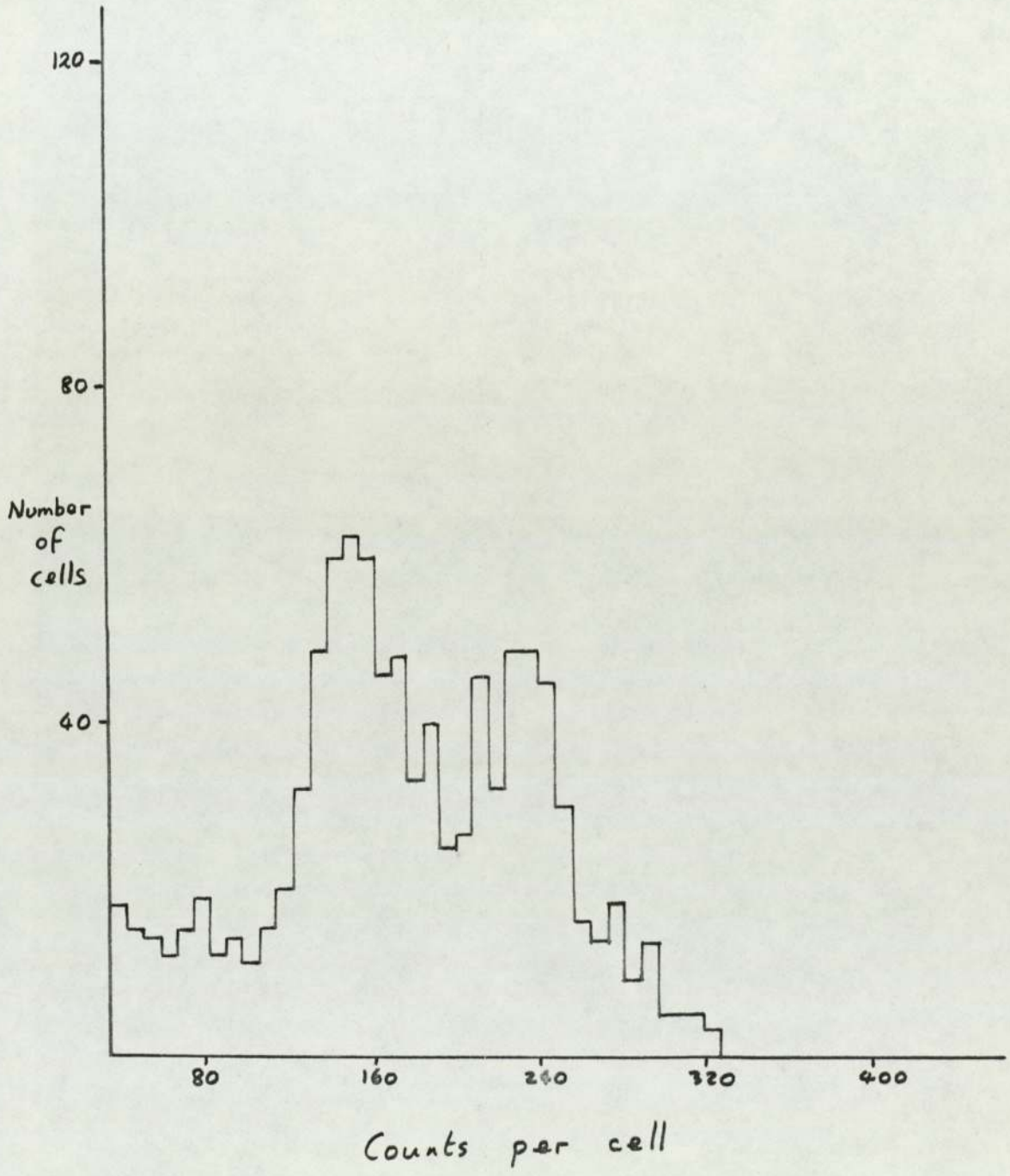

Figure 4.4 Count rate histogram. Lateral view. A case of Paget's disease of the skull.

Aside from the incidental finding mentioned above, it was found that the vast majority of scans exhibited a count-rate histogram in which a single well defined peak occured at low count rates. Analysis of over 500 scans showed that this occurred most commonly at a count rate between 104 and 112 counts per cell. In each case, therefore, the position of the maximum of the histogram was determined, and all the count rate data were modified by a factor designed to shift the maximum into this count range. This procedure cannot be expected to produce properly normalised count rate patterns where the histograms are unusually diffuse, and in cases where the maximum of the count rate histogram is less than 70 cells an appropriate error message is output and no further analysis is undertaken. The histogram can then be plotted out from the values held in a buffer area of the computer memory.

4.3 Normalisation Of Spatial Coordinate Data

The count rate data obtained after normalisation are searched to find the first and last cells in each line containing count rates higher than 64. Having identified these cells, the corresponding X coordinate data are read and these, together with the differences in X values (L) are stored in a buffer area.

The line length data are searched to find all lines within about $\pm$ 5 mm of the length of the line containing the radiological baseline. These lengths are averaged, as are the left-most X coordinates (X min) for these lines, to give $\bar{L}$. The mean length of the scan baseline was thus established, and was printed out.

It is also necessary to find the height of the vertex above the baseline. The best way of establishing a figure which could be used consistently for standardising the spatial coordinates was to find the

line in which $L_n = \frac{L}{2}$. The difference between the Y coordinates for the two lines gives the vertex height. (The actual vertex will be a line or two higher, but the point at which the operator judged the scan to have finished varied considerably from scan to scan).

Analysis of the data for baseline length and vertex height gave a mean ratio of 1.45 : 1 for the two sets of values. It was therefore decided to adopt a standard frame of reference 39 cells wide and 27 cells from the baseline to the vertex as defined above. The actual frame will be larger than this, as there are data below the radiological baseline, and also some data above the vertex as defined.

The scan data were now projected into the new coordinate system. The origin of the new coordinate system was taken as the interception of the X_{min} value and the baseline Y value. The X and Y increment values were calculated by dividing the baseline length by 39 and the vertex height value for an individual scan by 27. The coordinates of any point in the new frame of reference could thus be established, and the count rate value for that point was calculated by interpolation from the surrounding four points in the original data frame. Thus a normalised scan was obtained in which both count rate values and spatial coordinate values conformed to a certain specified standard. Apart from its obvious use in deriving a composite normal scan, individual normalised scans were useful in the semi-automatic analysis of certain variations in normal anatomy.

4.4 Use of normalised scan data to establish patterns of isotope uptake in the choroid plexus region

It has already been noted that normal brain tissue does not take up the pertechnetate ion from the bloodstream. Certain highly vascular structures in and around the brain do, however, contain higher

concentrations of the ion than would be expected in the main mass of the brain and therefore show as areas of higher than average activity. Structures which show up in this way include the venous sinuses, and the choroid plexi. The venous sinuses are situated peripherally, and activity in these does not usually obscure lesions in the brain, but the choroid plexi, located within the ventricles, may be mistaken for lesions, or may make the interpretation of the scan difficult.

When sodium pertechnetate is used as radio-pharmaceutical, it has become an almost universal practice to adminster oral potassium perchlorate prior to injection of the isotope, to act as a thyroid blocking agent. The pertechnetate ion concentrates in the normally functioning thyroid gland, and if the perchlorate is not given, unnecessary radiation exposure to this organ results. It was found that administration of perchlorate also had the effect of preventing concentration of the isotope by the choroid plexus, without, apparently, affecting the uptake in lesions of the brain (Barfield and Holmes, 1967). The dosage of potassium perchlorate varies widely at different centres but 200 m.g. orally appears to be a fairly well accepted dose. There were however some situations in which the adminstration of the premedication by the oral route was most inconvenient. These were, firstly, in the case of the seriously ill or unconscious patient, in which oral administration was at best difficult, and at worst impossible. Secondly, oral adminstration to out-patients prolonged the waiting time, as normally half an hour was allowed to elapse to permit absorption of the potassium perchlorate before isotope was injected intravenously. Because of these disadvantages of the oral route, a trial was conducted to test the effect of administration of 10 m.g. sodium perchlorate intravenously. Analysis of scan data was undertaken to determined if the sodium perchlorate

adminstered at the time of the isotope injection was as efficient as 200 m.g. oral potassium perchlorate as a choriod plexus blocking agent.

A number of scans reported as being visually normal were presented to an experienced observer, and he was asked to report on the visibility or otherwise of the choroid plexus. As choroid plexus activity is a normal variant of the isotope brain scan, activity in this region is not normally remarked upon in the scan reports. A small number of these normal scans were reported as showing different degrees of choroid plexus activity.

On a second occasion, a number of normal scans were reviewed. Without the knowledge of the radiologist, those scans from the first series which were reported as showing choroid plexus activity were included in the second series, and the rsults on these scans were compared.

In some cases scans reported as showing choroid plexus activity on the first occasion, were reported similarly on the second occasion. However a number of scans reported as showing some choroid plexus activity on the first occasion were reported as normal on the second occasion.

This exercise suggested that a more objective means of assessing choroid plexus activity was required.

4.4.1. Objective Assessment of Choroid Plexus Activity by Area of Interest Analysis

The area of interest analysis program may be called as a subroutine from the main scan normalisation program. Areas of any shape may be specified by a table of cell addresses.

For this particular application, the mean count rate in the area in which choroid plexus activity is most usually seen was compared with a similarly sized area in the frontal lobe. The areas chosen for comparison are shown in Fig. 4.5. Both areas are rectangular, of size 8 x 5 cells,

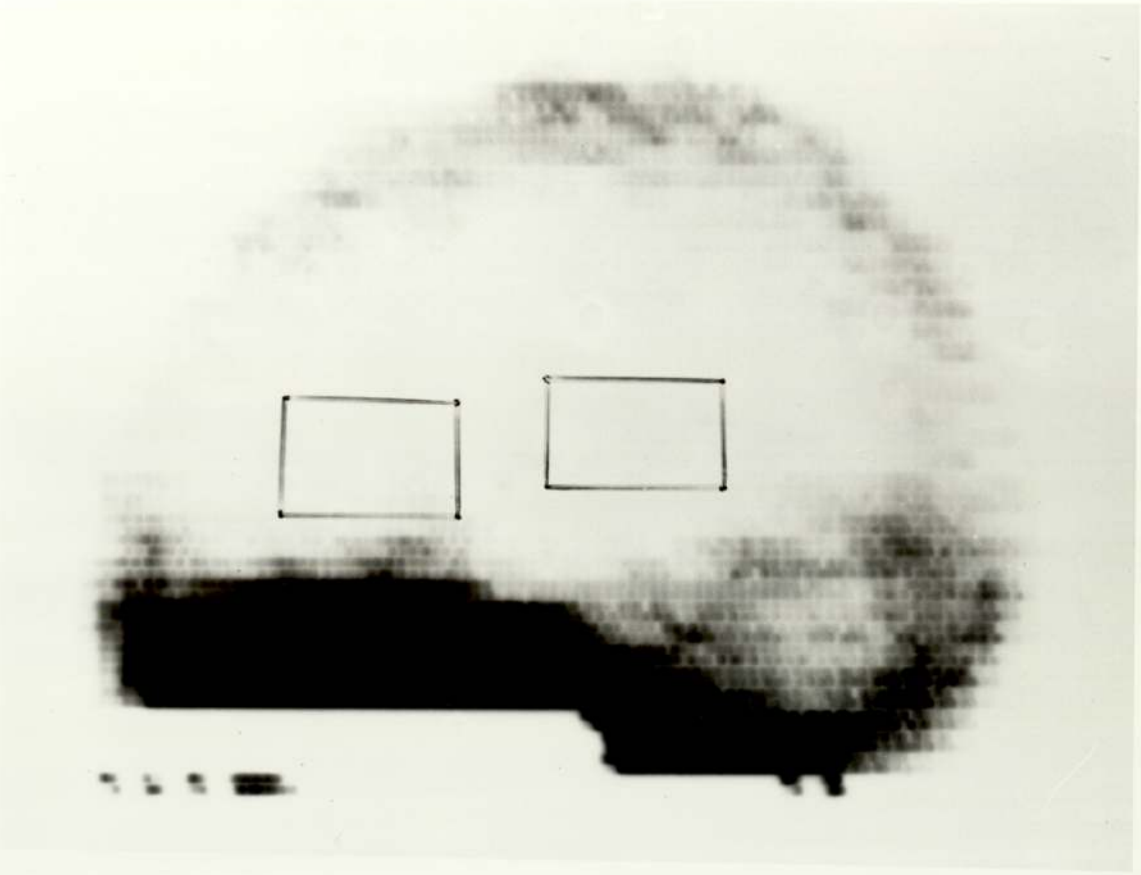

Figure 4.5 Computer generated scan image showing areas of interest used in the evaluation of choroid plexus activity.

i.e. approximately 32 x 20 mm.

The subroutine looks up the cell addresses in a table, extracts each count rate value Cn from the normalised data stored in the 50/50 storage and display unit frame 1 and converts the binary value to floating point format. The values ΣCn and $\Sigma (Cn)^2$ are calculated and stored, also in floating point format.

When all values in the area of interest table have been referenced the mean count rate $\Sigma Cn/N$ is calculated, and the standard deviation S is computed using the expression:

$$S = \sqrt{\frac{\Sigma (Cn)^2 - \frac{(\Sigma Cn)^2}{N}}{N-1}} \qquad \ldots(4.1)$$

The values for mean count rate and standard deviation for area 1 are printed out, and the corresponding values for area 2 are then computed and printed.

Area of interest analysis was carried out on fifty cases in which the patient had received oral potassium perchlorate (200 mg.) as premedication, and in a further fifty cases in which 10 mg. sodium perchlorate had been administered intravenously.

For each case, the ratio of the mean count rate in the choroid plexus region to that in the comparison region was formed. In the case of the 50 results obtained with intavenous sodium perchlorate, the mean ratio R_{Na} was found to be 1.0042 with a variance of 3.6799×10^{-3}, giving a standard error on the mean of 0.0087

i.e. $$\overline{R_{Na}} = 1.0042 \pm 0.0087$$

For the cases receiving 200 mg. potassium perchlorate prior to injection, the mean ratio $\overline{R_K}$ was 0.9889, the variance was 6.4631 x 10^{-3} and the standard error on the mean was 0.0115.

To assess the significance of the difference in the mean ratio between the two agents, a 'Student t-test' was applied. The value of t is 1.074 which gives p = 0.3, i.e. the difference is not significant. If there is a real difference it is too small to be demonstrated in samples of this size.

The significance of the variance in the two series was also tested. The variance ratio test gave a value of p of about 0.05. This is more nearly a significant difference, and may indicate that the oral potassium perchlorate has a more variable effect on individuals. This would occasion no surprise, as the efficiency with which the oral agent is absorbed from the alimentary tract to the bloodstream is almost certain to vary between individuals, and the time lapse between administration of the premedication and adminstration of the isotope is probably also of some importance.

As no significant difference between the mean ratios of the mean count rates in the two areas of interest using the two agents was demonstrated, it was considered that no account need be taken of the premedication used in selecting material for deriving an accumulated normal count rate pattern. The methods by which this pattern was obtained will be described in the next chapter.

CHAPTER 5

The derivation and use of composite normal scan images

5.1 Computation of the Composite Normal Scan from Normalised Patient Data.

Having developed methods of normalising individual patient data as described in the previous chapter, it was now necessary to combine these data into composite normal patterns to permit comparison with further individual patient data. This comparison will highlight areas of abnormal uptake, and should permit a quantitative assessment of the degree of departure from the expected pattern of uptake. In effect, for each projection, two composite normal patterns were required. These were, firstly, the mean nomalised counting rate and secondly, a pattern consisting of the calculated standard deviations of the individual points in the composite pattern. The standard deviations will be greater than those which would arise merely from the effect of the statistical nature of the radiation emission, as normal anatomical and physiological variation will also play a part.

As previously described, individual patient scan data are stored on magnetic tape files and are read into the memory of the 50/50 storage and display system for normalisation. This read cycle is destructive, i.e., any data already in the 50/50 storage and display memory is overwritten and therefore magnetic tape cannot be used as an input medium in building up composite patterns. It was decided to punch onto paper tape those normalised patterns from which the composite normal pattern was to be derived. These records could then be read back into the 50/50 memory on a point by point basis, and the appropriate arithmetic could then be performed on the data points.

The standard deviation, σ_t , can be derived from the individual data points, C_i , using either of the equivalent expressions:

$$\sigma_t = \sqrt{\frac{\Sigma(C_i - N)^2}{n-1}} \qquad \ldots\ (5.1)$$

or,

$$\sigma_t = \sqrt{\frac{\Sigma C_i^2 - (\Sigma C_i)^2/n}{n-1}} \qquad \ldots\ (5.2)$$

Where N= mean value of an element

n= number of patterns contributing to this element.

Use of the second expression is attractive, as it does not require prior knowledge of the mean value, N. In principle tables could be stored of $\Sigma(C_i)^2$, ΣC_i and n from which both the mean and the standard deviation could be derived.

Unfortunately, due to the very limited memory space of the 50/50 system, it was impossible to implement this algorithm. The total storage space available for data was only 12K words, and a typical normalised lateral scan contained up to 1350 data points, organised within a 40 x 64 matrix. Within the normalised count rate patterns, some cells will contain count rates in excess of 300, and the count capacity of a 12 bit word may be exceeded for $n > 14$. It is therefore necessary to use double precision arithmetic for storing ΣC_i and treble precision (or floating point arithmetic) for storing $\Sigma(C_i)^2$.

It was therefore decided to implement expression 5.1 using a two pass system. On the first pass, tables of ΣC_i and n are stored from which N are calculated, and a second pass computes a table of $\Sigma (C_i - N)^2$ from the input data and the stored values of N from which values for the standard deviation will be calculated on completion of the second pass.

The value of n will not necessarily be the same for all

points in the composite pattern. The setting of the scan limit switches depends upon the judgement of the operator, and precisely the same area will not be scanned in every case. It would be unwise however, to exclude a data point from the composite merely because data were not present from this area in every scan. Some useful data from peripheral regions, especially in the posterior fossa region may be derived from a smaller number of records than the number available in the more central regions of the scan.

In the first pass, tables of ΣC_i and n were calculated. ΣC_i data were stored in bits 0-17 of the 24 bit word of the 50/50 memory (giving a number range of 0 - 262,143) and n was stored in bits 18 - 23. It was clearly inadvisable to compute the mean where n was very small, as the mean was likely to be inaccurate. Therefore, on completion of the first pass, means were calculated for data points where $n \geq 8$. This also served to limit the total number of data points to a value less than one third of the total available memory words, thus allowing a table of $\Sigma (C_i - N)^2$ to be stored in floating point format in a single memory field. Values of data points where $n < 8$ were deleted from the record on the completion of pass 1.

The tapes were then read in a second time, and for each non-zero data point the deviation was calculated and stored in floating point format in sequential locations in field 1. On completion of this pass, the standard deviation of all data points were calculated, and these values, converted to single precision binary numbers, were stored in sequence in the higher unused addresses of frame 0. Values for the standard deviation were stored in bits 0 - 7 of these memory words, leaving bits 8-11 for the storage of n values. In this way, tables of mean values, standard deviation, and n could be accomodated within a single memory field. Finally, a paper tape of these

values was punched. This was later used to enter these values into memory field 1 of the computer as part of the 'compare' program.

Three composite normal patterns were calculated by the above method, for left and right lateral projections and the A.P. projection. If required, these data may be stored as records on the cartridge tape recorder of the 50/50 system, and input as required into field 1 of the computer for purposes of comparison with patient scan data. Each pattern was a composite of between 11 and 14 scans.

5.1.1 The Variance of the Composite Normal Scan Data

The standard deviation values obtained as above represent the observed variance in a series of proven normal patient scans. This variance is made up of two elements, one being the contribution from the finite number of counts in each element, and the other being related to the patient- to- patient variation. As the scans have been normalised with respect to the low count rate areas over the cerebral hemispheres, the patient-to-patient variance over these areas should be small, but appreciable patient-to-patient variance may be expected in the peripheral regions, due to real differences in uptake between individuals, anatomical variations such as the intensity of radioisotope concentration in the venous sinuses, and due to differences in head shape. If σ_t^2 is the total observed variance from the sampling error of the counts, and σ_p^2 is the patient to patient variance, then:

$$\sigma_t^2 = \sigma_c^2 + \sigma_p^2 \qquad \ldots\ (5.3)$$

σ_c^2 can be obtained from a knowledge of the count rates in the original scans making up the composite normal, since $\sigma_{ci}^2 = C_i$ where C_i is the un-normalised count rate of an element in the i th

scan, and σ_{ci}^2 is the variance of this element due to the stochastic nature of the radioisotope decay.

A complication is introduced into the calculation by the fact that the individual scan count rates are normalised. The mean count rate for an element is N where

$$N = \frac{\sum k_i C_i}{n} \qquad \ldots\ (5.4)$$

the term k_i being a normalisation factor. Values for k_i in a series of scans are distributed around unity, and their differences from unity are generally small. It would be expected, therefore, in a large series, that σ_c^2 would approximately equal N, and it may be permissible to use the approximate expression

$$\sigma_c^2 = N \qquad \ldots\ (5.5)$$

rather than the strictly more accurate expression for the average variance

$$\sigma_c^2 = \frac{\sum C_i}{n} \qquad \ldots\ (5.6)$$

Taking the left lateral composite normal scan as an example, σ_c^2 was computed using both expressions. It was found that the normalisation factors for the scans in this series varied between 0.57 and 1.3. The two tables for average count rate variance were compared, and it was found that expression 5.5 tended to slightly underestimate the variance. The difference was, however, very small and was nowhere greater than 5% of the mean count rate. It was therefore decided that use of the approximate expression given in equation 5.5 was justified.

Substituting into equation 5.3. the normal patient to patient variance may now be expressed as

$$\sigma_p^2 = \sigma_t^2 - N \qquad \ldots\ (5.7)$$

Using equation 5.7, plots of patient to patient variance were computed. It was found that in the periphery and posterior fossa, as expected, patient to patient variance was relatively large, at about 15 - 20% of the mean count rate. In the cerebral hemispheres, patient to patient variance was small, in the order of 5% of the mean count rate.

5.2 Comparison of Individual Patient Scan Data with the Composite Normal pattern

In this retrospective study, patient scan data were read from magnetic tape and normalised in the usual way, the result being stored in frame 1 of the 50/50 memory. The normalised patient record is then subtracted, point by point, from the composite normal pattern, the modulus of the result being stored in frame 2.

The significance of any difference found must be assessed in terms of the combined variance of the two count rates, i.e. as

$$\sigma_D^2 = \sigma_{cp}^2 + \sigma_p^2 + \sigma_t^2/n \qquad \ldots\ (5.8)$$

where $\sigma_{cp}^2 = C_p$ and C_p is the un-normalised count rate for the element under consideration. When the count rate data are normalised,

$$P = kC_p \qquad \ldots\ (5.9)$$

where k is a normalisation factor, and P is the normalised individual patient count rate. The standard deviation σ_{cp} of the count rate

value is also increased by the factor k, and the variance becomes

$$\sigma_{cp}^2 = k^2 C_p \qquad \ldots\ (5.10)$$

Substituting from equation 5.9,

$$\sigma_{cp}^2 = kP \qquad \ldots\ (5.11)$$

It is now possible to express the difference between the individual patient data and the composite normal data as a number of standard deviations from the expected value, i.e. as

$$D = \frac{P - N}{\sqrt{(\sigma_{cp}^2 + \sigma_p^2 + \sigma_t^2/n)}} \qquad \ldots\ (5.12)$$

Substituting from equations 5.3, 5.5, and 5.11 this becomes,

$$D = \frac{P - N}{\sqrt{kP + (\sigma_t^2 - N) + \sigma_t^2/n}} \qquad \ldots\ (5.13)$$

which may be simplified to

$$D = \frac{P - N}{\sqrt{kP - N + (n-1)\sigma_t^2/n}} \qquad \ldots\ (5.14)$$

an expression which closely resembles that used by Popham, Bull and Emery (1970). Values of D were calculated using expression 5.14 and printed out on the teleprinter. The symbol used in the printout is obtained by reference to a lookup table such that values of $|D| < 2$ were indicated by a dot. This threshold can readily be altered by changing a single value in the lookup table.

5.2.1 A check on the validity of the composite normal pattern variance

For the left lateral composite normal, comparisons were made between the individual patient scans contributing the the composite normal, and the composite normal pattern itself.

Assuming that the differences between the two patterns follow a normal distribution, one would expect that 5% of the points would differ by two standard deviations or more. An average lateral scan image contains about 1300 data points, and of these, some 60 would be expected to have $D \geq 2$. In fact, the average for the series was found to be 57. Occasional points exhibited $D \geq 3$; the theoretical probability of this is at the rate of about three cells per scan ($p = 0.0027$). Bearing in mind the comparatively small number of scans in the series, it was thought that these results were sufficiently close to the theoretical values to indicate the validity of the composite normal data and the expression used to calculate D.

Although the results for the series as a whole were in accordance with prediction, there were noticeable differences between some of the individual scans. Two or three of the scans showed remarkably few points where $D \geq 2$, whereas others showed quite large areas, especially in the region of the transverse sinus and the pituitary gland where $D \geq 2$. As these latter cases had been shown to possess no focal abnormalities, these differences must be ascribed to anatomical or physiological variation.

5.3 Criteria for abnormality

The criteria for abnormality of areas within radionuclide scan images were discussed by Haybittle (1966) and later by Griver et. al. (1976). For an area A of the individual patient scan which has a difference D of greater than three standard deviations from the normal

value, the probability, p, that this is due solely to random variation is equal to 0.0027. As noted above, if a lateral scan contains approximately 1300 elements, on average three such elements would be expected to show deviation of this order.

The criteria for abnormality adopted will depend upon what is considered to be an acceptable false-positive rate. Most workers have adopted a figure of 5% false positives and on this basis one scan in twenty would be expected to show an area A of greater than three standard deviations difference from normal arising purely from statistical uncertainty.

If T is the whole area of the scan, and A is the abnormal area, then the probability p' of finding such an area is given by

$$p' = \frac{T}{A} \cdot p \qquad \ldots\ldots (5.15)$$

Putting p' = 0.05 (for a 5% false-positive rate), p = 0.0027 (for a three standard deviation limit), and T = 1300 (for the total number of elements in the scan), it appears that scans containing 70 elements of greater than three standard deviations difference can be regarded as abnormal. If the analysis is repeated with p = 0.000061 (for four standard deviations difference) A = 1.6. Evidently any points of greater than four standard deviations difference from the expected value can be taken to show a degree of significance, and several such points, especially if they were grouped together, would be highly significant.

5.4 Results of a trial based on 50 individual patient scan data

A series of 50 consecutive cases in which the scan data were complete and a confirmed diagnosis was available was assessed in terms of the criteria for abnormality derived above. The results are

	true positive	false positive	true negative	false negative	equivocal
observer	19	3	16	6	6
computer	15	3	20	12	0

Figure 5.1 (a). Reporting accuracy of an experienced observer with access to clinical details against the accuracy of the computer printout with an assumed 5% false positive rate, in a series of 50 clinical results.

	true positive	false positive	true negative	false negative
observer	23	5	16	6
computer	15	3	20	12

Figure 5.1 (b). Reassessment of the above table assuming that an equivocal result is considered to be positive.

given in fig. 5.1 and will be discussed in more detail in following sections.

In reviewing the cases which were judged to be abnormal on the basis of the computer printout, it was noted that all contained significant numbers of cells of greater than four standard deviations difference from the expected values. In most cases, such cells were closely grouped together, and contained within a larger area comprising cells of greater than three standard deviations difference. In only four cases (out of 18 positive reports) did the area of the abnormality contain more than 70 cells of greater than three standard deviations difference; for this criterion to be fulfilled the abnormal area would have to exceed 11 cm^2. Abnormalities of this size are relatively unusual. It seems possible that the adopted criteria are rather imprecise, particularly in the important range between three and four standard deviations. By substituting into equation 5.15 values for p corresponding to standard deviation differences in the range 3 - 4, the table given in figure 5.2 is obtained which could be useful in the assessment of borderline cases.

A curious fact was noted in regard to two cases, both diagnosed as infarcts, and both regarded as visually equivocal, in that the most significant differences were noted on the lateral view opposite to the abnormality. In both cases, correct lateralisation was given by the AP view, though in neither case was the AP view sufficiently abnormal to be reported as such. This illustrates the importance of correlating the various projections available for each case, and demonstrates that non-significant differences noted on other views can be useful in supporting an abnormal finding. In these two cases, the obtained result was presumably due to the operator setting the plane of focus incorrectly.

D	p	S
3.0	2.7×10^{-3}	70
3.1	2.0×10^{-3}	52
3.2	1.4×10^{-3}	38
3.3	1.0×10^{-3}	26
3.4	7.0×10^{-4}	18
3.5	4.9×10^{-4}	13
3.6	3.3×10^{-4}	9
3.7	2.2×10^{-4}	6
3.8	1.5×10^{-4}	4
3.9	9.5×10^{-5}	2.6
4.0	6.1×10^{-5}	1.6

Figure 5.2 Number of cells, S , at different levels of significance which fulfil the criteria for abnormality

In one case, illustrated in fig. 5.3, strict adherance to the criteria for abnormality as defined led to the conclusion that this obviously positive scan was in fact negative, and it has been entered in fig. 5.1 as a false negative. Even reference to the more precise criteria given in figure 5.2 is unhelpful in this case because the anomaly contains only three points with differences greater than 3.6 and only one point with a difference greater than 3.9. This case appears obviously abnormal on visual inspection of the printout because it is well defined, i.e. all the points which differ by significant amounts from the expected values are very closely associated, and this factor is not allowed for in defining the criteria for abnormality. As an exercise, it was decided to compute the difference from the expected value of a group of points containing this apparent abnormality using expression 5.14. In this case, values of P, N, and σ_t^2 refer to the sums of these values for the points in the group.

For such a group comprising an area of 3x3 cells centred on the anomaly, the computed difference from the expected value was 10.5 standard deviations, and for a rather larger area of 5x5 cells, the difference was 14.4. These differences are highly significant, but they arise mainly because these points, mostly exhibiting differences of three or more standard deviations computed on an individual cell basis, are very closely associated. The number of cases in which this analysis would reveal a lesion not meeting the standard criteria would probably be small; inspection of the false-negative results for the current series of 50 cases showed no other case in which this area of interest analysis would be likely to be of value. It is possible that the method could occasionally be helpful if the computer analysis revealed an anomaly of doubtful significance in an area where the clinical information strongly suggested the possibility of a lesion.

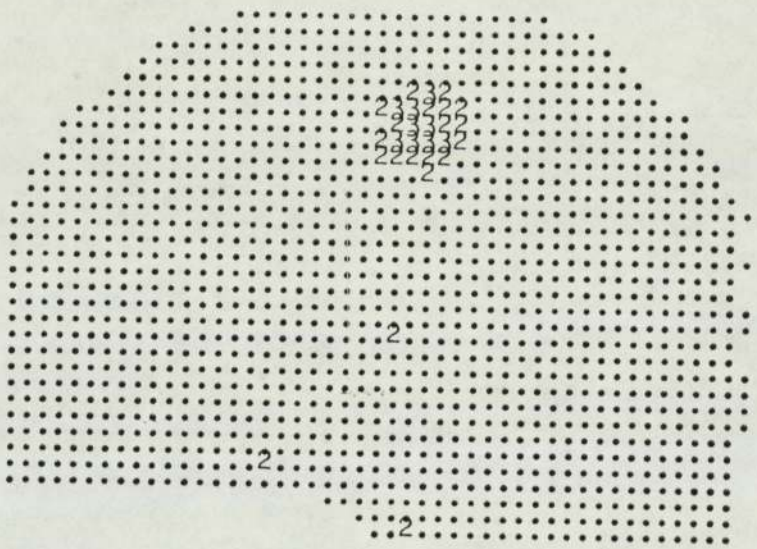

Figure 5.3 Simulated computer printout of a left lateral projection showing an apparent abnormality in the vault which failed to meet the criteria for abnormality.

5.4.1 Correlation between views

In this study, cases have been reported as abnormal if an abnormality meeting the stated criteria was recognised on a single projection. Most results were obtained on the basis of the lateral scan findings.

The sagittal views were analysed in a similar manner to the lateral views, by production of a composite normal pattern. This was in contrast to the approach of Popham et. al. and Dowsett and Perry, who took advantage of the natural symmettry of these scans about the midline to compare equivalent areas on the two sides of the single patient scan under analysis. These workers recognised the obvious drawbacks of this approach in that it would be insensitive in the case of lesions which cross over the midline. Another problem, noted by Popham, is that the PA projection is not always very symmettrical even in normal cases, because of normal anatomical variations in the position and size of the venous sinuses.

An attempt to produce a composite normal PA view was abandoned because of the problems of variability in the normal case material, the comparatively small number of normal cases available for analysis (since this projection was often only carried out if a posterior fossa or occipital lesion was suspected) and the impossibility of estimating the angle at which the scan had been performed. The production of a composite normal AP scan also presented some problems. The anterior aspect of the brain was normally examined in a Townes projection, at an angle to the radiological baseline estimated by the operator to be 15^{o}, to make correlation with the plain skull X-rays easier. The actual angle of the scan could be calculated on computer analysis by reference to the anatomical point data punched onto the paper tape. It was found, in fact, that the angle varied quite widely, with a mean

of 9^{o} 30' and a standard deviation of 5^{o}. It was therefore decided, in selecting cases suitable for computer analysis to form a composite normal, to reject cases showing extreme angular differences from the mean value, but otherwise to take no account of the angle of the scan. This proceedure was not entirely satisfactory, and it seems likely, in retrospect, that Popham's method of symmettry analysis would have given more consistent results. The AP scan analysis of individual patient data was useful in confirming the lateralisation of lesions seen on one or both lateral views, but no significance was attached to the few cases which showed an apparent abnormality on the AP scan which was not confirmed on either lateral.

5.4.2 Analysis of the trial results

The results set out in fig. 5.1 (a) compares the accuracy of the computer analysis against that of an experienced radiologist with access to the patient's clinical details and X-rays. It will be noted that the computer analysis has detected fewer true positive results and more true negative results than the visual assessment. The false positive rate for the computer analysis is close to the predicted value. The observer's results also yielded six equivocal reports, of which four were shown on contrast X-ray examination to correspond with lesions. If the equivocal reports are taken to be positive, the observer's accuracy improves to the values shown in fig. 5.1 (b). The overall reporting accuracy in this case (i.e. true positives + true negatives) amounts to 78% of all cases in the series. The overall reporting accuracy for the computer assessment was 70%.

It is interesting to compare these values with those reported recently by Griver et. al. (1976). In the equivalent situation, comparing the reporting accuracy of an experienced observer with access

to clinical details against that of a computer assessment with an assumed 5% false positive rate, the observer recorded a 78% accuracy and the computer 62%. The results of the current study are therefore substantially better, but still fall short of the results obtained by visual assessment. A number of ways in which the computer assessment could be further improved are evident. An area of interest analysis technique has been shown in section 5.4 to be capable of detecting small, relatively low uptake lesions, and a better means of analysing sagittal projections would undoubtedly improve the overall reporting accuracy; it was noted that two true-positive results obtained by the observer but missed by the computer were obtained solely on the basis of the asymmetry of the sagittal projections. With these refinements the reporting accuracy of the computer would probably be very close to that of an experienced observer, and if the two methods of reporting were to be correlated, there seems little doubt that the overall reporting accuracy would be slightly improved.

If analysis is undertaken of the cases in which the conclusions reached by the two methods in this trial differed, it is noted that in the the 14 such cases, the observer was correct 9 times and the computer 5 times. In the 9 cases in which the computer failed to detect the lesion, 6 were lesions of the posterior fossa or very close to the periphery, i.e. precisely those areas which were known to exhibit a large patient to patient variation. Of the 5 cases in which the computer assessment alone detected the lesion, 4 were in the cerebral hemispheres. The conclusion might therefore be drawn that the computer performs as well as an experienced observer in detecting lesions within the cerebral hemispheres, but the method is less sensitive in those areas which are difficult to examine by conventional

radionuclide imaging, the posterior fossa and the base of the brain. In order to examine these regions in detail, other methods are necessary.

It should be emphasised that, although the computer assessment alone failed to match the accuracy of the observer, the combination of the computer and visual assessments detected 88% of the lesions in the series, a highly significant improvement. For this improvement in accuracy to be realised in practice an independent and sensitive method of examining questionable regions of the scan is necessary. Such a method should also be applicable to the difficult regions low in the brain. The following chapters describe the development of one such technique.

CHAPTER 6

Transverse axial radionuclide tomography

6.1 Medical Radiographic Imaging Techniques

The conventional diagnostic x-ray image is formed by the superimposition of all the information contained within the various layers of the object under examination. Referring to Fig. 6,1, if f_i is the fraction of the incident x-ray intensity transmitted by element i of the object, and $x_i = \ln f_i$, the response obtained at the detector, d, can be defined by the equation

$$\ln d = A_0 \sum_{i=0}^{i=N} x_i$$

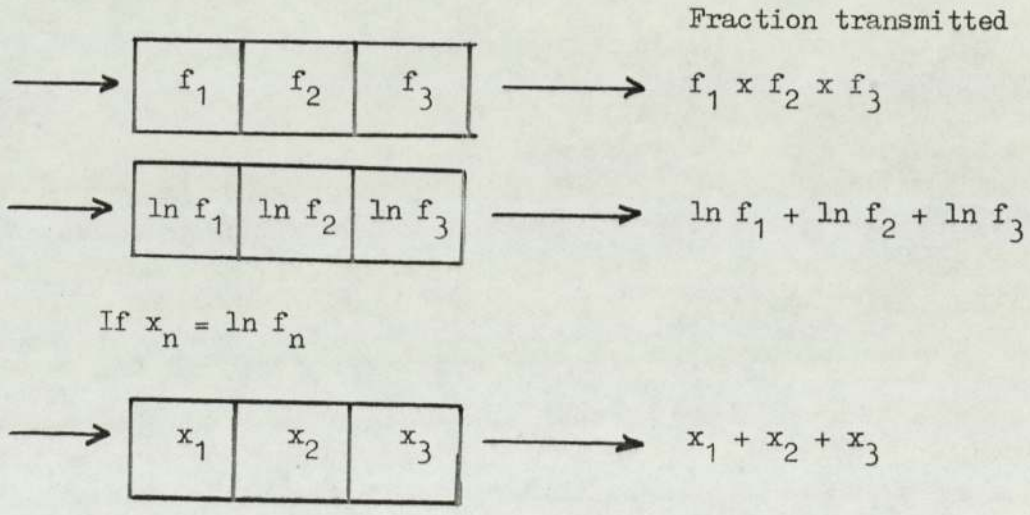

Fig. 6.1 Narrow beam absorption of X-rays

The above treatment is idealised, in that it is assumed that the detector receives only direct radiation. In practice some low angle scattered radiation will also be received by the detector despite the collimation provided by a lead-strip grid placed in front of the detector.

In the case of the conventional x-ray photograph, this means that only elements containing tissue of high x-ray absorption coefficient will be visualised, and that even these will be visualised less clearly as the distance from the element to the detectors is increased. At the photon energy of a typical diagnostic x-ray set, where most absorption is by the photoelectric effect, only volumes of relatively high electron density and large Z will be seen. Volumes containing low electron density material will not in general be seen, unless they are surrounded by even lower electron density material such as gas.

There are two available means of partially overcoming this limitation of the conventional radiograph. Firstly, by introduction into body cavities of high electron density material (contrast radiography) and secondly, tomography, in which the radiation source and radiation detector are moved relative to each other in such a way that only information contained within a specified section is imaged clearly.

6.1.1. Contrast Radiography

For this method to be successful, a high concentration of radio-opaque material must be maintained in the cavities of the organ under examination for the time necessary to complete the investigation. As modern diagnostic x-ray sets can produce a high x-ray photon output, exposure times can be as short as a few milliseconds, so, for example, the arteries in an organ can be visualised, providing the injection of radio-opaque material is made rapidly at a point close to the organ. This procedure is known as angiography. Similarly, veins and the lymphatic vessels can be examined in the procedures of venography and lymphangiography. These procedures are usually complicated, and can be hazardous in any but the most expert hands. Radioisotope investigations are analagous to contrast radiographic examinations but because select-

ive concentration of radioactive material takes place by biochemical processes at a relatively slow rate, and because the amounts of radiopharmaceutical present are in general minute, because of the high specific activity of the material, these procedures are much simpler and safer.

6.1.2 Conventional X-ray tomography

This procedure relies on relative movement of the radiation source and detector to blur out information not contained within the chosen plane of focus. Fig. 6.2 illustrates the principle of the method. It should be noted that information from other planes is still present, but it is spread over a relatively large area of the image plane, and thus it may contribute to the 'background' if it falls on the photographic emulsion, but it will not be sharply focussed. If a naturally radio-opaque structure is defocussed in this way, an artefact may be obtained. The high background obtained is partially suppressed by suitable exposure of the film, taking advantage of the non-linear exposure/density characteristic of the photographic emulsion.

The success of this method depends largely on having sufficiently large relative movement of the source and detector. Very complex mechanical devices have been constructed to give a large relative movement and this technique, though complicated, is often quite successful. A combination of tomography and contrast radiography (usually negative contrast, using air) can give good results.

6.1.3 Tomographic Isotope Examinations

Isotope imaging shares a common problem with conventional x-ray imaging, in that the images of all layers of the organ under investigation are superimposed, leading to a loss of contrast. There has therefore been interest for a number of years in methods of obtaining tomographic isotope images. A number of methods have been described.

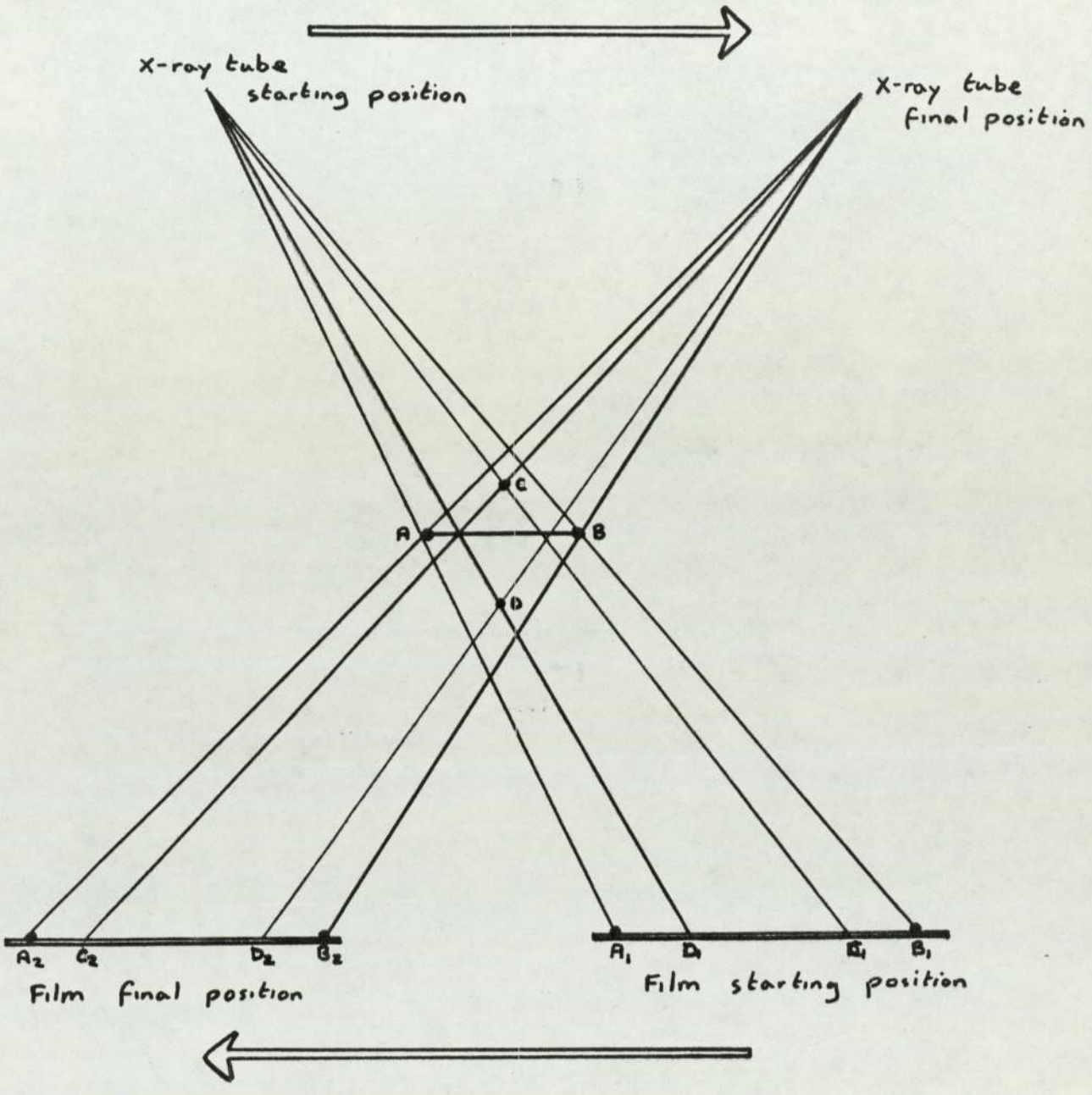

Figure 6.2 The mechanism of conventional X-ray tomography

Most methods use the same principles as x-ray tomography, relying on a defocussing technique to blur out-of-plane sections. As with x-ray tomograms, artefacts are introduced, and a high background is usually obtained. There seems, therefore, to be a considerable case for the type of transverse sectional tomographic examination first proposed by Kuhl and Edwards (1963) in that all the information detected contributes to the final image, and that information outside the plane of interest does not enter the radiation detectors. To be successful this method requires mathematical reconstruction of the image, instead of the purely optical methods used by other techniques. The principle of Kuhl's method is shown in Fig. 6.3

More recently, Kuhl has described further development of his technique, and other transverse axial imaging devices have been described by Patton, Brill and Erickson (1969), and Robertson, Marr, Rosenblum et al. (1973). A dual detector isotope scanner is now commercially available which is mechanically capable of producing transverse axial isotope tomograms, as well as conventional radioisotope images. This machine was described by Keeling (1971) and a similar device was used in this investigation.

6.2 Development of A System For Routine Transverse Axial Isotope Tomography

As indicated above, transverse axial tomography using radioisotopes requires a mathematical reconstruction of the isotope distribution from one dimensional 'profiles' obtained at a number of different angles around the object. There is no simple analogue method of accurate reconstruction, although a method described as film exposure summation was attempted by Kuhl. (Kuhl and Edwards, 1968).

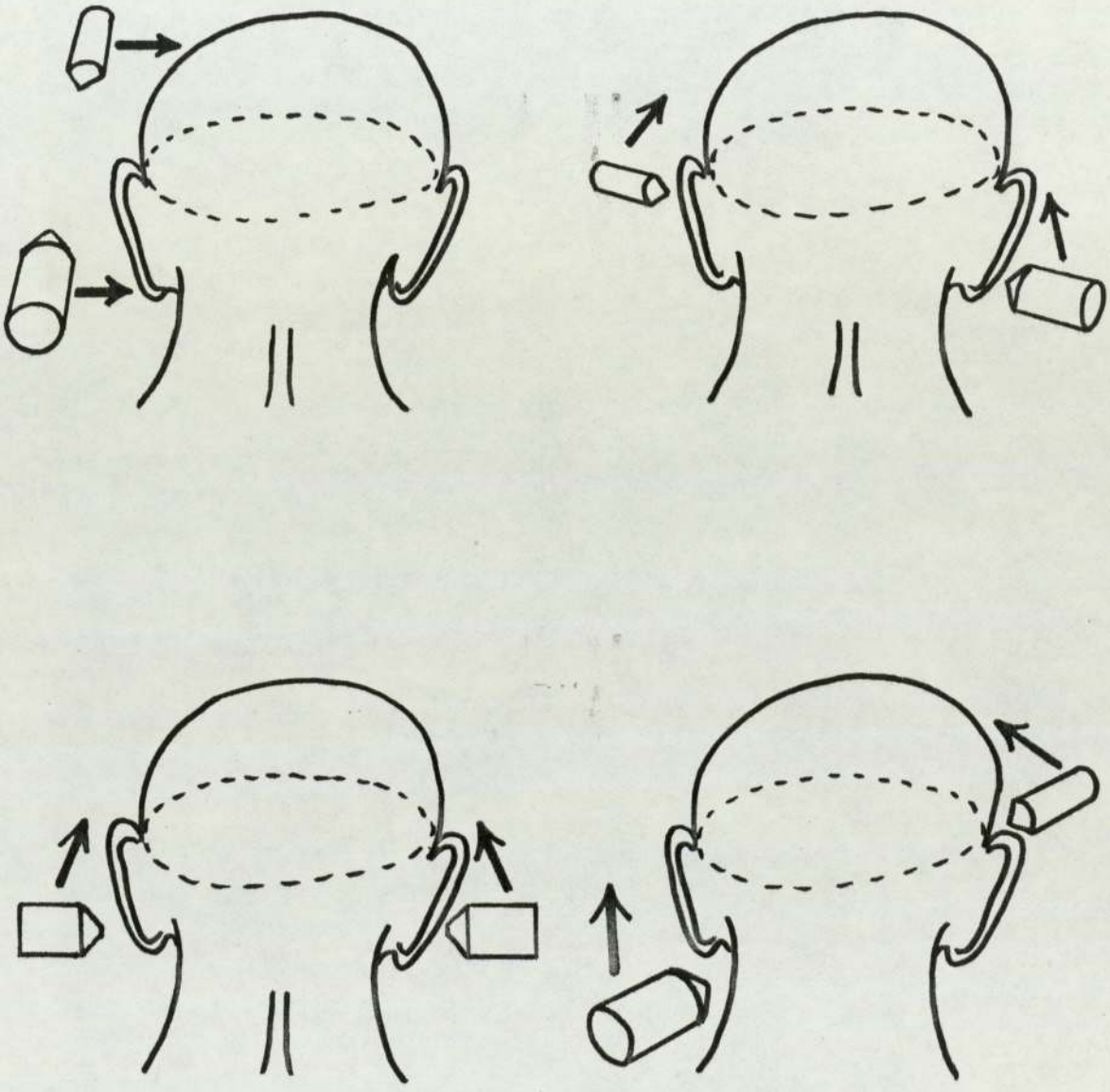

Figure 6.3 Method of transverse axial isotope tomography proposed by Kuhl and Edwards (1963)

Reconstruction of an image in this way is a general problem and occurs in a number of different areas of work, e.g. electron microscopy and radioastronomy. A large number of reconstruction methods have been proposed, and several excellent review papers are available. A problem seems to be that the accuracy of a particular method seems to have some relationship to the type of structure being examined and the random statistical variation of the detected intensity data. This problem was discussed in some detail by Herman and Rowland (1973). However, a more recent paper in which the same data were reconstructed using six different algorithms yielding very similar results has suggested that the results may in fact be noise-limited, and that the choice of reconstruction algorithm for images of the brain may not be critical where accurate projection data are available. (Smith et al (1975)).

For the preliminary work on the present project, a computer program was used which had been developed by Keyes at Aberdeen University and which had been shown to give excellent results in brain imaging. This program was based on the convolution method of Bracewell and Riddle (1967) and the method has been described by Keyes. (Keyes, 1976). Early results with this program were very encouraging and the program was subsequently developed to provide rapid and efficient processing within the constraints of the very small data processor being used, whilst retaining the basic method used by the Aberdeen University group.

6.2.1 The J & P Engineering Limited MS 430 Scanner

The MS 430 is a dual detector isotope scanner, and is illustrated in Fig. 6.4. The two collimated 4" diameter sodium iodide crystals are mounted in frames, and can be moved in two dimensions by lead screws driven by stepping motors. The two scanning frames are

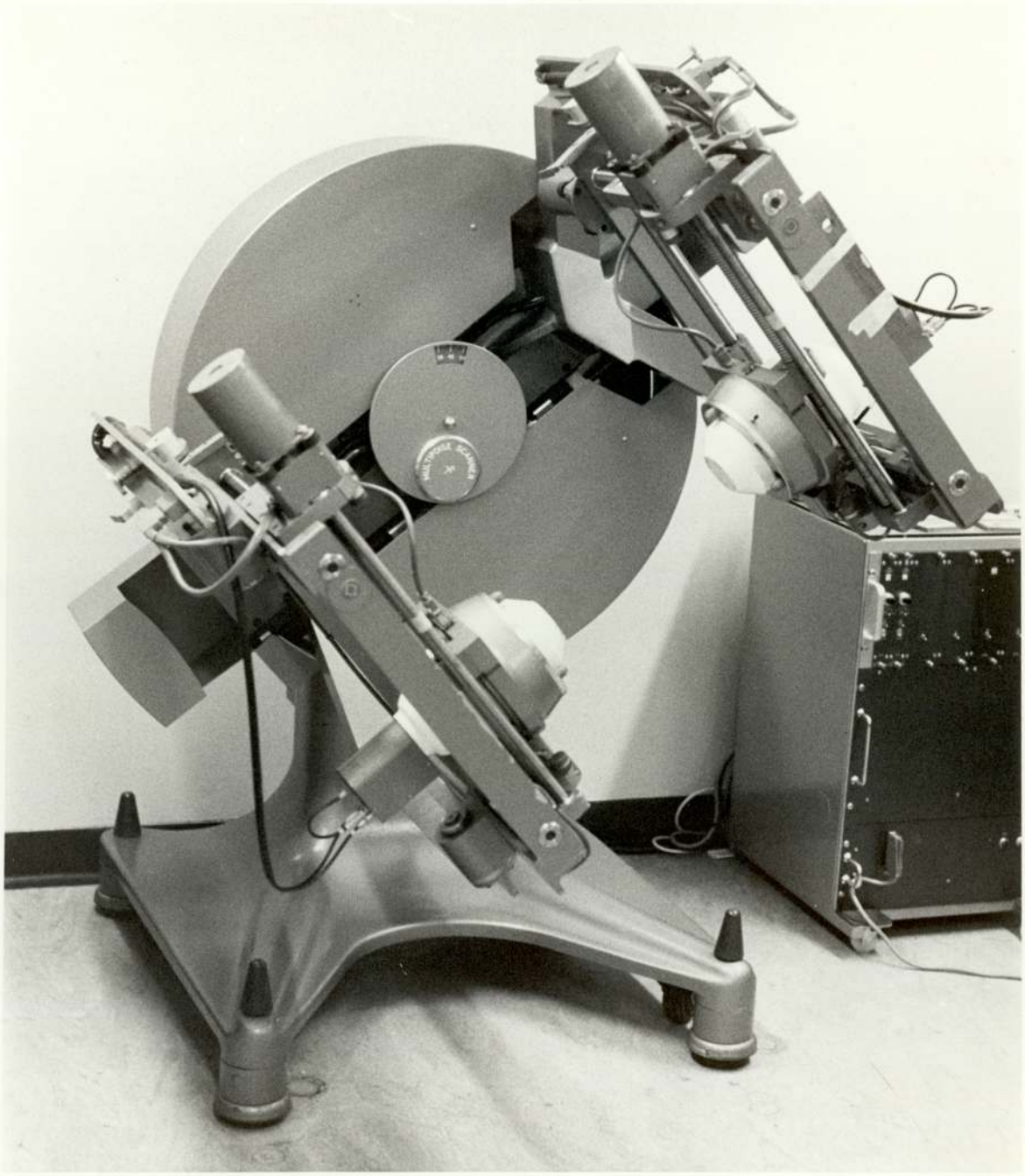

Figure 6.4 The J & P MS 430 Isotope scanner

mounted within a yoke, and can be pivoted with respect to the yoke through an arc of $\pm 15^0$ by a hand wheel driving a sector rack and pinion. This facility is particularly useful in obtaining angled sagittal views of the brain. In particular, very good visualisation of the posterior fossa can be obtained.

The yoke on which the scanning frames are mounted can be rotated through an arc of 270^0. This rotation can be accomplished by switching a motor from the manual control module or a programmed rotation can be obtained. The latter facility is used in isotope tomography, a pre-selected rotation of between 1^0 and 19^0 being performed at the end of each scanning line. The required angular increment is selected by a thumbwheel switch on the scanner control console.

The display, consisting of dual colour dot printers and dual photoscans (exposing 17" x 14" X-ray film) is driven by stepping motors in the x and y directions. The stepping motor pulses are derived from the same source as the pulses used to drive the detectors, therefore, the movements of the detectors and display are synchronised.

A four track cassette tape recorder is provided which records data during a scan. Two data tracks contain pulse data from the two radiation detectors and the remaining two tracks record stepping motor pulses. It is thus possible to redisplay the results of any investigation.

6.2.2 Design & Construction Of Scanner/Computer Interface

The scanner-computer interface was designed to be suitable for conventional linear scanning data acquisition as well as transverse sectional data acquisition.

For conventional scanning data acquisition, positional data are derived from the drive pulses applied to the stepping motors driving

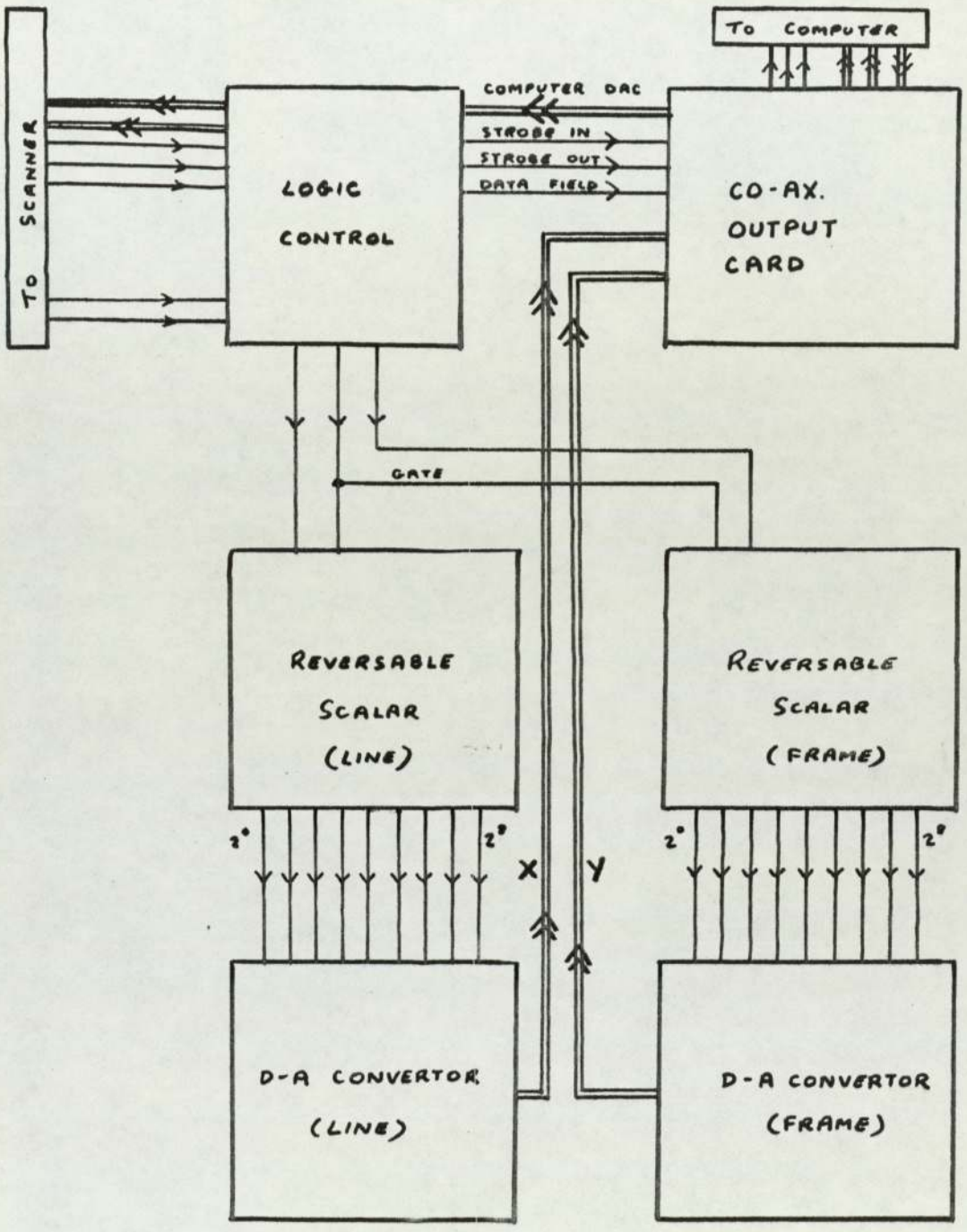

Figure 6.5 Block diagram of scanner/computer interface circuits

The design of this interface was largely dictated by availability of commercial hardware. A simpler and better system would be to interface the digital outputs of the scalars directly to the computer bus.

the detectors. These are counted in reversable scalars, with appropriate gating at the ends of lines to give a correction for scalloping. In this application, the scalars perform the function of serial-parallel converters. The values in the two scalars are then applied to the inputs of digital-to-analogue converters. Thus two analogue voltages are obtained which are proportional at all times to the position of the detectors within the scanning frame.

Each time a detector gives a pulse which is accepted by the pulse height analyser for that detector, a 'strobe' pulse is produced. This is a 0V to 5V pulse of approximately 5μS duration. Simultaneously, a level is generated on a second line which identifies the detector in which the pulse originated.

Further strobe pulses are obtained at each cell boundary. The number and frequency of these is determined by the 'cell size' setting of the scanner and also by a switch which determines the maximum number of cells in any profile, limiting the maximum to 64,128 or 256 cells per line.

A block diagram of the scanner part of the scanner/computer interface is given in Fig. 6.5.

The signals transmitted by the scanner are applied to the analogue-digital interface of the Nuclear-Data 50/50 data acquisition and display system. As the positional data are analogue levels, it is necessary to use analogue gate circuitry to adapt these signals to an appropriate form for analysis. The 50/50 ADC modules contain linear gate circuitry, and it was necessary to utilise this circuitry for the analysis of the signals.

Inspection of the circuit diagrams for the ADC's (Fig.6.6) suggested that it would be most appropriate to use the DIRECT -5V input

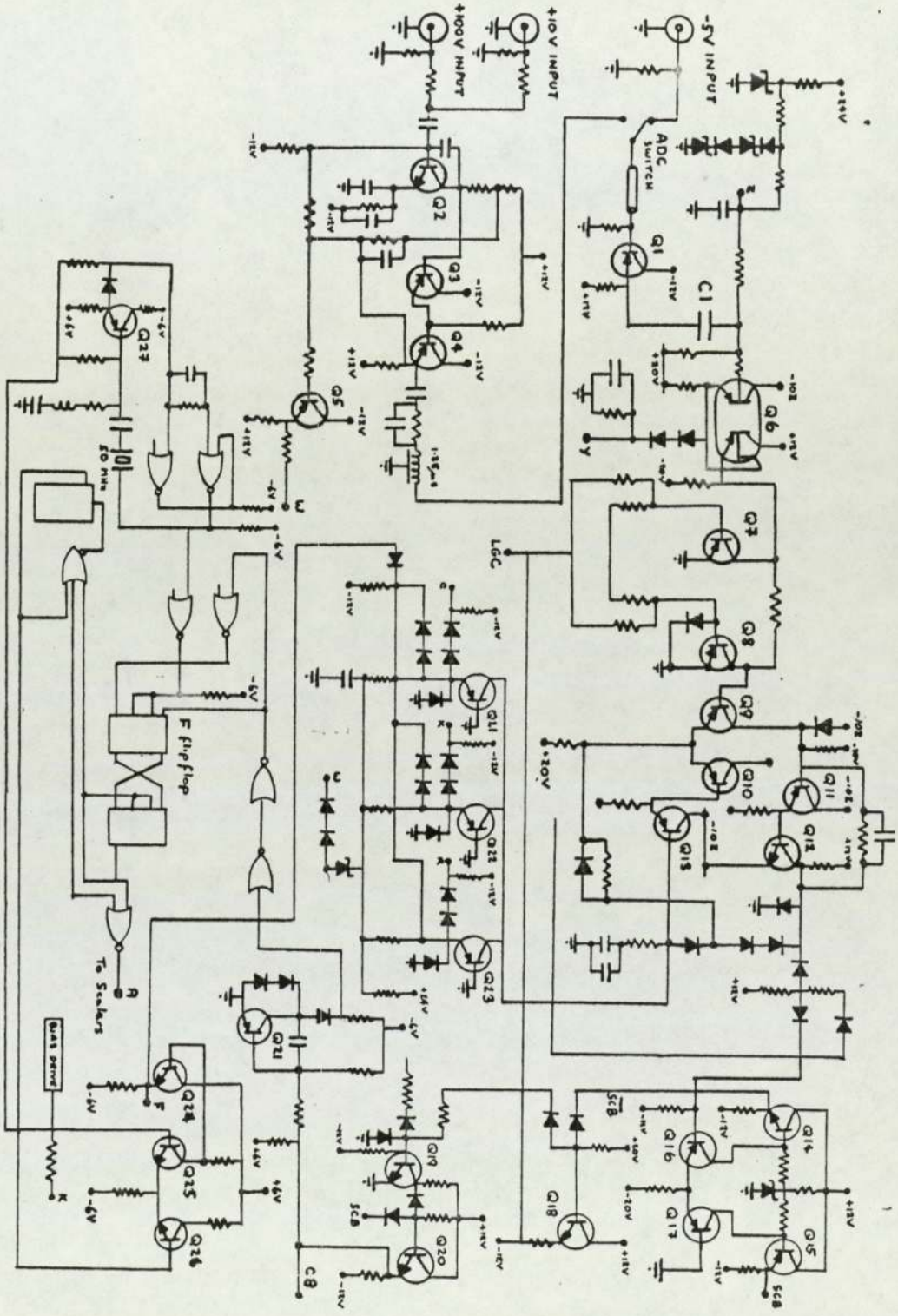

Figure 6.6 Input circuits of 50 MHz analogue/digital converter

to the ADC's. This input can be coupled through an emitter follower, Q1, to the input of the double transistor Q6 by shorting out the decoupling capacitor C1. The transistor Q6 forms the input stage of the linear gate circuit Q7, Q8. This gate is opened by signal LGC which is derived from the input applied to the COINCIDENCE input BNC, provided the linear gate front panel switch is in the 'open' position.

If the analogue levels representing the scanner detector positions are applied to the DIRECT -5V inputs to the ADC's, and the appropriate strobe pulse is received, the analogue level will be sampled by the linear gate circuitry. The output of the linear gate circuit is then applied to the sweep circuit, comprising transistors Q9 to Q13 and associated components. The sweep circuit produces a signal which goes up for a length of time proportional to the amplitude of the input signal. This signal is applied to the shaping and inverting circuits associated with Q14 to Q17 which generate signals SCB and $\overline{\text{SCB}}$, the former being held up during the interval in which the output signal of the sweep circuit is up, and the latter being held down during this interval.

Signal $\overline{\text{SCB}}$ is used to block the linear gate until a signal is provided indicating that the data handling circuits are ready to handle another conversion. Any strobe pulse occurring in this time interval will be unable to open the linear gate, and these data will be lost.

Signal SCB is inverted by Q20 to provide signal CB. This signal is gated with the next pulse from the address oscillator (running at 50 MHz) to reset the 'F' flip-flop. Unless this flip-flop is reset the sweep circuit is inhibited by signal F from permitting the linear discharge of the sweep capacitors. The discharging operation is therefore synchronised with the oscillator.

During the time interval after the F flip-flop is turned on, and until signal SCB goes down (indicating the end of the linear discharge of the sweep capacitors) the address advance oscillator pulses are used to 'run up' a scalar. When signal SCB goes down, the total count stored in the scalar is proportional to the sweep capacitor discharge interval, and hence to the input signal amplitude.

In order to avoid any non linearity which may occur at the start of the capacitor rundown ramp, a small negative voltage is applied to each input signal, and the offset thus obtained is later removed by inhibiting one of the 'carry' signals in the scalar. The offset is applied by the F signal via a diode coupled capacitatiive timing circuit associated with transistors Q21 to Q23. Inspection of the circuit reveals that the offset voltage obtained is dependant upon the position of the 'CONVERSION GAIN' switch, since inputs C, K and R are derived from this switch.

As previously noted, the DIRECT -5V input BNC was D.C. coupled to the input of transistor Q6 in order to permit the analysis of the very slowly varying levels applied to the input. Unfortunately, removing the decoupling capacitor means that the entire circuit, comprising linear gate, sweep, shaping and inverting circuits and offset circuitry, is D.C. coupled throughout. This means that the offset applied through the conversion gain switch will result in a bias level at the input. The magnitude of this bias is dependant on the setting of the conversion gain switch.

It was established that the signal level required to give full scale output from the ADC was, in fact, -3V, not the -5V nominal value. To obtain a zero output fron the ADC, the input signal required an external offset of approximately 130 mV for a 4K conversion gain, and no

less than 900 mV for a 128 conversion gain. As each ADC was required to provide either a row or a column address in order to define a point within a 64 x 64 square matrix, in the usual case only 64 discrete levels were produced by the scanner digital-to-analogue converter, i.e. each voltage step had a magnitude of approximately 50 mV. It was felt that the ADC could be set up to give a 130 mV offset (this representing only about $2\frac{1}{2}$ voltage increments) and still remain stable, but to attempt to obtain an offset of 900 mV would result in instability and hence uncertain results. There was thus no alternative to using a 4K conversion gain setting for the ADV's.

The problem then arose of combining two 12bit binary numbers to form a single 12 bit address. It was necessary to modify the data pathways to do this without, if possible, preventing the system from carrying out the general purpose data acquisition for which it was designed.

If reference is made to the general block diagram of the data processing system (Fig. 3.2) it will be noted that data are passed from the two ADC inputs to the storage and display system via a module referred to as a 2 parameter ADC control. This module interfaces the ADC's to the storage and display unit, and in addition to providing certain control signals, can be used to define the storage configuration of the memory. A number of prewired program plugs are provided which will, for example, select eight storage matrices of 32 x 32 cells x 12 bits, or two of 64x64 cells x 12 bits. A special program plug was designed and made up in which the least significant 6 bits of each ADC output was disregarded, and only the most significant 6 bits were used to form the address. In addition, an 'overflow' bit input provided on the front panel program plug socket was wired in parallel to a BNC socket that was added to the

front panel. This socket was connected to the "data field" input of the scanner interface and depending upon the state of this line at the time of a conversion event, data was added to the appropriate channel in either the least significant 12 bits or the most significant 12 bits of the 4K x 24 bit memory in the storage and display unit.

The only disadvantage that is apparent in using the method described above to form the address of a particular scintillation event is that use of a 4K conversion gain increased conversion time, and some events may be lost by coincidence.

The oscillator in the ADC runs at a 50 MHz rate, therefore the conversion time for a full scale signal is $4K/50 \times 10^6$ seconds or approximately 80 μ seconds. The percentage of losses is position dependant, which could result in significant distorsion of the data, but for the fact that the average count rate is low.

The maximum count rate observed in a typical section scan of the brain using 10 mCi of ^{99m} Tc is approximately 400 counts per second. If C_a is the actual count rate, C_o is the observed count rate and t is the effective 'dead time' of the system,

$$C_a = \frac{C_o}{1-C_o t} \qquad \text{.....(6.2)}$$

In the worst possible case, with a count rate of 400 counts per second occurring in the last cell of the line, the losses amount to 3.2%. In actual practise, the losses are not as severe as this, because the maximum count rate occurs during the central portion of the line, and the count-rate has fallen to background levels near the end of the line. Losses due to the rather long conversion time should nowhere exceed 2.5%.

During development of the scanner interface, it became

apparent that the comparatively long data lines (approximately 17m) were causing problems. A terminating module was constructed by the scanner manufacturers which provided R-C networks to match the output impedances of the analogue lines, and in the case of the digital (strobe) lines monostable circuits to provide clean 'strobe' pulses of approximately 5 μ second duration in place of the rather noisy pulses received at the end of the transmission line.

6.2.3 Display Of Computer Processed Results On Scanner Display Circuits.

In addition to transmitting data from the scanner to the data processor for analysis, it is necessary to return processed data from the data processor to the display circuitry of the scanner. This was considered essential in order to provide a full size display with a good grey scale. The only alternative would be to photograph the display oscilloscope, but this would yield small polaroid prints of rather inferior quality because of the very limited grey scale capability of the oscilloscope.

The method used to transmit information from the data processor to the scanner for display purposes was as follows. The scanner was set in motion, in the 'computer playback' mode, and as before provided X and Y voltages to define position in the scanning frame. In this mode, a strobe pulse was transmitted at the end of each cell in the display pattern. The strobe pulse caused sampling of the X and Y levels, and formation of an address by the two parameter ADC control.

For playback of information to the scanner the two parameter ADC module was put into the 'computer control' mode, The accepted input address was put into the last channel of the storage and display unit memory from whence it was read into the computer. The computer was then

programmed to read the value of the given address in lower memory and hold this value for approximately 10 milliseconds. When playing back to the scanner the 50/50 display circuits were disabled, and holding the value by a computer generated loop caused an analogue level proportional to the value in the addressed channel to be generated by the 'live time display' circuitry. This analogue level was sampled by the scanner and displayed by one of the scanner displays.

After 10 milliseconds, the computer addressed the value in the given channel in upper memory, and held this until another strobe pulse occurred. The scanner again sampled this level, and displayed it in the second display channel. Thus two frames of picture data were simultaneously displayed.

At the end of the display sequence, the scanner stop button was pressed and the strobe pulses ceased. The computer recognised the cessation of strobe pulses, and switched off the analyser. Both raw data and picture data were stored on magnetic tape.

6.3 The suitability of the detector system for transverse axial reconstruction techniques

To provide accurate, quantitative reconstruction of the transverse axial distribution of radioactivity in an organ, the characteristics of the radiation detection system are of considerable importance. Ideally, the resolution and sensitivity of the detection system should be uniform throughout the entire thickness of the section under examination. This condition is almost impossible to achieve in practice. If, for example, very small detectors were used with small bore parallel-hole collimators the resolution would be uniform throughout the section, but the sensitivity would not be, because of the effects of scattering. If larger detectors with focussing collimators are employed, the effects of scattering can be overcome to some extent, but the resolution

will vary through the section. A compromise solution may be found in the use of relatively small detectors, parallel opposed and fairly widely separated with long focus multi-hole collimators. This approach was used in the Aberdeen Section Scanner (Bowley, Taylor, Causer et al. 1973) Kuhl's approach was similar (Kuhl and Edwards, 1963).

The present study was designed to assess the suitability of the J & P section scanner detection system for this purpose, and if necessary, make recommendations for improving the detection system.

A water tank was constructed, in which a 1 mm. diameter Co^{57} radiation source could be accurately positioned, to plot out the characteristics of the detection system. The dimensions of the tank were 20 x 20 x 20 cms. and in the floor of the box were mounted two pieces of perforated fibre-board, pierced on a 0.1 inch matrix, and separated by a few mm. (see Fig. 6.7). The Co^{57} source was mounted in a perspex holder, the base of which had three locating pins. The source could be accurately and reproducably positioned at a large number of points within the box. Dual scalar/discrimators were used to record the counts, and for most positions within the box counts of at least 10K were recorded, giving good counting statistics.

The water filled box was positioned between the two detectors, and the collimator point source response functions were plotted. It was found during the course of this task that the axes of the response functions did not quite coincide with the apparent machanical axes as obtained from measurement of the detector housings, and slight adjustments were made to bring the axes into alignment. The sector racks were marked up so that the detectors could accurately and quickly be set up parallel opposed for routine section scanning.

Having obtained the individual collimator characteristics the curves were combined for a number of collimator separations to determine

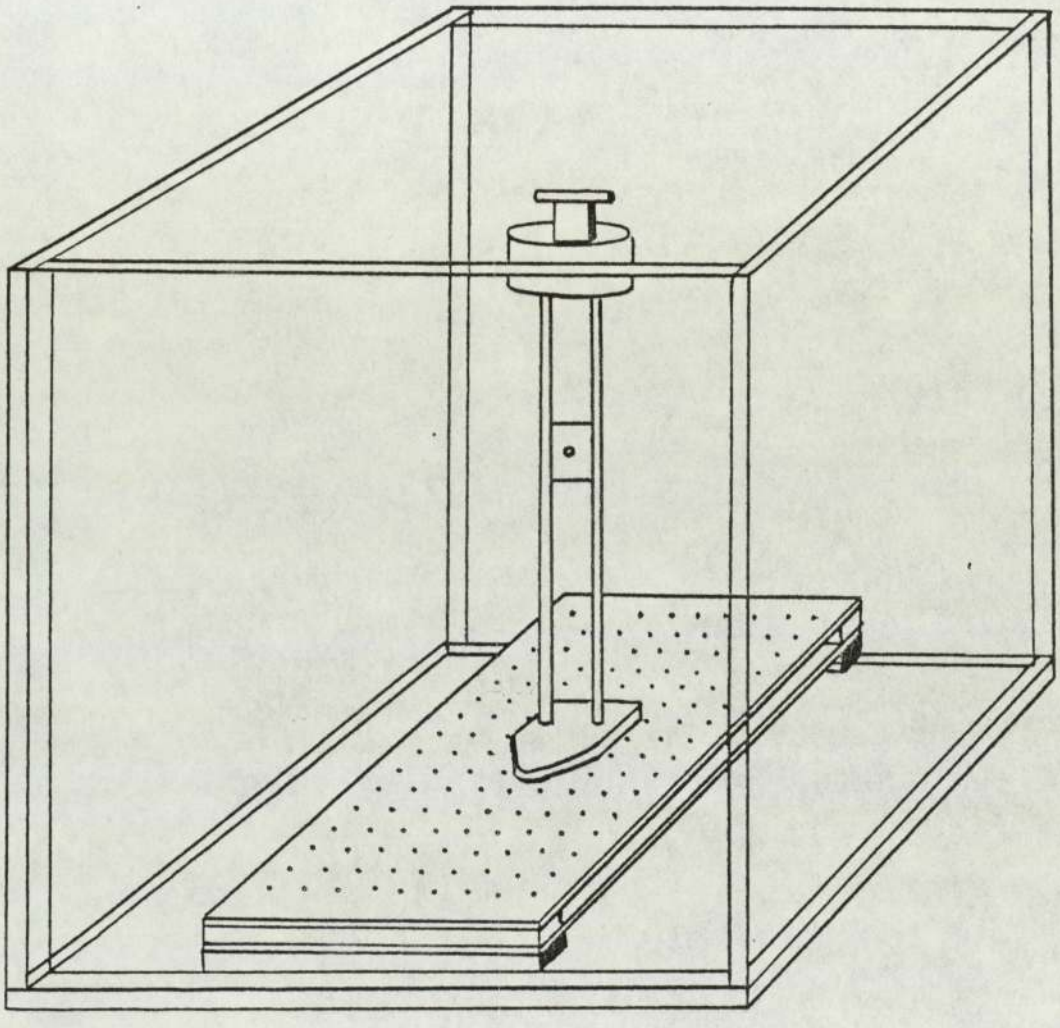

Figure 6.7 Tank used for plotting collimator characteristics

the separation which would give optimum uniformity of resolution and sensitivity for an object roughly the size of the human head. It was found that resolution (expressed as the full width half maximum of the point source response function)did not vary greatly with collimator separation, but axial sensitivity varied quite considerably. This was to be expected, since the collimators were of fairly short focal length, about 12.5 cms. The curves obtained are plotted in Fig. 6.8. The best compromise for the detector separation with the available collimators appeared to be 32 cms. With this separation, the axial sensitivity varied by ± 20% in a 20 cm. thick water equivalent object. An improvement could be obtained by using longer focal length collimators, and such collimators would be essential for body section scanning.

6.3.1 Mechanical Characteristics Of Detection System

Before the scanner could be used for transverse axial scanning, it was necessary to determine accurately the position of the axis of rotation in relation to the mechanical parts of the scanner. This was done by the arrangement shown in Fig. 6.9. A plate was fixed to a steel rod which was rigidly mounted on the central section of the scanner yoke. An external pointer was fixed close to the plate and the point of contact marked. As the scanner was rotated, the pointer traced out a circle. The centre of this circle lay on the axis of rotation. The position of the axis could thus be fixed in relation to the mechanical parts of the scanner.

The MS 430 scanner was designed specifically for brain scanning, and the scanning frame (i.e. the area through which the detectors can be moved) is only 24 cms. square. This is however, sufficient to accommodate all but the very largest head size. Unfortunately, however, the midpoints of the scanning lines were not coplaner with the axis of rotation of the machine. The plane containing the axis of rotation intersected

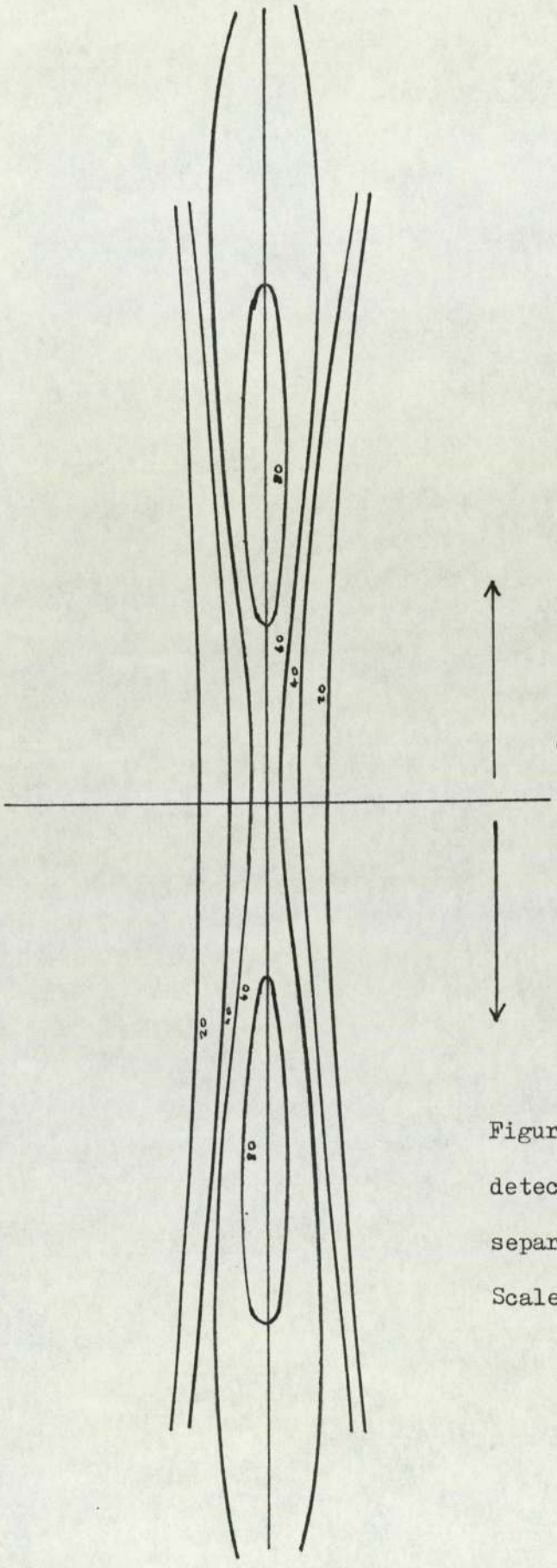

Figure 6.8 Isocount contours for detector system, with collimator separation of 32 cm
Scale: full size

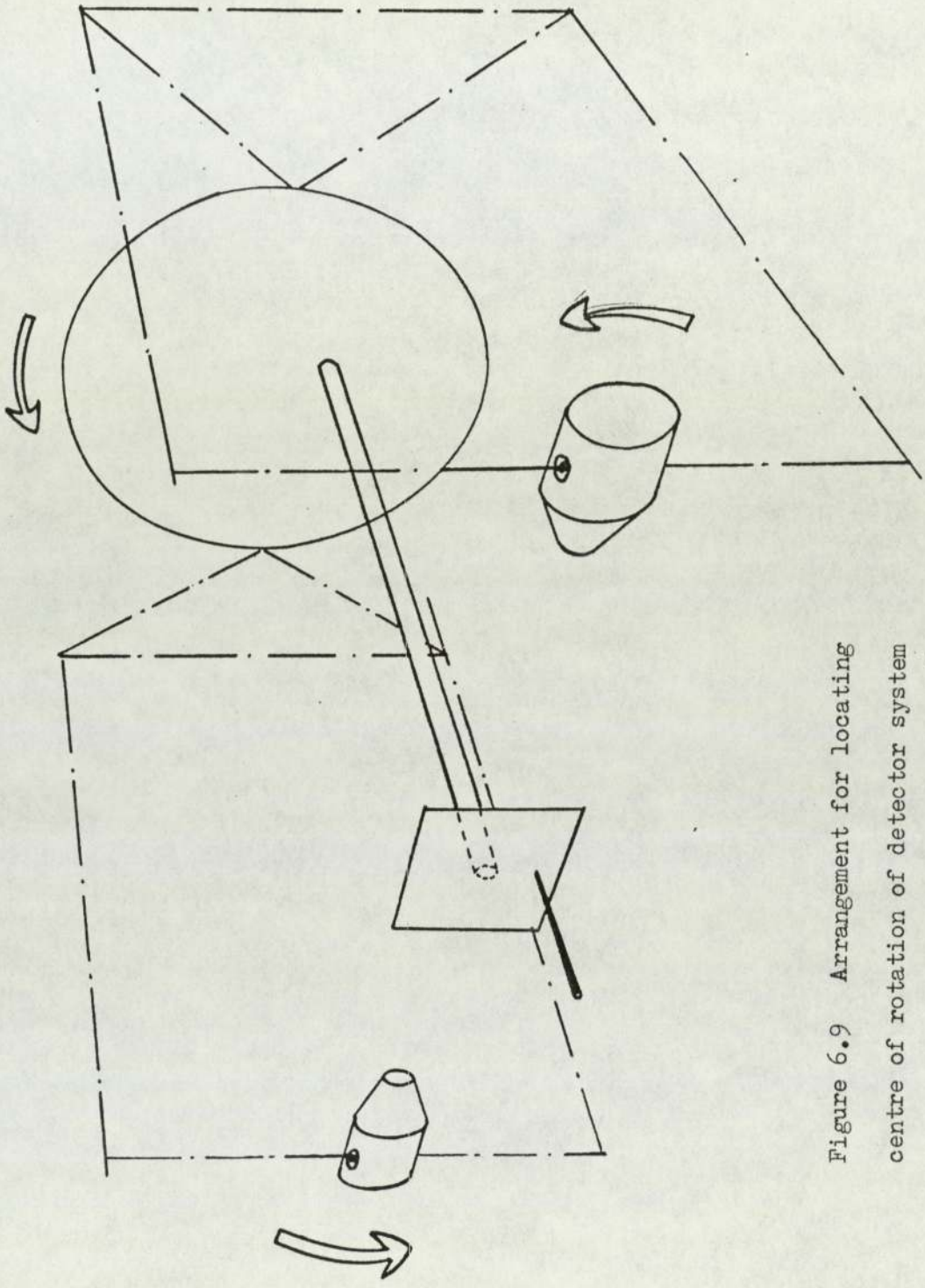

Figure 6.9 Arrangement for locating centre of rotation of detector system

the scanning frames at a point only 10.6 cms. from the limiting microswitch at one end of the scanning line. This gave a 'swept volume' when the scanner was rotated through 180° of only 21.2 cms. diameter, which would accommodate only rather small head sizes. Roughly 50% of patients would be expected to have heads larger than this.

The movement of the detector heads is limited by a series of microswitches. At each end of the scanning line are 'deceleration' microswitches which when struck by the detectors cause reversal of the detector motion. Thus if the scanner controls were inadvertantly set to drive the detectors beyond the permissable limits of the line, the microswitches would reverse the detector motion at the appropriate point, and prevent damage to the detectors or the motors. These microswitches were placed a few mms. clear of the yoke, to allow the detectors space to decelerate and reverse motion before striking the yoke. The scanner was designed to work at speeds of up to 5 cm/sec, but in fact the higher speeds were not used at all for brain scanning. It was therefore decided that if the speed were to be restricted to a normal maximum of 2.5 cm/sec the microswitch could be moved 1.4 cms. giving a usuable line length for section scanning of 24 cms. or 60 cells of 4 mm. width, which coincided conveniently with the buffer storage area of the computer. With the microswitch set in this new position, the detector assembly would strike the yoke if set to overun at a scanner speed of 3 cm/sec. There was thus an ample safety margin.

6.4 Image Reconstruction Methods

Fig 6.10 illustrates two scans of an object containing two active areas in a volume of uniform low activity. The two scans are performed at angles θ_1 and θ_2 and each is a line integral of the activity distribution function, which may be termed $g(x,y)$. The line integrals

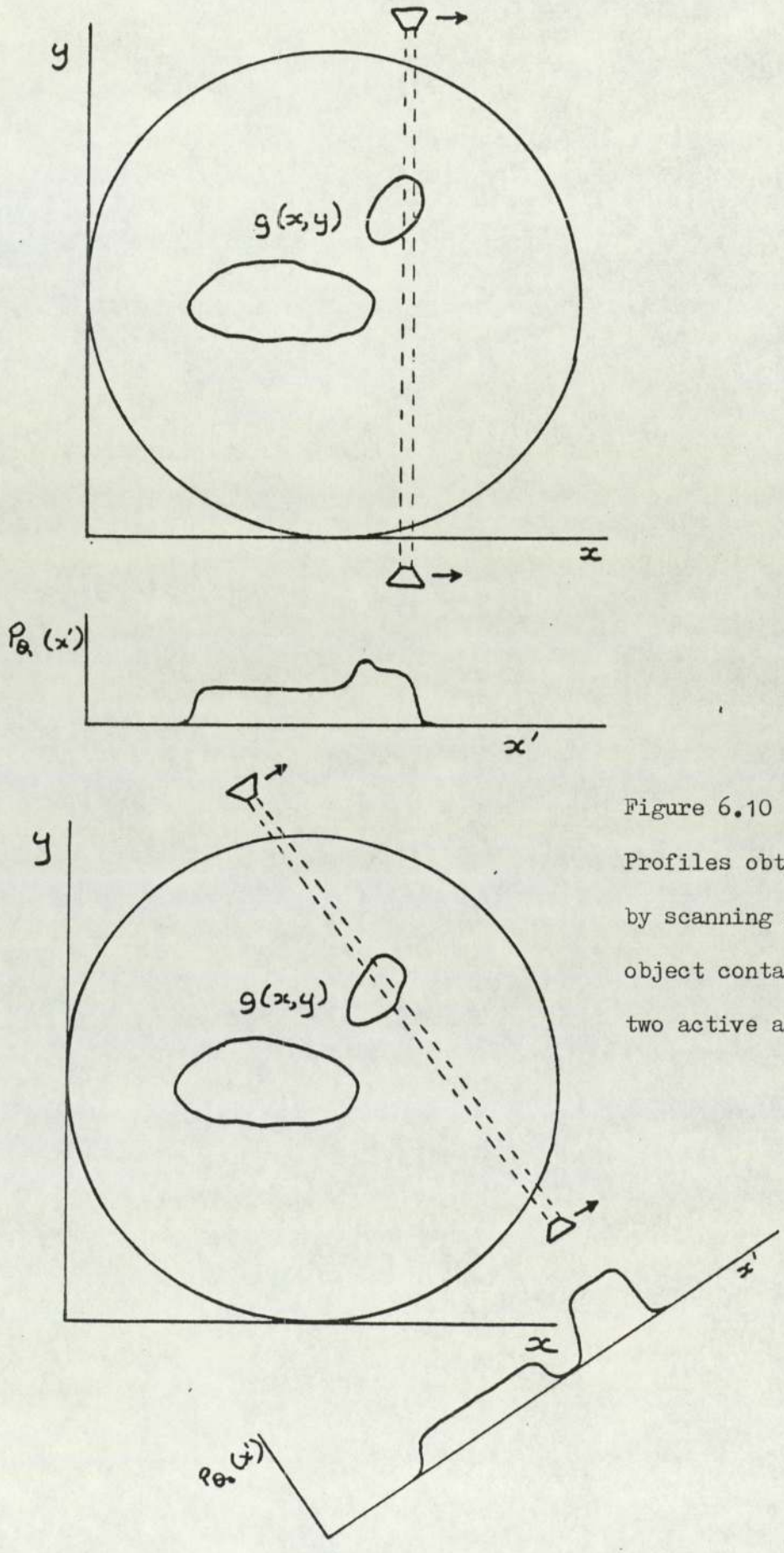

Figure 6.10
Profiles obtained by scanning an object containing two active areas

are referred to as projections for convenience. After one pass of the detectors over the object, the function $P_\theta(x')$ is known for all values of x', that is a profile at angle θ to some arbitrary baseline. If working in Cartesian coordinates, it is usual to take the x axis as the baseline, and the profile can then be expressed in terms of the rotated Cartesian axis in terms of x' only, where

$$x' = x \cos\theta + y \sin\theta$$

$$y' = x \sin\theta - y \cos\theta$$

The simplest means of reconstructing the image, given a series of profiles at different angles, θ, is 'back projection'. This method is illustrated in Fig. 6.11. Although this method does reveal the positions of the small circular sources of activity within the object, it will be noted that each source in the reconstructed distribution is a focus for a star-like artefactual distribution. In the limit, for an infinite number of profiles, the artefact becomes a 1/r function (for $r > r_{min}$ where r_{min} is the radius of the object) as illustrated in the figure. This method therefore, although yielding an approximate representation of the function $g(x,y)$ gives a high 'background'. The reconstructed image may be improved by subtracting a background term, but the method is clearly only capable of yielding a very approximate solution.

6.5. Successive Approximation Reconstruction Methods

Successive approximation reconstruction methods, in general, take an approximate solution to the intensity function, and work out the profiles which would be obtained from this initial solution. The calculated profiles are then compared to the actual profiles obtained from the object, and correction factors are worked out which are used to refine the model. This process goes through a number of iterations until the calculated profiles are in reasonable agreement with the actual profiles. The

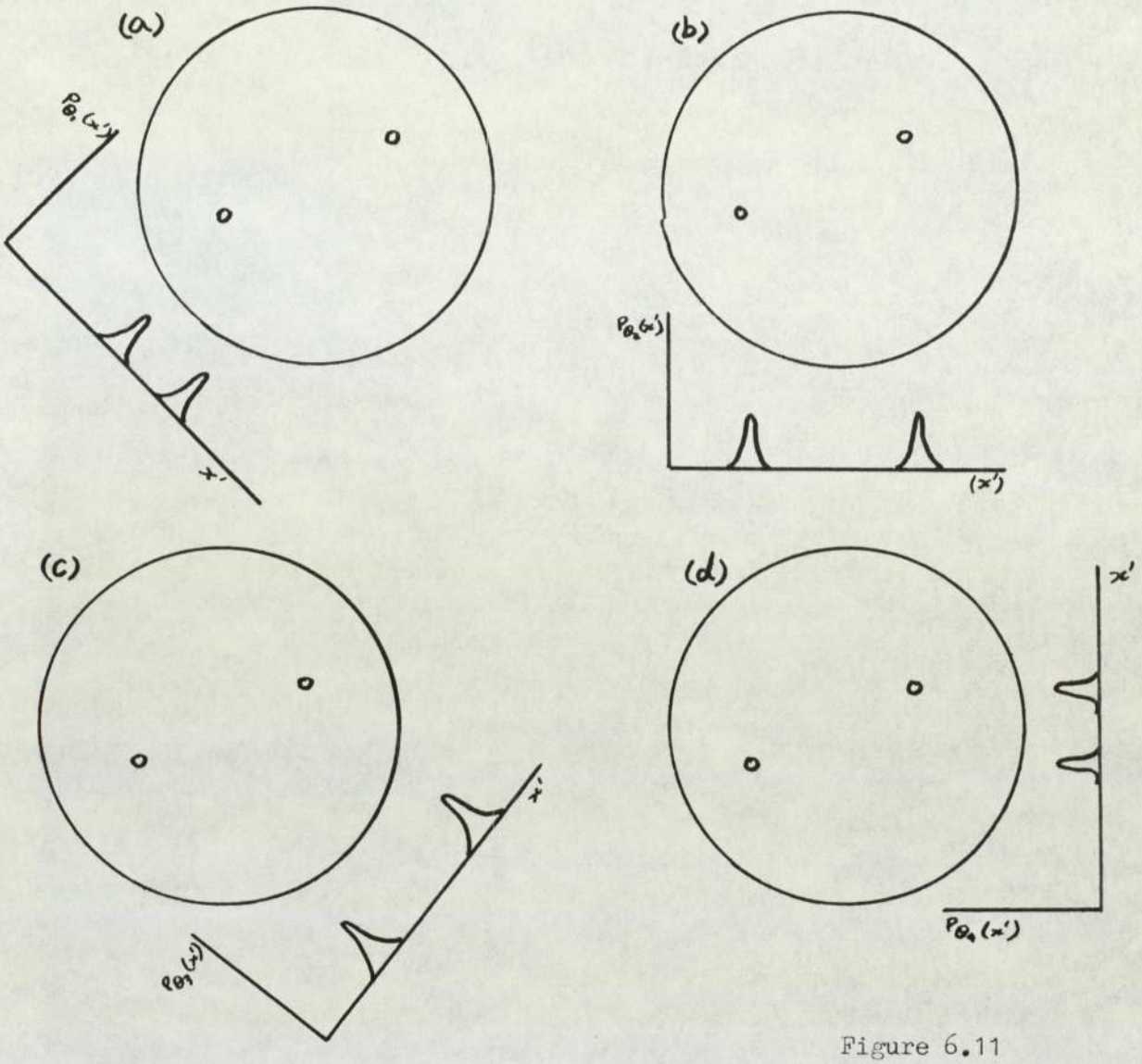

Figure 6.11

Back projection

of four profiles

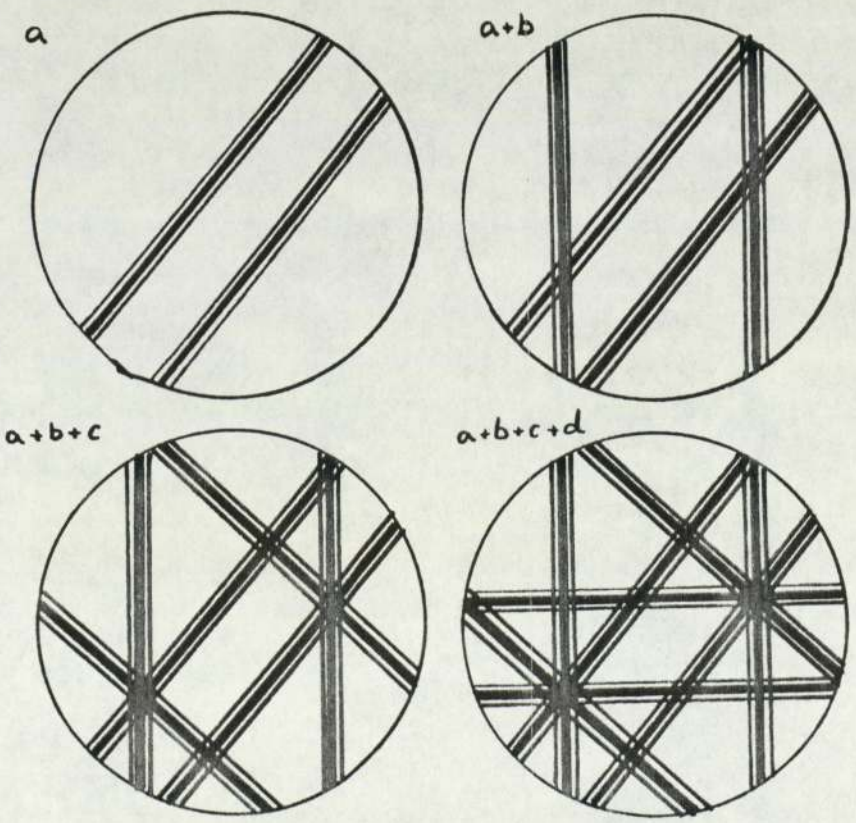

calculated intensity function should then resemble the actual intensity function.

There are two main groups of successive approximation methods. They differ in the way in which the correction factors to the matrix values making up the model are calculated. The two groups of techniques are often referred to as ART (Algebraic Reconstruction Technique) and SIRT (Simultaneous Iterative Reconstruction Technique).

6.5.1. Algebraic Reconstruction Technique

This method makes a new approximation based on the error resulting from the previous approximation. All points are corrected for each projection. The general form of the equation is

$$p^{n+1}(x,y) = p^{n}(x,y) + \frac{P_\theta(x') - R_\theta^n(x')}{N_\theta(x')} \qquad \ldots(6.5)$$

Where $p^n(x,y)$ is the value of a matrix element (x,y) in the 'reconstruction frame', n = number of iterations, $P_\theta(x')$ is the value of the projection of the actual intensity function at angle θ on a ray passing through (x,y), $R_\theta^n(x')$ is the calculated value of a projection of the 'reconstruction frame' at angle θ on a ray passing through (x,y) in the latter frame, and $N_\theta(x')$ is the number of matrix elements which lie along this ray.

A very simple example is shown in Fig.6.12 (a). In this case, a correct solution to the intensity function is obtained in two iterations.

A second example is given in Fig. 6.12 (b). In this case, an apparently correct solution is also obtained in two iterations, but the solution is not, in fact, identical to the original intensity function.

These examples illustrate one problem inherent in the method. There may not, in fact, be a unique solution to the problem, as the number

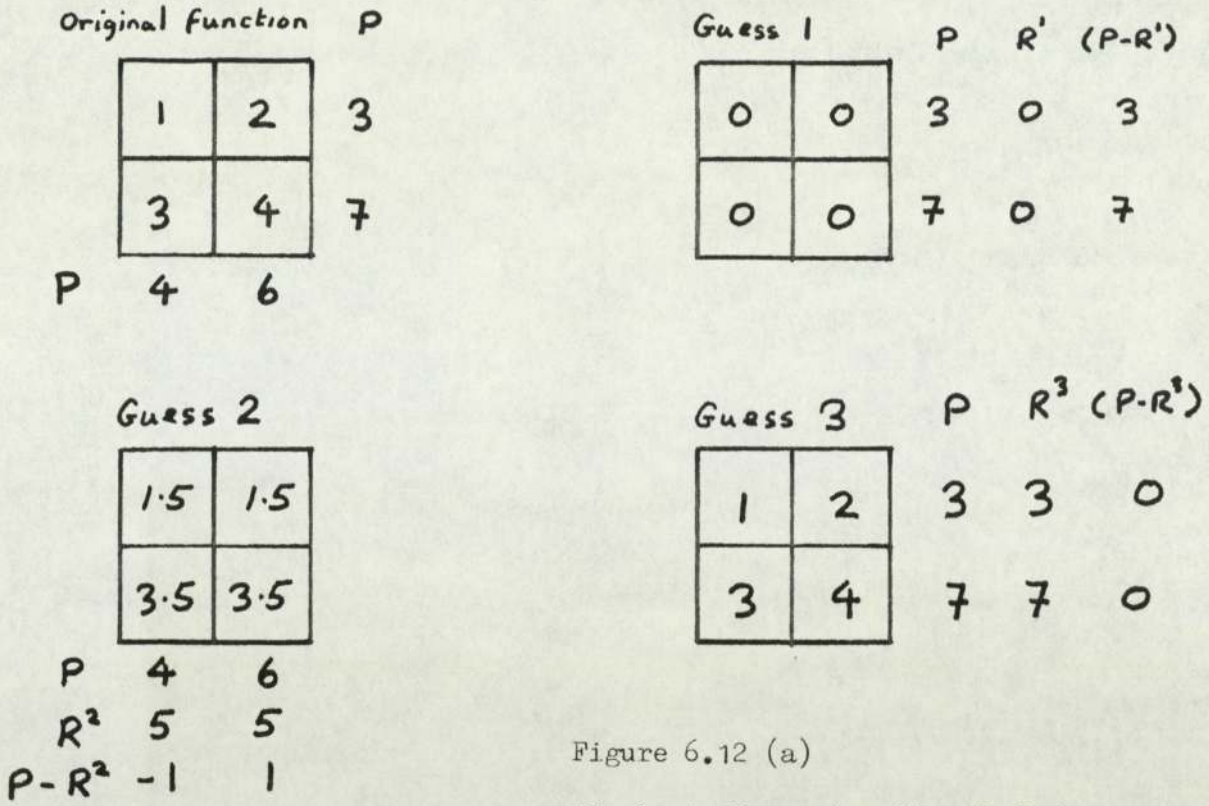

Figure 6.12 (a)

Algebraic Reconstruction Technique

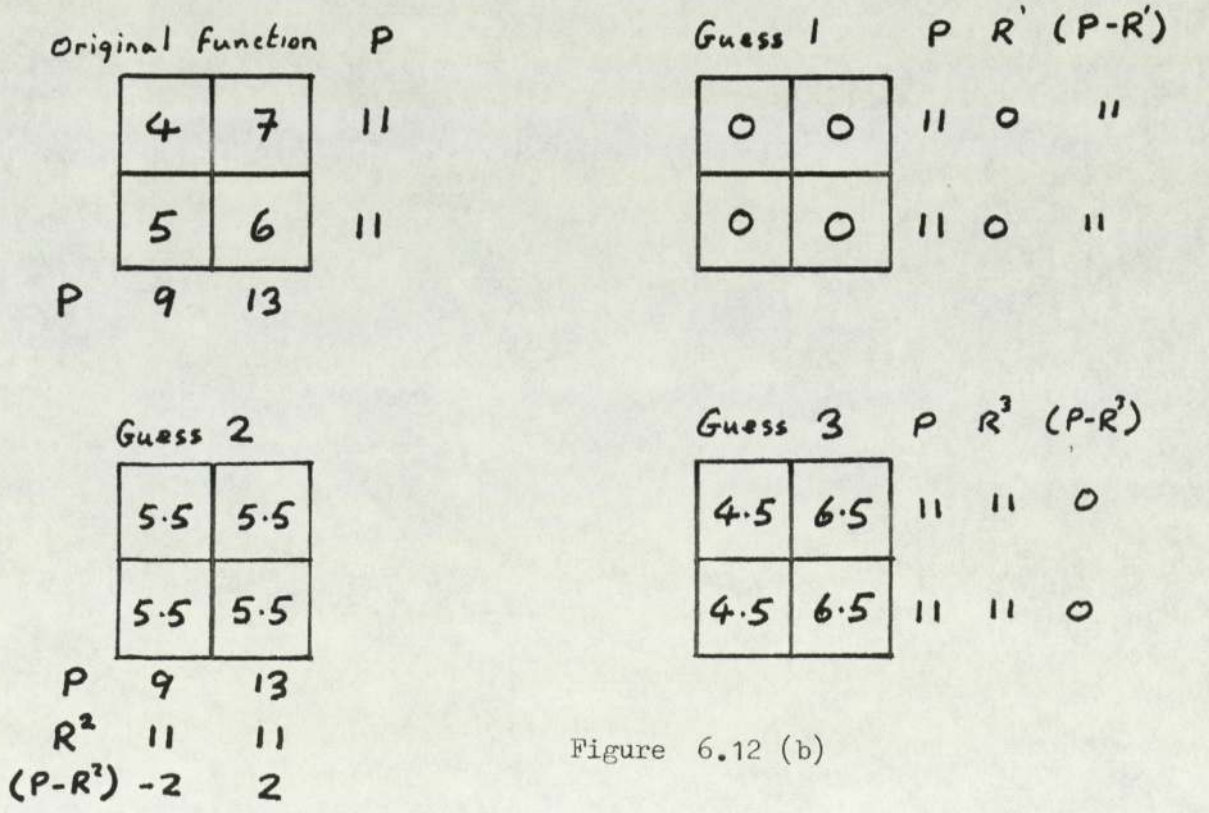

Figure 6.12 (b)

of equations one can obtain from the projection data may well be fewer than the number of unknowns. One may therefore be faced with the problem of selecting, from a number of solutions that satisfy the equations equally well, one which for some additional reason is considered most likely to provide the best approximation to the original intensity function.

In the real situation, there are two further factors which have to be taken into consideration. Firstly, the projection data are obtained experimentally and in most situations will contain appreciable statistical uncertainty.It is thus likely that the equations are inconsistent and that there is no exact solution at all. In this case, some means has to be found of determining the best approximate solution.

Secondly, the number of required unknowns and the number of equations may become so large that standard methods of solution become computationally unfeasible. The limitations imposed by computational speed must be carefully considered in implementing any proposed reconstruction algorithm.

In view of the above complicating factors, a modification of ART is often used in which some contraint is placed upon the values which matrix elements can be assigned. Such a method was proposed by Gordon et al. (1970) in which a matrix element was reassigned value 0 if the application of a correction factor would assign a negative value to the element. It is sometimes possible to apply considerable constraints because of prior knowledge of the main features of the intensity funtion. An obvious example is in the case of transverse section of the brain, where it is known that the relatively low activity of the normal brain tissue will be enclosed within the relatively high activity of the scalp. There is much scope for ingenuity in devising suitable constraints to improve the speed and accuracy of the reconstruction.

A further problem has been noted by Gilbert (1972 a). He notes that with real experimental data, as a consequence of the inconsistency of the intensity data, the first few results obtained by the unconstrained ART algorithm represent better and better solutions, but if the iterations are continued beyond a certain number, the results then become progressively worse. A means must thus be found for stopping the iterations at an appropriate point. This problem has been further examined by Herman. (1973)

6.5.2 Simultaneous Iterative Reconstruction Technique

This method was proposed by Goitein (1971) and later by Gilbert (1972 b). Whereas in ART, all points are corrected for each projection, in SIRT, each point is corrected for all projections. The general formula is

$$p^{n+1}(x,y) = p^{n}(x,y) + \frac{\sum_{\theta} P_{\theta}(x') - \sum_{\theta} R_{\theta}(x')}{\sum_{\theta} N_{\theta}(x')} \qquad \ldots (6.6)$$

An example of the use of SIRT is given in Fig. 6.13. Herman and Rowland have suggested that this method had particular value where the projection data are very noisy. A disadvantage is that a much larger computer memory is required to implement SIRT than is required by ART.

6.6 Methods Using The Fourier Transformation

The basis of this method is the theorom which states that the Fourier transform of a two dimensional projection of a three dimensional object is identical to the corresponding central section of the three dimensional Fourier transform of the object. Since, in transverse sectional tomography we are essentially concerned with a two dimensional object, that is, a 'slice' through the real three dimensional object, we can reduce the above theorom to the two dimensional version; the Fourier transform of the one dimensional projection of a two dimensional object is identical to

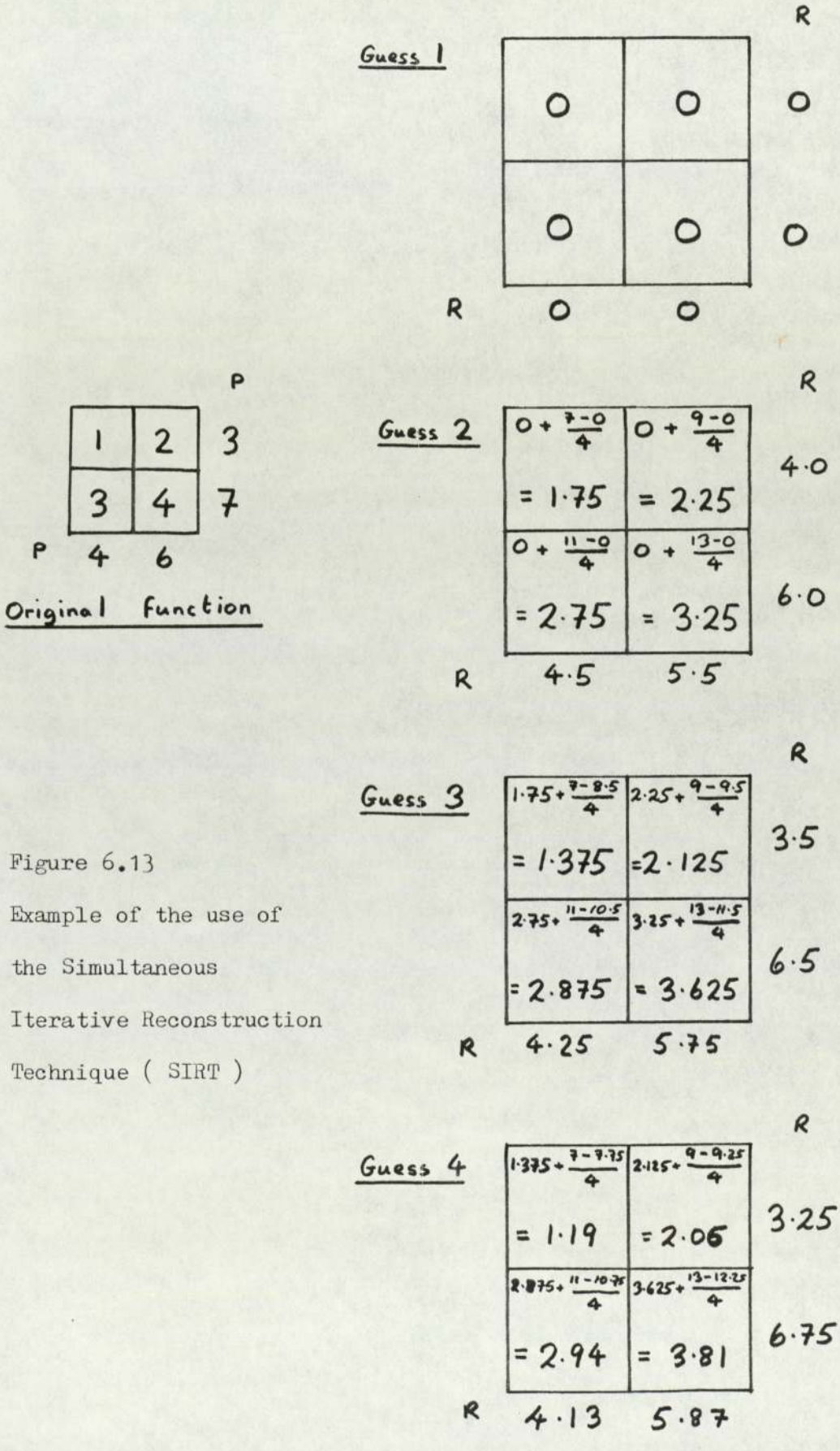

Figure 6.13
Example of the use of the Simultaneous Iterative Reconstruction Technique (SIRT)

the corresponding central section of the two dimensional transform of the object.

In mathematical terms, if $g(x,y)$ is the original intensity function, and P_θ is the projection of this function onto a line making an angle θ to the x axis, then if F is the Fourier operator, and X' is the distance along the central section at angle θ in Fourier space.

$$F\left[P_\theta(x')\right] X' = \int_{-\infty}^{\infty} e^{-2\pi i X' x'} \left[P_\theta(x')\right] dx' \qquad \ldots (6.7)$$

Thus if the projections in real space are known, it is possible to calculate a series of central sections of the two dimensional Fourier transform $F(X,Y)$ at various angles, θ, to the X axis.

Having obtained these central sections, it may then be possible to interpolate between them to obtain $F(X,Y)$ for any values of X,Y. Having now obtained the two dimensional Fourier transform, it is possible, by using the inverse Fourier transform operation, to obtain the original function $g(x,y)$.

This technique appears at first sight to offer distinct advantages over the successive approximation methods, in that it is mathematically precise.

In practice, however, the reconstruction mode can never be more than an estimate of the original intensity function for the following reasons:

(a) The physical projection data are only approximations of the functions $P_\theta(x')$, $P_{\theta_2}(x')$ ...

(b) Any interpolation procedure can only give approximate values for the points X, Y in the two dimensional Fourier transform which do not lie on the central sections.

(c) The integrals in the Fourier transforms have to be evaluated numerically and some error is inevitable.

The development of algorithms for fast Fourier transforms and purpose built microcomputers which allow the very rapid evaluation of Fourier transforms have made this method a potentially attractive one in certain applications, particularly in x-ray transverse axial tomography, where the very high photon flux permits reasonably accurate projections to be obtained. Such a method has been described by Peters et. al. (1973).

6.6.1 The 'Convolution' Method

This group of methods derive from work by Radon, published in 1917. He discussed the following question. If $g(r,\theta)$ is a density function (expressed in polar coordinates) and $P_\theta(x')$ is the projection of this function onto an axis at angle θ', is a knowledge of projections $P_{\theta'}(x')$ for all θ' sufficient to determine $g(r,\theta)$?

He was able to show that:

$$g(r,\theta) = \frac{1}{2\pi^2} \int_{-\pi/2}^{\pi/2} \int_{-\infty}^{\infty} \frac{dP_{\theta'}(x')}{dx'} \cdot \frac{1}{r.\sin(\theta - \theta') - x'} .dx'd\theta' \qquad .....(6.8)$$

A formula of this type can be used to estimate the function $g(r,\theta)$ from the projection data $P_\theta(x')$ without having to perform Fourier transforms. The formula above is exact, and under ideal conditions as with the Fourier transform method, will reconstruct the function exactly.

A number of methods of reconstructing a density or intensity function can be derived from Radon's equation. These include the methods of Bracewell and Riddle (1967), Ramachandran and Lakshminarayanan (1971), Gilbert (1972b) and Vainshtein and Orlov (1972).

These workers used somewhat different approximations in the

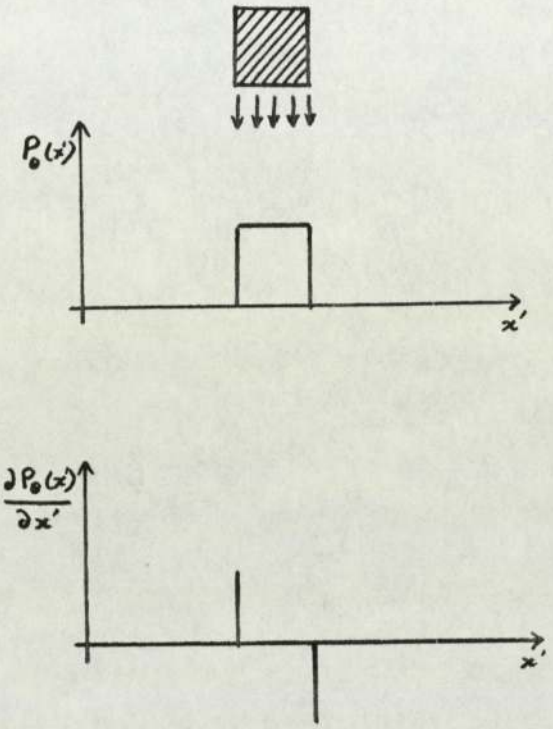

Figure 6.14

Example of the use of a 'convolution' algorithm (Equation 6.10)

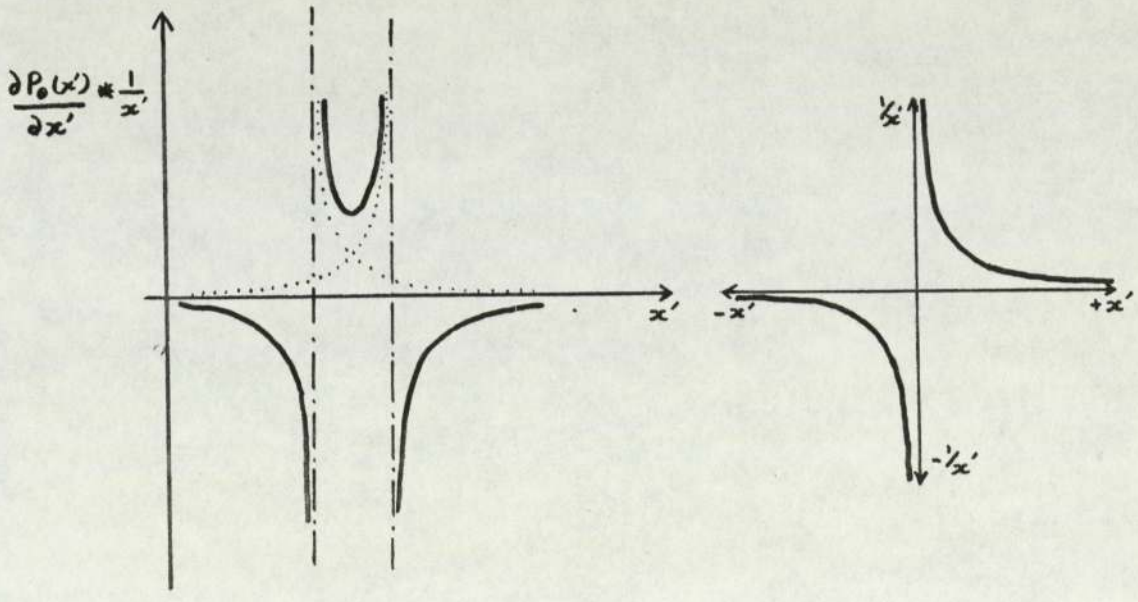

evaluation of equation (6.8), so the results lead to different estimates of the structure to be reconstructed. The most appropriate approximation for reconstructing a particular type of object can often only be found by experiment.

In principle, the above methods seek to obtain a function $G_\theta(x')$ which can be computed from the projections, such that

$$g(x,y) = \sum_\theta G_\theta(x') \qquad \ldots (6.9)$$

Gilbert showed that:

$$G_\theta(x') = \frac{dP_\theta(x')}{dx'} * \frac{1}{x'} \qquad \ldots (6.10)$$

is such a function, where* represents the convolution operation. The similarity to the Radon equation is evident. A simple example of the use of Gilbert's equation is given in Fig. 6.14. If the functions resulting from this operation for all values of θ are back projected, the result will be an accurate reconstruction of the original object. The blurring of the image resulting from the straightforward back projection process is removed by the modification of the profiles prior to the back projection in accordance with the above equation.

Bracewell and Riddle proposed a different approximation which does not require differentiation of the profiles, but is simply a convolution with a modification function. This method has been used very successfully by Keyes to reconstruct transverse sectional isotope scan data provided by the Aberdeen Sectional Scanner. Keyes programs were used in a pilot study to establish the suitability of the convolution algorithm to the problem of reconstructing data provided by the J & P MS 430 Scanner. The methods and results of this study will be discussed in the next chapter.

CHAPTER 7

A pilot study of radionuclide tomography

7.1 A Pilot Study Of Transverse Axial Isotope Imaging Examinations

In order to carry out a pilot study into the potential value of transverse axial isotope imaging examinations it was decided to use established and tested programs. Of the few groups in Europe with experience in this technique, the group in Aberdeen had by far the most experience, and they generously allowed their programs to be used. Fortuitously, they also used a Nuclear Data 50/50 system, although their equipment configuration was not identical to the Midland Centre for Neurosurgery 50/50 system. Even so, very few program changes were necessary in order to run the Aberdeen programs on the Midland Centre system. New input and output procedures were, however, necessary, as were procedures to store raw and processed data on the Ampex tape deck which is used for bulk storage on the Midland Centre system. Initial investigations were carried out using a phantom, and then a small series of clinical cases, both normal and abnormal, were scanned. The results correlated well with data obtained from more conventional investigative procedures and gave some indication of the additional information which could be obtained from the section scan. Some limitations of the method and some practical difficulties were also noted, and a development program was undertaken to resolve some of the latter problems.

7.2 The Reconstruction Algorithm.

The methods used in these programs have been fully described by Keyes (1976). A brief description of the method is reproduced here.

The method used was that of Bracewell and Riddle, in which the original profiles were modified so that when back projected, they reconstructed the original intensity function.

The effect of the operation was to multiply the Fourier transform of the profiles with a ramp function (i.e. amplification directly proportional to spatial frequency) out to a limiting spatial frequency R_M. Any spatial frequencies above R_M were removed. The reconstructed density at a point (in the ideal case) was then given by the integral of all the modified projections through that point.

$$g_{BR}(x,y) = \int_0^{\pi} G_\theta(x')\, d\theta \qquad \ldots (7.1)$$

where G_θ represents the modifed projections. This modification was performed in accordance with the equation

$$G_\theta(x') = P_\theta(x') * R_M\left[\frac{\sin 2\pi R_m x'}{\pi R_m x'} - \left(\frac{\sin \pi R_m x'}{\pi R_m x'}\right)^2\right] \ldots (7.2)$$

In the realisation of the method described by Keyes, the profiles were convoluted with a symmetric non-recursive digital filter with 31 weighting values, calculated according to the equation

$$Wi = W_{-i} = Rm\left[\frac{\sin 2\pi R_m i\Delta}{\pi R_m i\Delta} - \left(\frac{\sin \pi R_m i\Delta}{\pi R_m i\Delta}\right)^2\right](.54+.46\,\frac{\cos 2\pi i}{31}) \ldots (7.3)$$

for $i = 0, 1 \ldots\ldots 15$. Δ was the interval at which the data from the scanner were sampled, typically 4 mm. The cosine term was a window function of the type described by Gold and Rader, (1969) and was necessary to prevent oscillations due to truncation of the convolution function after 15 values. It was also useful to reduce statistical noise in the data. The values calculated as above were stored as a look up table in the reconstruction program. Using Keyes program, convolution of a single profile took approximately 4 seconds.

7.3 Implementation Of The Algorithm.

In the Aberdeen system, the data collected by the section scanner were punched on paper tape. The data consisted of the number of gamma rays detected during a preset increment of scan line, typically 4 mm. At the end of each scan line, the detector system rotated an amount (typically 6°) about a fixed axis and another scan line was performed in the reverse direction. These data were read into the Aberdeen Nuclear Data system upper memory using a program stored in the PDP8 memory field 1. The data were then assembled using a program stored in the PDP8 field 0 (with some subroutines in field 1). The reconstruction programs were written in DEC 4K FORTRAN, with PAL3 subroutines. The reconstruction program fell into three parts: an

alignment check on the data, the modification of the profiles with a digital filter, and a back projection procedure.

7.3.1 Check On The Alignment Of The Data.

It was most important that the data should be aligned with respect to the axis of rotation. The back projection program assumed the position of the axis of rotation to be at cell position (32,32) where reconstruction was performed on a 64 x 64 matrix. It was necessary that the data be similarly aligned, or artefacts would be produced when the data were reconstructed.

For the purposes of the reconstruction program only 30 profiles at 6° angular increments were required, i.e. profiles P_{θ} ($\theta = 0, 6^{\circ}. \ldots\ldots 174^{\circ}$). In order to carry out an alignment check, a 31st profile was scanned, at 180°. This profile should be identical to the 0° profile except that, because the detector system had rotated through 180°, the profile would read from right to left, instead of left to right as in the case of the 0° profile. It was possible that (a) the scanning line length for a particular case may be insufficient to provide data for all 64 cells allocated in storage for each profile, or (b) the limit switches might have been set so that the number of cells in the profile is not symmetrical with respect to the axis of rotation. The 1st and the 31st profiles were therefore compared and any misalignment was corrected by shifting all the profiles by a calculated number of cells, in order to store the data in a symmetrical manner around cell 32 of the line.

The required shift was calculated by computing the centre of gravity of the first profile about the left hand edge and the centre of gravity of the final profile about the right hand edge. If a discrepancy was found, the required shift, N, to align the data was calculated, and the storage locations for all data were shifted by the required number of cells. This subroutine was such that for a left to right shift, data in the last N cells of profile P_R will appear after

the shift operation in the first N cells of profile P_{n+1}. As these values represent only background, no great inaccuracy was introduced.

7.3.2 Modification of the data profiles

Having performed the shift operation, the program then modified all the profiles by convolution with the pre-calculated digital filter values. These values were stored in floating point format, each occupying three 12 bit words, but since the filter was symmetrical (and $W_o = 1$) it was necessary to store only 15 fractional values, ie 45 words of memory. It was not necessary to convolute the 31st profile, as this was not used in the subsequent back projection operation.

7.3.3 Back projection of the modified profiles

Values obtained by the modification of the data profiles by convolution with the digital filter were stored in the Nuclear Data upper memory field. The lower memory field was used as a 'reconstruction field' for the back projection of the modified profiles.

The back projection part of the program took each point in the reconstruction frame in sequence, once for each profile, and for the particular value of θ applicable to this profile, calculated the address of the value in upper memory to be added to the value of the point in the reconstruction frame.

The origin of cartesian coordinates was taken as the centre of the reconstruction frame, i.e. at position 31.5, 31.5. After rotation through θ (see fig. 7.1),

$$X' = r \cos (\phi + \theta) \qquad \ldots (7.4)$$

If the side of the square data cell is taken as unit length, then

$$x = i - 31.5 = r \cos \phi \qquad \ldots (7.5)$$

$$y = j - 31.5 = r \sin \phi \qquad \ldots (7.6)$$

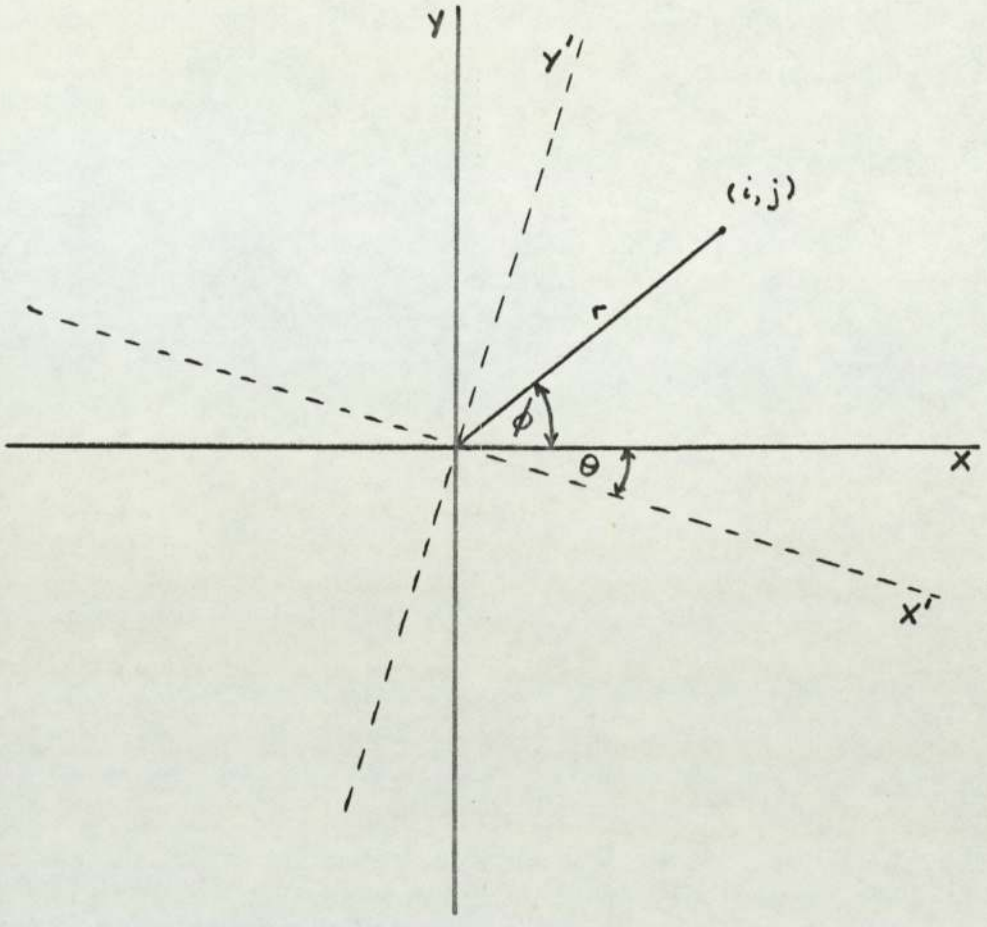

Figure 7.1 Rotation of cartesian coordinate system

Address of point in data frame is (i,j)

where i = 0,63; j = 0,63

Expanding equation 7.4. and substituting for r cos ϕ and r sin ϕ from equations 7.5 and 7.6 gives the expression..

$$X' = (i - 31.5) \cos\theta - (j - 31.5) \sin\theta$$

$$= i \cos\theta - j \sin\theta + 31.5 (\sin\theta - \cos\theta) \quad ...(7.7).$$

The address of the value to the taken from the appropriate profile in upper memory is $(X' + 31.5)$. As the address is an integer value which is obtained from the calculated value by truncation, it is necessary to add 0.5 to the calculated value before truncation to correct any error in rounding off.

Hence, if M is the address of the value to be taken from profile P_{θ}!

$$M = X' + 31.5 + 0.5$$

$$= X' + 32 \quad ...(7.8)$$

Substituting for X' from (7.7)

$$M = i \cos\theta - j \sin\theta + 31.5 (\sin\theta - \cos\theta) + 32 \quad ...(7.9)$$

Since the profiles are stored sequentially in upper memory, 64 is added to the address for each new profile, ie.

$MQ = M + IM$ where $IM = 64, 128 ...$

MQ is the absolute address in upper memory of the appropriate data point to be added to point (j,k) in the reconstruction frame. It is necessary to check that the value of M is an integer between 0 and 63 as some points in the reconstruction frame will be beyond the limits of certain profiles. The limit of valid results in the reconstruction frame is a circular area of diameter 64 units.

7.4 Additional Software Required To Implement Aberdeen Programs.

Because of the different methods of data capture, storage and display used at Aberdeen and Birmingham, some additional programming was necessary.

7.4.1 Input Procedures.

Data was normally captured 'on line' to the computer, the

data from the two detectors being stored separately in Nuclear Data upper and lower memories.

Storing the data in this way admits the possibility of combining the data in ways other than straightforward addition. It had been demonstrated in plotting the collimator characteristics that there appeared to be a significant difference in sensitivity between the two detectors. In the early results, therefore, a multiplication factor was applied to one set of data before adding the data together and storing in upper memory. Subsequent detailed examination of the detectors showed that one of the detectors had been incorrectly assembled. Correct assembly virtually eliminated the difference in the sensitivities, and addition of the two sets of data was subsequently employed.

On occasion, the computer was not available when required for a section scan, and in this case, data were stored on the magnetic tape cassette system of the scanner. Unfortunately, when data stored in this way were played back to the computer, the data were modified by the addition of a small Y offset, usually amounting to two or three Y increments. It was necessary to remove this before the data could be reconstructed.

The data input program incorporated a procedure which could be entered if data were acquired off-line rather than on-line. In the former case, data were entered from the tape recorder, and after data entry, an integral value was entered manually from the teletype keyboard to specify a shift of the data by N profiles. The data were then in a suitable form for analysis, and reconstruction could proceed.

Before entering the reconstruction program, data were stored on 7 track digital magnetic tape. Data in the 50/50 lower memory were shifted up by one profile, and a record identification consisting of the patient's name and departmental reference number was written

into the first profile. Both data frames were then written onto magnetic tape, and data in lower memory were then restored to the original form before reconstruction commenced.

7.4.2 Output Procedures.

Data were reconstructed on a 64 x 64 cell matrix, each matrix element representing an area of 4 mm x 4 mm. The form of output most useful to the neurosurgeon is a full size one, as measurements can then be taken which are of value in planning the operation. If, however, a 4 mm square cell is used to display the result, the pictures appear very coarse grained, and interpretation is difficult. Most interpreters of the results therefore prefer a 2 mm square cell in the final presentation of the data, and this preference was catered for in displaying the results. A procedure was written which employed a 5 point smoothing function to display the result in each 4 mm square cell as four 2 mm square cells.

To display the results, intensity data in the form of analogue voltage levels in the range 0 - 1 V have to be transmitted to the scanner in response to each address generated by the scanner interface. This analogue level was derived from the signal applied to the Y input of the display oscilloscope by suitable selection of the display switches. The scanner was capable of displaying independently two channels of information, but in this application identical information was presented to both display channels. This was of value, because although the 'set intensity' circuits of the scanner display were disabled during computer playback, the 'background subtract' circuits were not. It was therefore possible to set different background suppression values for the two display channels, and this was sometimes of value in enhancing the appearance of any lesions detected.

For playback, the two parameter ADC control was set into the 'computer playback' mode, and the 'strobe out' pulses generated by the scanner interface were selected by a switch in the scanner dataway terminating module in the Nuclear data 50/50 system. The 'strobe out' pulses were generated by the scanner at the end of each 2 mm x 2 mm cell as the scanner scanned over the display field. When the 'strobe out' pulse occurred, the X and Y inputs were sampled, and an address was generated which was stored in the last channel of the 50/50 memory. The value stored in this channel was sampled by the computer, and when a non-zero value was found (indicating the generation of an address) the value of that particular display point was calculated, and a suitable voltage was applied to the Y input of the oscilloscope. This value was held for sufficient time to allow the scanner display circuits to sample the analogue level and after clearing the last channel of memory, the computer then set the value in the last channel of 50/50 memory to zero and awaited the generation of the address of the next data point to be displayed.

7.5. The Computer Program

The input, data storage, reconstruction and data display elements of the program were combined into a single program, which occupied almost the whole of the 8K core memory of the PDP8L, in addition to the 4K 24 bit memory of the 50/50 storage and display unit. Total core requirements were thus approximately 16K 12 bit words of memory.

The complete program as described above took approximately 10 minutes to run, and displaying the result full size using 2 mm square elements required a further 15 minutes. Scanning the patient took approximately 7.5 minutes for each complete section. Considerable operator intervention was required to set the computer and 50/50 switches to the appropriate positions for different phases of the program. Despite these limitations, however, useful results were

obtained which enabled a preliminary assessment of the value of the method to be made.

7.6. Design of a phantom to test the section scan method.

In order to make a preliminary assessment of the section scan method in practice, a phantom was constructed by the University of Aston. This phantom is illustrated in fig. 7.2.

The phantom consists of a perspex cylinder of 15 cm. internal diameter, with a flange at one end into which a rubber O ring is fitted. The cylinder can be closed with a circular face plate screwed against the flange, and filling holes are provided in the flange to allow the cylinder to be filled with a radioactive solution.

The cylinder contains a liner which holds in position radioactive targets. The usual target configuration is a central tube 2 cm. in diameter containing a radioactive solution, and an off axis tube (also 2 cm. in diameter) situated 3.5 cm. from the central axis. It is possible, by removing the central tube, to fit a transverse axial tube to give some indication of the variation of resolution and sensitivity across a diameter.

In order to simulate absorption and scatter in the bone of the skull, the perspex cylinder may be enclosed within a close fitting aluminium sleeve 3mm in thickness.

7.6.1 Results obtained with Aston University Phantom.

Scans were carried out with the radioisotope concentrations in the surrounding fluid, the central tube and the off axis tube in the ratio 1 : 5 : 3, both with and without the aluminium shell. The concentrations were such as to give counting rates similar to these encountered in brain scanning with Technetium 99m.

The results are shown in fig. 7.3 (a) and (b). Both 'targets' are clearly resolved, and the central tube appears 'hotter' than the off axis tube. If the maximum intensity in the reconstruction of the

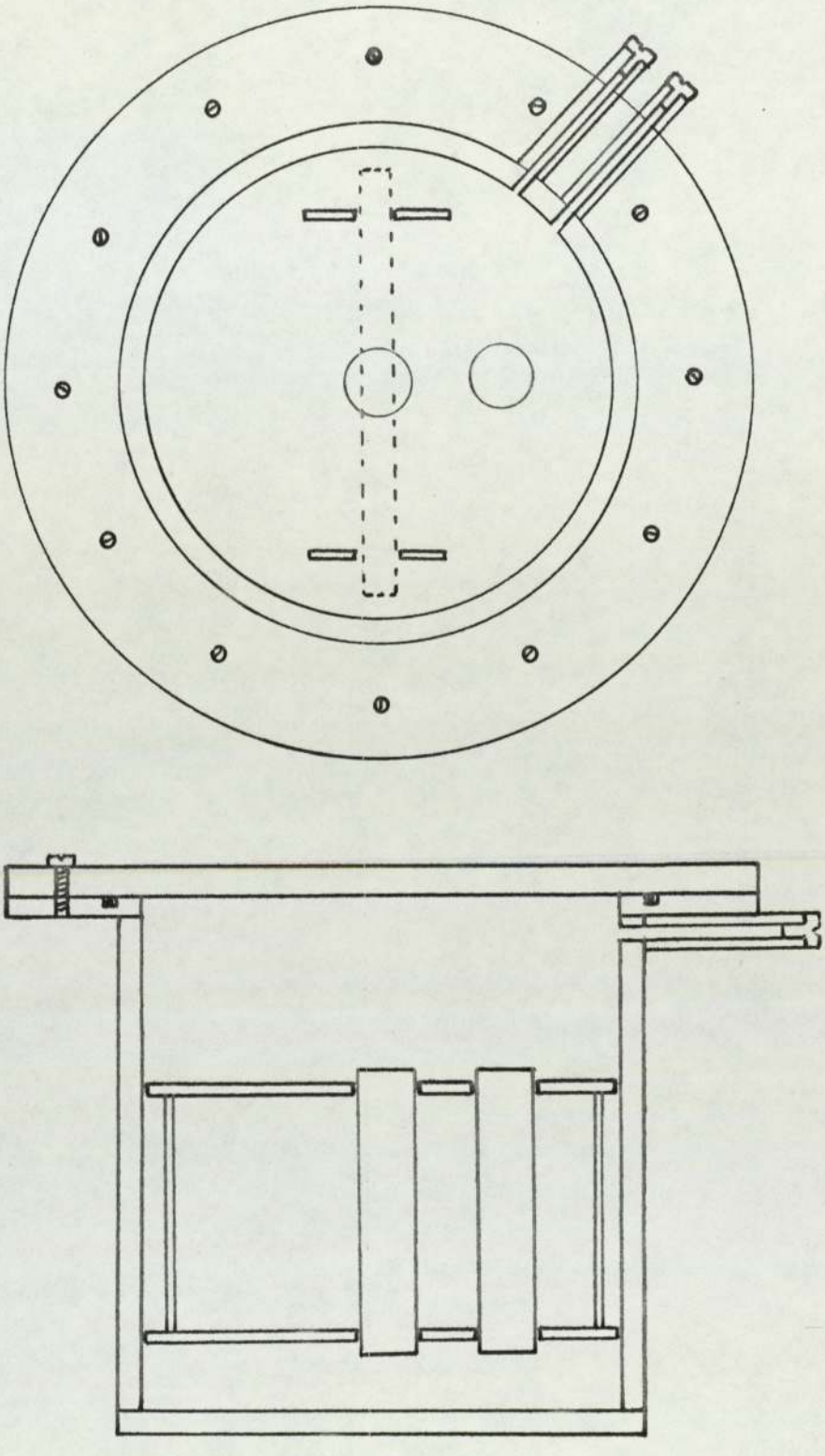

Figure 7.2 The University of Aston phantom.

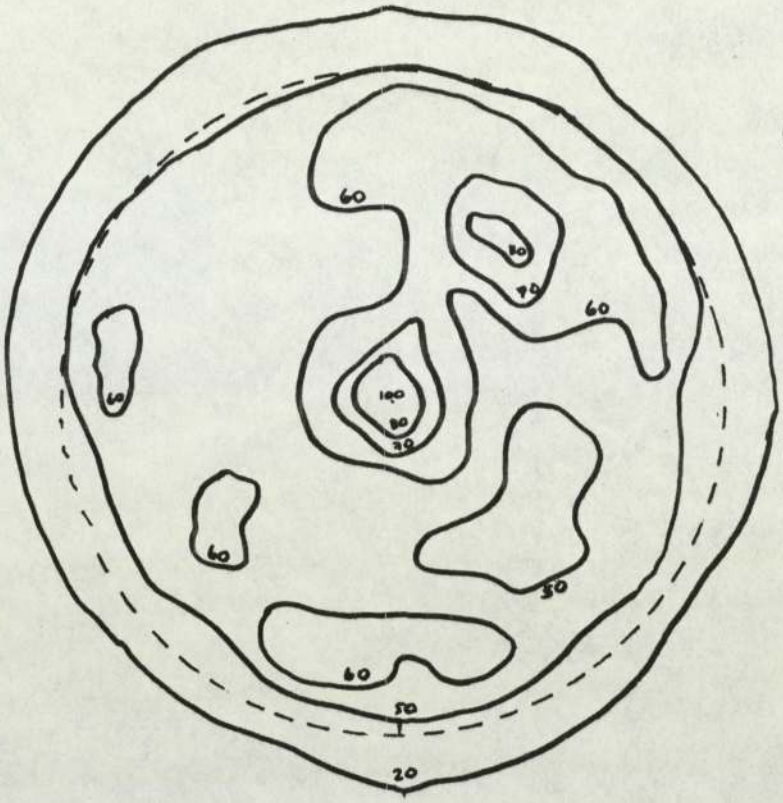

(a)

Figure 7.3 Scans of phantom fitted with central tube of activity 5 units/ml and off axis tube of activity 3 units/ml in surrounding fluid of activity 1 unit/ml, (a) without (b) with aluminium shell

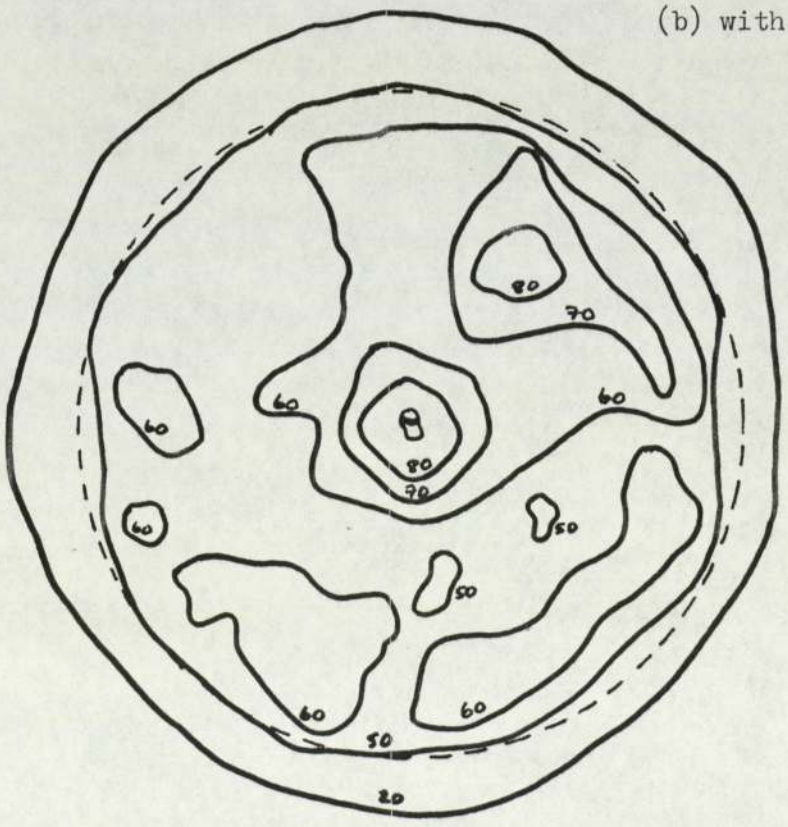

(b)

central tube is taken as 100%. the maximum in the region of the off axis tube becomes 90% and the general level in the surrounding solution about 60%. The general level of the background is therefore a good deal higher than expected. It is also evident, from a study of fig. 7.3. that in the reconstruction too much activity has been attributed to the superficial rim of the phantom. This is only to be expected in view of the collimator characteristics discussed previously (as fig 6.8). Obviously some correction must be made for the non-uniformity of the detector system if quantitative results are to be obtained.

Fig. 7.4. shows the reconstructed result obtained when a transverse axial tube was fitted in place of the central tube in the phantom. The axial tube is 1.4 cm. in diameter, or about the same order as the collimator resolution. The radioactive concentration in the axial tube is five times that in the surrounding fluid. Because of the relatively small diameter of this tube very careful positioning is required to ensure that the tube is fully in the plane of the section being scanned. This is especially difficult when the aluminium shell is fitted.

Results obtained with this source configuration confirm the impression given by the previous experiments, that sensitivity is reduced with increasing depth in the phantom.

7.7. Patient investigations:-

Initially a number of apparently normal patients were examined, i.e. patients in which the conventional radioisotope scans had revealed no abnormality. Sections were taken in a plane about 4 cm. above the orbit-meatal baseline.

The first results obtained were a little puzzling. The skull outline was clearly shown, but the intensity in the region of the skull was rather non-uniform. Within the skull, the reconstructed intensity distribution presented a curious mottled appearences. This may be seen

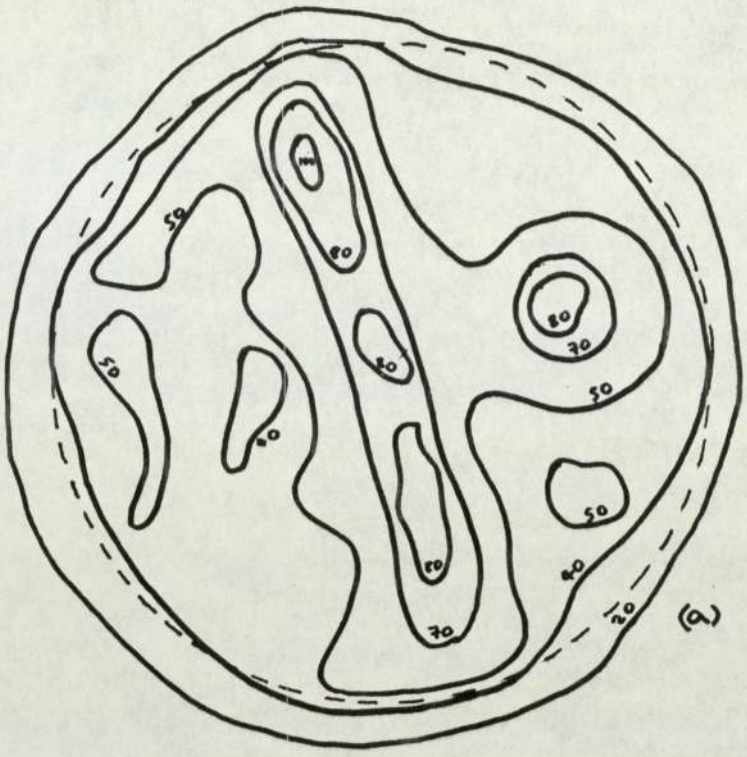

Figure 7.4 Scans of phantom fitted with transverse axial tube of activity 5 units/ml, off axis tube of activity 3 units/ml in surrounding fluid of activity 1 unit/ml, (a) without (b) with aluminium shell. Broken line indicates edge of phantom.

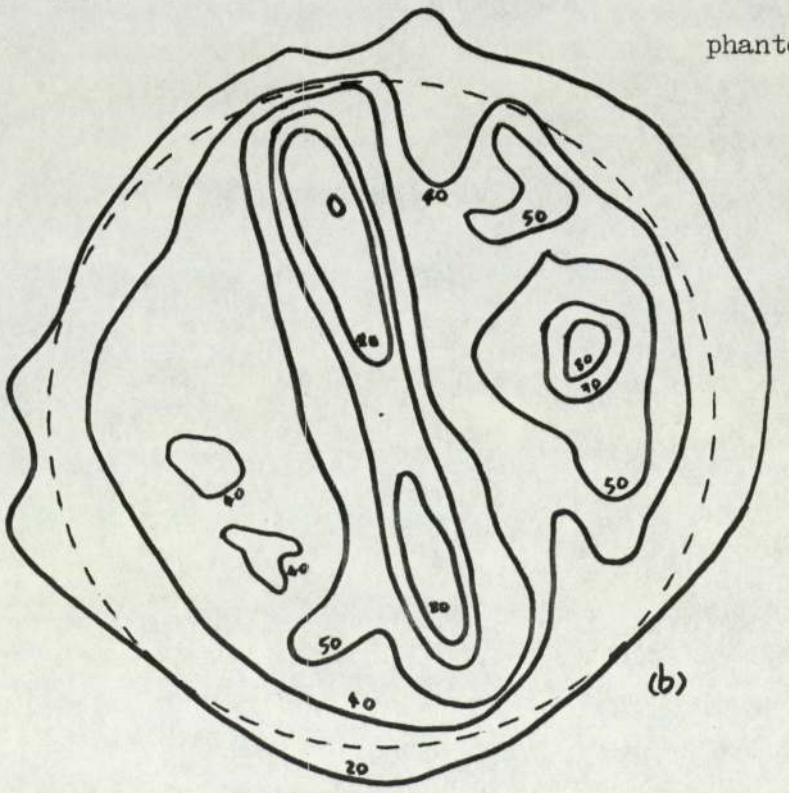

in the two normal scans reproduced in fig. 7.5. It was at first thought that these dark bands might be due to structure within the brain, but it was eventually concluded that they were artefacts. The use of a 10%-15% background subtraction when replaying the image will remove this mottled appearance, and improve the visibility of any lesion present.

A number of cases showing positive uptake of isotope on the conventional scan were also section scanned using the Aberdeen program. Two examples are given in fig. 7.6.

The patient whose isotope brain scan is reproduced in fig. 7.6. (a) was well until he suffered a paroxysm of laughter whilst watching television which led into an epileptic fit. He had a further attack two weeks later. An isotope brain scan at this time showed a small rounded lesion, which angiography revealed to be a malignant tumour. Two further brain scans, at intervals of about three months, revealed the rapid growth of the tumour. On the occasion of the third isotope scan, a section scan was also performed.

The section scan revealed that the tumour had a highly irregular structure. This finding was not believed at the time, but subsequent experiences with isotope section scans, and more recently with the E.M.I. X-ray scanner has shown that such an apperance is not at all unusual in cases of malignant tumours, and is, indeed, a useful pointer to be diagnosis of malignancy.

The patient whose scan reproduced in fig. 7.6 (b) had a very short history of being muddled in his thoughts, associated with a specific kind of speech difficulty, known as dysphasia. Dysphasia usually indicates a lesion in the 'speech area' of the brain, usually situated on the left side of the brain.

The conventional lateral scan revealed what appeared to be reasonably uniform abnormal uptake of isotope in the region of the apeech area. The section scan, however, revealed quite clearly that the central part of the lesion did not take up the isotope to the same extent as the peripheral part. This finding, coupled with the roughly

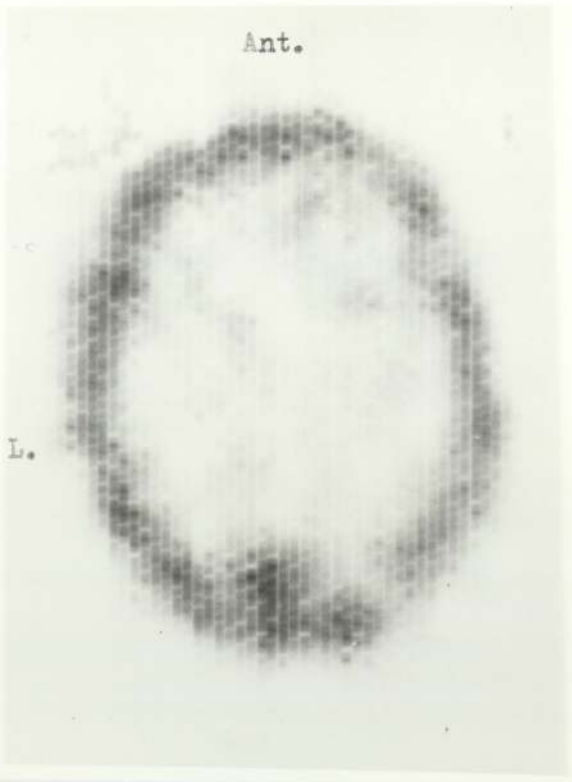

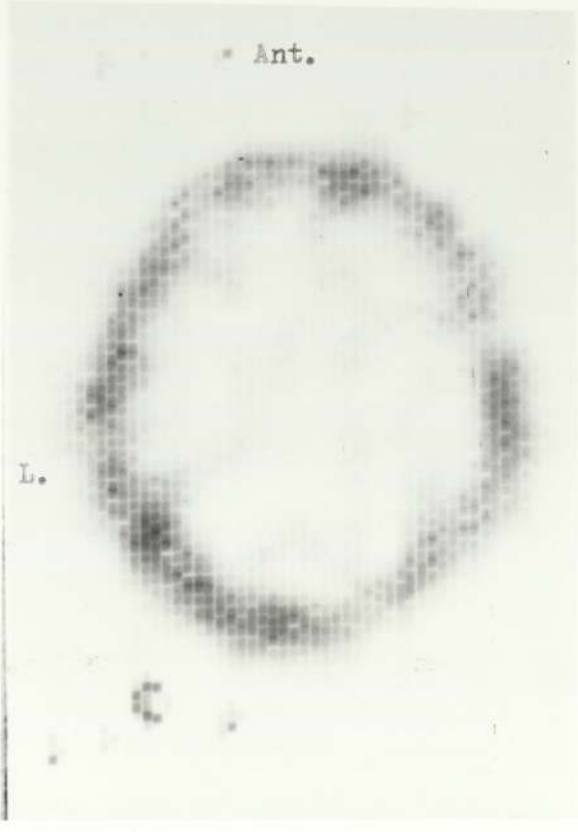

Figure 7.5 Two normal section scans

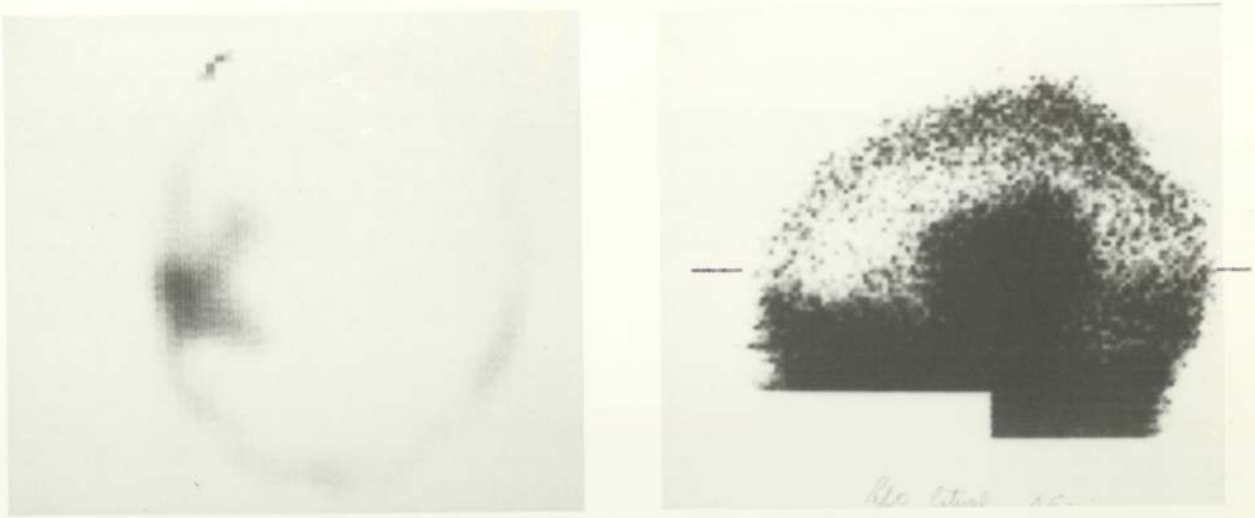

Figure 7.6 (a) Large malignant tumour. Line indicates plane of section.

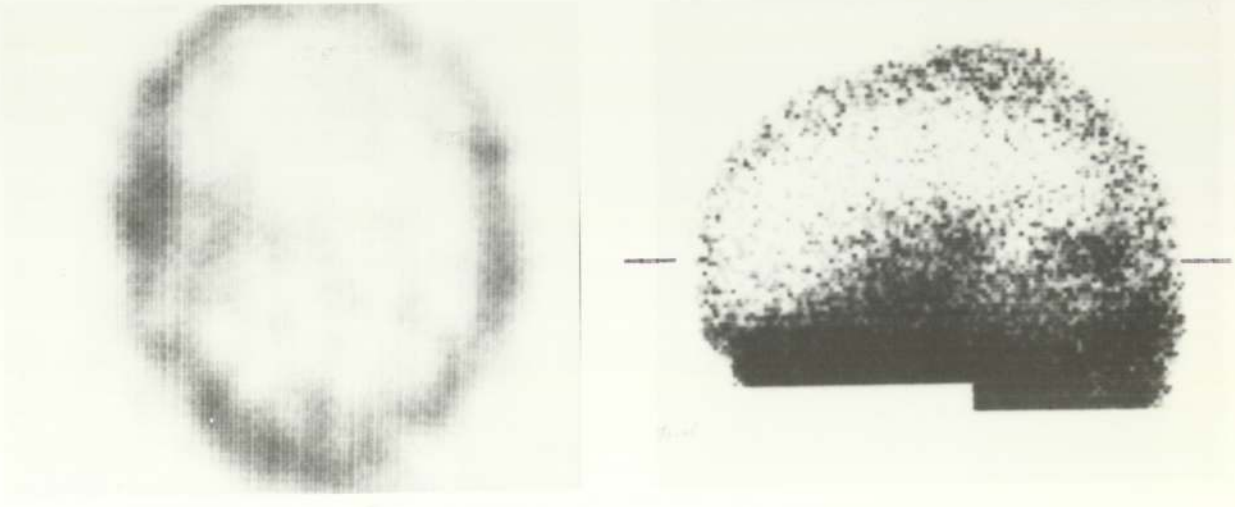

Figure 7.6 (b) Small malignant tumour with necrotic centre.

circular shape of the lesion very strongly suggested a tumour rather than a vascular lesion. At operation, a small malignant tumour with a cystic central part, of a size corresponding to the size shown on the section scan was found.

These results, and others obtained during the pilot study of the section scan method, showed quite clearly the value of the transverse axial view in elucidating the structure of a lesion. This was frequently of great value in making a diagnosis.

The pilot study yielded much useful information, but also highlighted some shortcomings of the method of implementation. The Aberdeen University program requires some switch manipulations, and more are required in order to display the result. As the computer is located some distance from the scanner, and in another room, this was most inconvenient. A development program was therefore initiated, intended to (a) considerably speed up the computation, (b) to eliminate completely switch manipulations so that the system could be controlled by a VDU in the scanner room and (c) to substantially reduce the amount of computer storage required so that a very small and unsophisticated computer could be used. These developments together with clinical results obtained using the new programs will be described in the next chapter.

CHAPTER 8

Further development of the tomographic imaging method

8.1 Development of the Section Scan Method

In order to develop the section scan technique into a method suitable for routine use in a busy department, certain developments and refinements of the equipment and technique were necessary.

It was necessary first of all to eliminate the switch manipulations required to implement the Aberdeen program. Secondly, the computation required speeding up, so that results were available on completion of the scan, in order to allow decisions to be taken on the necessity or otherwise for further sections to be scanned. These developments in the system will now be described.

8.2. Hardware developments.

Most of the data acquistion functions of the 50/50 processor could be controlled by software in addition to hardware control via the front panel switches. In the original version of the computer/scanner interface, however, computer control was not provided for, and it was necessary to switch manually the interface to allow the appropriate set of strobe pulses to address the data acquisition system.

To allow the computer to control the selection of the appropriate set of strobe pulses for different parts of the computer, a special logic module was designed and constructed. Peripheral data transfers are handled by the PDP 8L with octal instructions commencing with prefix 6. The complete instruction bits are output by the computer as pulses which appear as Buffered Memory Register bits (BMR bits). The second and third octal numbers (bits 3-8) are pulses 4.8 μ secs in length and specify one particular peripheral, or one type of operation within a peripheral. The last 3 bits are transmitted as IOP pulses (Input/Output pulses) and are 1.6 u secs in length. IOP pulses are transmitted serially, and it is therefore possible for operations to be microprogrammed, provided they share a common device code. (See fig. 8.1)

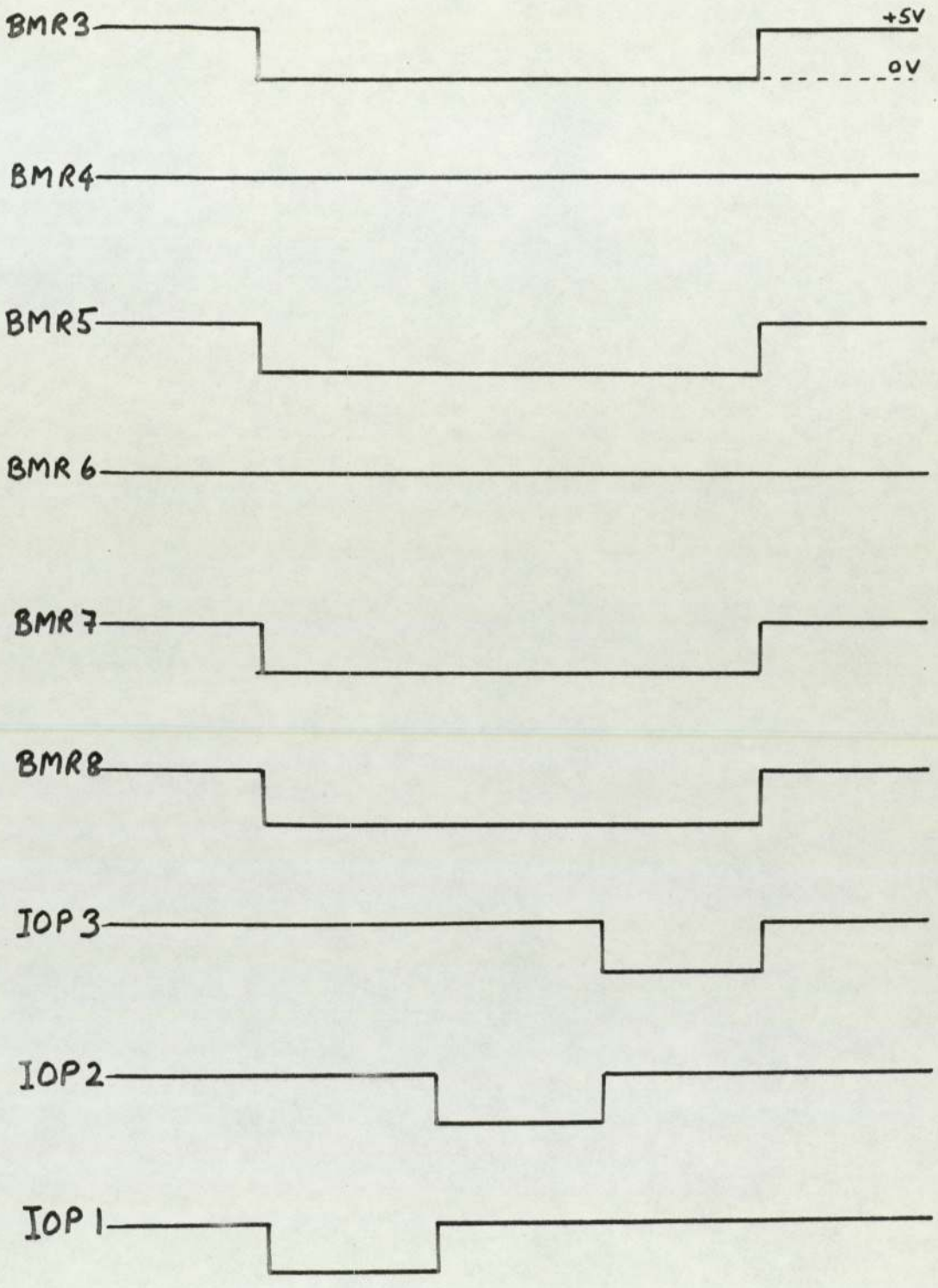

Figure 8.1 Buffered memory register signals during a typical peripheral transfer operation.

The above signals represent a 6537 operation

In the scanner/computer interface, two sets of strobe pulses, STROBE IN and STROBE OUT are always present when the scanner is in motion. STROBE IN pulses occur when the single channel analyser in either detecter system registers a pulse. STROBE OUT pulses occur at each cell boundary.

In the J & P designed dataway terminating module, monostables are used to clean up the rather noisy strobe pulses received from the scanner (see fig. 8.2). The new dataway terminator/(fig. 8.3) contains in addition a decoding network which sets a flip-flop, the output levels of which are gated with the STROBE pulses to allow only the appropriate pulses through to the linear gate circuitry. The system is thus equivalent to a software switch, and manual selection of the strobe pulses is eliminated.

8.2.1 Dataway Terminating Module Circuit Description.

Two additional peripheral reference instruction, STIN (STROBE In, Code 6102) and STOUT (Strobe OUT, Code 6101) were defined.

Interconnections with the BMR and IOP lines in the two-parameter ADC control module were made. Decoding of the device code bits was performed by the invertor G.1.1 and the 8 input NAND gate G2. When an instruction with the correct device code is received, the output of G2 goes low, This output is inverted by G1.2 and gated with IOP pulses. If the instruction was a STIN (6102) code, the output of G3.2 goes low, and this resets flip-flop F1. The $\bar{Q}$ output of this flip-flop is then gated with the Q output of monostable S1, and enables STROBE IN pulses to be transmitted to the ADC control module linear gate input. STROBE OUT pulses are disabled.

To select only STROBE OUT pulses, a STOUT (6101) code is output by the computer. This sets flip-flop F1, the Q output goes high, and gate G3.3 is enabled.

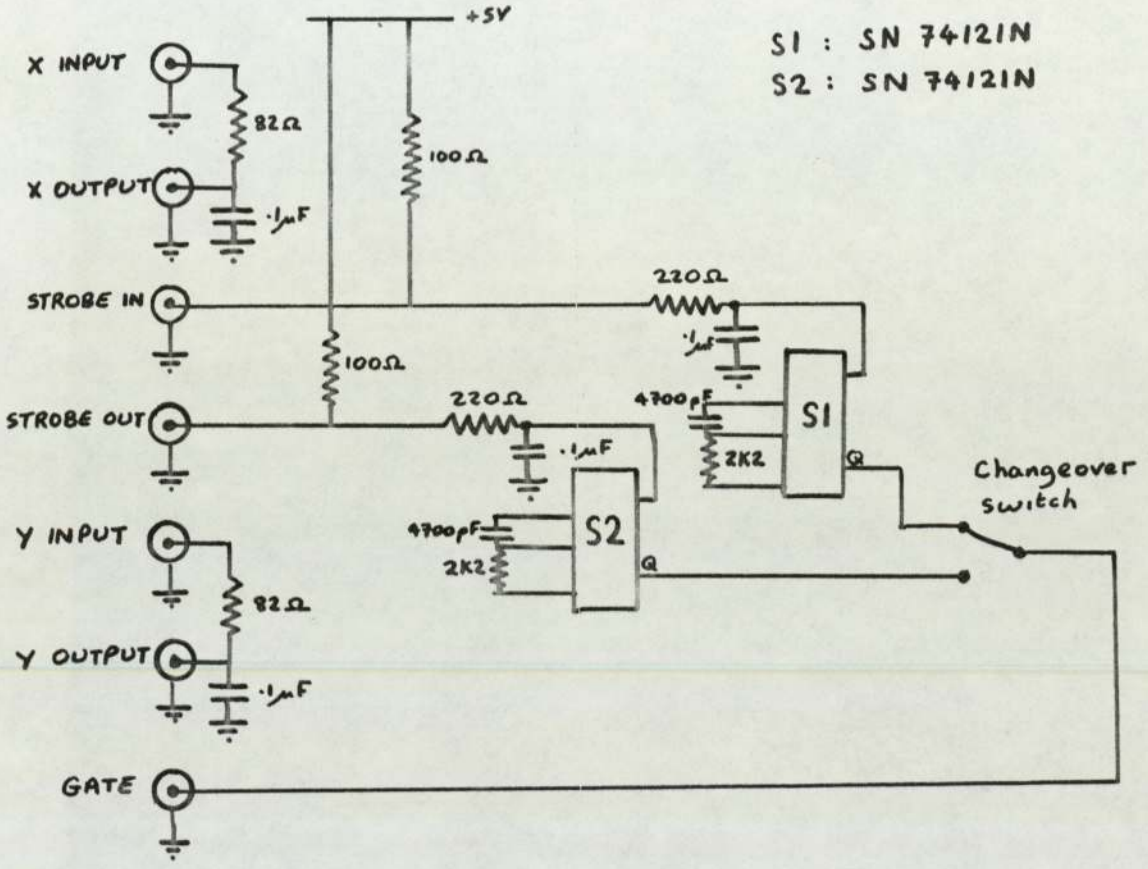

Figure 8.2 J & P designed dataway terminating module

A further refinement of the circuit subsequently proved to be necessary, In the subroutine which determines the position of the centre of rotation, described in section 8.3.1, it is necessary to determine the last cell in the first profile which contains counts. This is done by 'counting down' from the last cell in the first profile to determine the first cell containing data. Normally, the cells at either end of the data profile contain only background radiation, as these are beyond the skull of the patient. On average, each background cell will contain three or four counts, but occasionally no counts at all are recorded. The subroutine will then compute an inaccurate position for the centre of rotation in the data profile.

In order to ensure that every cell actually scanned contains at least one count, the Dataway Terminating Module was modified so that both STROBE IN and STROBE OUT pulses are recorded when data are being input.. This modification is shown in Fig. 8.3. The extra count in each cell is removed prior to reconstruction.

In the final version of the module the $\bar{Q}$ output of the flip-flop is gated with the Q output of the monostable S1 serving the STROBE IN pulses. If a STOUT instruction has been received, the flip-flop is set, and its $\bar{Q}$ output goes low. Thus gate G.3.4. is disabled, and its output is always high. This high output enables G.3.3. which is gated with the $\bar{Q}$ output from S2. Thus, STROBE OUT pulses are output from the module, as 0V to 5V pulses.

If a STIN instruction is issued by the computer, F1 is reset, and the $\bar{Q}$ output goes high, enabling G.3.4. STROBE IN pulses, from the Q output of S1 are transmitted by G.3.4., appearing at the output of the G.3.4. as 5V to 0V pulses. Now, either STROBE IN or STROBE OUT pulses will be transmitted by G.3.3., appearing on the output of this gate as 0V to 5V pulses.

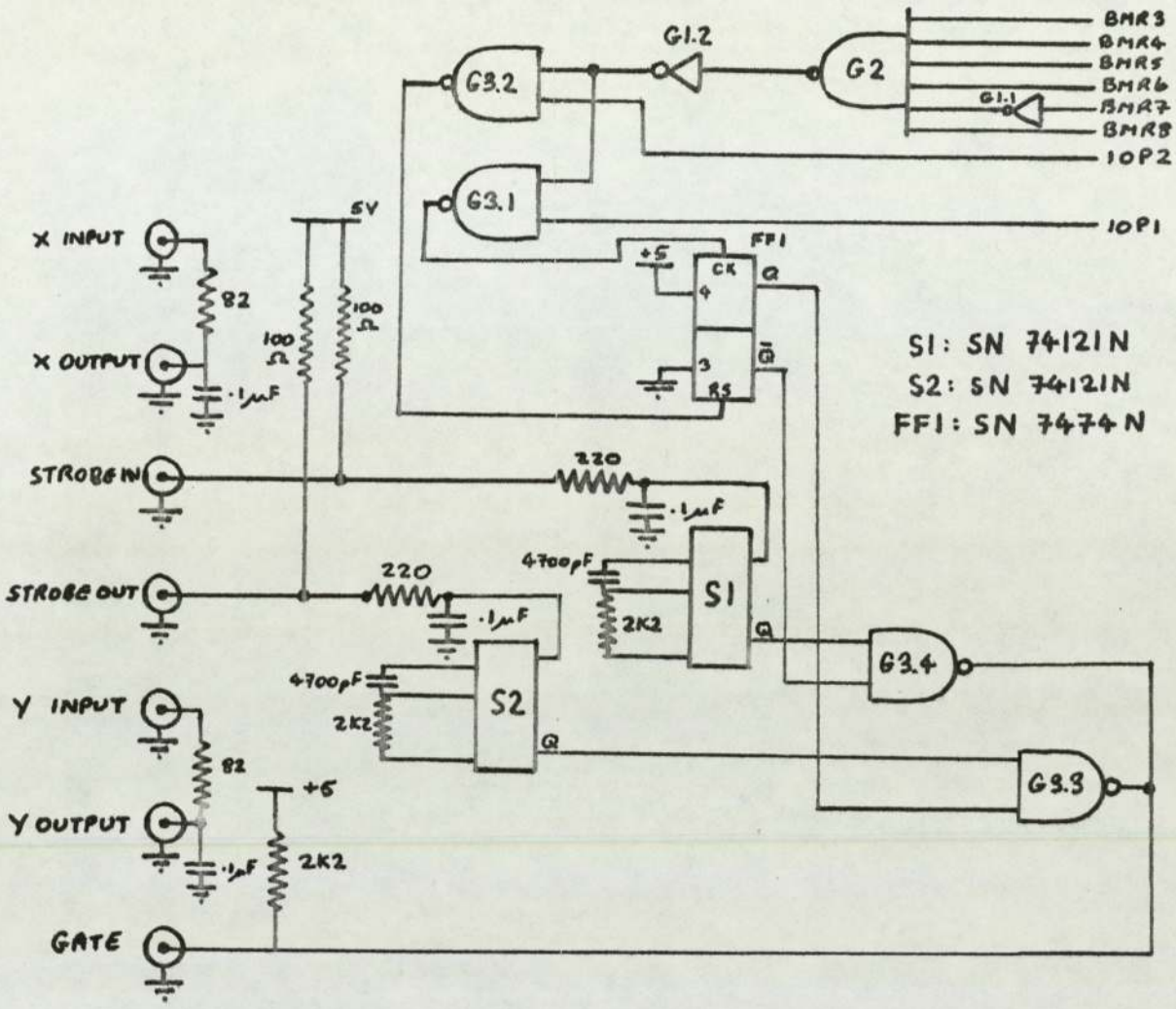

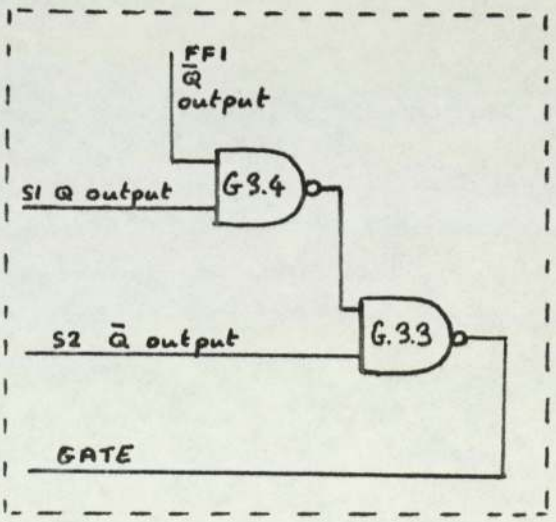

Figure 8.3 Redesigned dataway terminating module including computer control circuitry. (inset) Modification to allow mixing of strobe signals.

8.3. Software Developments

The algorithm used in Keyes program is of the convolution type, and is non-iterative. It is therefore unnecessary to collect all the data before commencing the reconstruction. Providing the program runs sufficiently fast, it is possible to filter and back project the information on a profile by profile basis, using the computer in real-time. The result is then available within four seconds of the completion of scanning. Display of the result can commence immediately, and should be completed in the time required to prepare the next patient for examination. Alternatively, the result can be viewed on the oscilloscope, and if necessary, other sections can be performed. In this case, the result is stored on magnetic tape for playback at a later stage.

Keyes implementation of the algorithm is not suitable for use in this way. The programs were therefore entirely rewritten, but using the same basic algorithm. In order to reduce the running time of the program, the DEC assembly language PAL 3 was used. Subroutines were adapted from those used for establishing the brain scan data base, and some parts of the DEC 23 bit floating point arithmetic package were also used. It became clear during this exercise that a very much small computer memory was now required for the implementation of the algorithm, compared with the FORTRAN implementation. Operation on a profile by profile basis means that it is only necessary to store two profiles of data at any time, saving almost 2K words of computer memory and a program written entirely in PAL 3 requires only a small fraction of the memory required by a FORTRAN program. Thus a smaller (and cheaper) computer could be used. The final version of the developed programs required a total of about 7K words of computer memory, compared with approximately 13K words required by Keyes program.

8.3.1. Alignment of the data.

Real time operation of the system precluded the method described earlier for aligning the data with respect to the centre of rotation of the coordinate system, since only a maximum of two adjacent profiles will normally be held in the input buffer. It was therefore necessary to find some other means of aligning the data.

It was realised that when the detectors on the scanner were in contact with the deceleration microswitches on the scanner yoke, the data from the detectors was 'gated off' even though the scanner might continue to move in the same direction for a few millimetres (depending upon the scanning speed) before reversing direction. The moment at which the scanner touches the microswitch (and the data consequently ceases) is thus a fixed reference point, independant of the speed of the scanner.

Providing, therefore, that the scanner display limit switches have been set to over run the scanning frame the last cell containing data in the first profile can be used to align the data in this and subsequent profiles by adding an integer N, to the address of the data points.

Since the scan is normally started a few mm clear of the deceleration microswitch at the commencement of the first profile, the scanning line length is insufficient to store data in all 64 cells of the first profile. There are normally one or two cells which do not contain data, since the buffer is cleared before starting the scan. In the first attempt at implementing this type of alignment check, it was assumed that the radiation background level close to the head would be sufficiently high to ensure that some counts would always be recorded in cells within the area traversed by the scanner. The first few trials showed that this was not necessarily true, and a modification was therefore made to the interface circuity to mix the STROBE OUT signals with

the input signals. A STROBE OUT pulse will occur in each cell indexed by the scanner, so any cell within the scanned area will contain at least one count. It is now permissible to take the last non-zero cell as a reference point from which the data can be aligned.

8.3.2. Data input procedures.

As discussed in section 7.4.1 the best results could be obtained merely by adding together data from the two detectors. There was little point in storing the data separately. By removing the 'field specification' line from the interface data from both detectors were stored in the same 12 bit memory location. If the 'field' input is open circuited, data are stored in the upper 12 bits of the 50/50 24 bit word, and if the 'field' input is shorted, data will be stored in the least significant 12 bits.

When the program is started, the computer requests the patient name and department number, and these are entered from the teletype keyboard, to form a permanent 'leader' to the magnetic tape record. The computer then types out via the control teletype instructions to the operator regarding the positions of switches on the scanner control console.

When the scanner is started the computer monitors the input of data. When data appears in the second profile, indicating that the first data profile has been completed, the computer asks the operator if data are being entered on-line, or off-line via the tape recorder.

If the response indicates that data are being entered on-line the computer calculates the 'shift' correction, filters and back projects the first profile into the lower memory field of the 50/50 storage and display unit. The computer then waits until storage of the second profile is complete and filters and back projects this profile. As the 31st profile is not required by the program, the reconstruction of the image is in fact completed a few seconds before the scanner completes the scan, and storage and display of the image on the scanner display circuits can commence immediately.

If the data are being entered off-line the computer requests a number specifying a Y shift. The tape recorder/scanner interface is such that the Y values are offset from zero, normally by about 1 cm. Data storage therefore normally starts at the 4th profile in the 50/50 memory, but this can vary slightly. In this case, the computer oscilloscope is inspected by the operator to determine by how many profiles data must be shifted for the reconstruction program. Once a value has been entered by the operator, the reconstruction proceeds as in the case of the data being entered on-line.

8.3.3 Data Storage and Display.

After completion of the reconstruction, the computer asks if data storage on the AMPEX magnetic tape deck is required. If the response is in the affirmative, the computer shifts the information in the 50/50 lower memory field up by one profile, and transcribes the patients name, department number and magnetic tape file number into the first profile. The contents of both memory fields are then written onto the $\frac{1}{2}$ inch magnetic tape system. Overwriting previous data is impossible under normal circumstances as a subroutine positions the tape at the beginning of blank tape, ie. after all previously recorded data.

Having stored the input data and the reconstructed image on magnetic tape, the computer overwrites the input data (stored in 50/50 upper memory) with an enhanced image of the reconstructed isotope distribution.

The image obtained in the reconstruction as in the case of Keyes program, usually comprises numbers in the range 0-1000. The digital filter process will have produced negative values, which are stored in the 12 bit word as numbers in the range 2048-4095. If the data were exact, these negative values would be entirely removed by the back projection process. In fact, a few negative values usually remain after reconstruction, and these appear as high positive numbers,

close to 4095, on the display.

Because of the statistical inaccuracies in the input data, and the limitations of the reconstruction algorithm, some 'background' is usually obtained surrounding the reconstructed image. This background is too low to have any significance, and its subtraction improves the appearance of the image.

The radiologists at the Midland Centre for Neurosurgery have a marked preference for full size photographic display on X-ray film of radionuclide investigations. In common with most photoscan display, the display of the J & P Scanner will output a very large number of grey levels. To the eye, there is no perceptable transition in going from one grey level to another. The display is therefore entirely qualitative. In order to take advantage of the full range of grey levels which the scanner is capable of displaying, it was necessary to multiply the number in the reconstructed image by a factor such that the maximum value of the reconstructed image is set to 4K. This is necessary because the computer/scanner interface circuitry is essentially a fixed gain amplifier, and maximum contrast of the image is only achieved by producing a full scale analogue level from the computer. Inevitably, enhancement of the data in this way will mean that the image is no longer strictly quantitative, but as the factors used in the enhancement are stored in the magnetic tape record, the quantitative image can be recovered if necessary.

The image enhancement subroutine performs three functions. Firstly, negative values are removed by setting these to zero. Secondly the 'background' level is established, and only values between maximum and background are selected for display, and thirdly, the range of values between background and maximum is expanded to cover the full number range provided by the 12 bit data word.

In order to compute the factors required by the enhancement subroutine, a cell count histogram was established covering all values

in the data frame. In the case of a section scan showing no abnormality, the main features of this are:-

(a) a large peak close to zero, representing cells generally outside the volume of the skull (ie.'background' counts).

(b) a small and broader peak representing the activity in the scalp.

(c) a small group of cells with very high values.

These latter are negative values left over from the filtering process, and they appear because of statistical inaccuracies in the data.

Having sorted the values in the reconstruction frame into the appropriate count rate categories, the buffer in which the count rate histogram values are held is searched to establish (a) the count rate value at which the maximum of the histogram occurs and (b) the count rate value at which the upper 'tail' of the histogram reaches zero. The value (a) represents the general level of background, most of these calls lying outside the skull outline and (b) represents a count rate slightly higher than the maximum count in the reconstructed distribution, excluding the negative values left over from the convolution operation. In most cases (b) was of the order of 1000 counts per cell and (a) was of the order of 100 counts per cell.

In order to display the result on the scanner display systems with optimum contrast, cells with a count outside the range (a+96) to (b) were set to zero, and counts within this range were expanded by multiplication with a suitable factor to cover the range 0 to 4095 counts. This gave displayed results showing few low count rate artefacts within the skull, thus enhancing the appearance of any positive uptakes. The background suppression introduced by this technique amounts to about 20% of the maximum count in the distribution.

8.4. Clinical results

To date, approximately one hundred confirmed positive section scans have been performed, and these have enabled some conclusions to be drawn as to the value of the method. Until now most section scans have been performed on cases showing a positive uptake on the conventional radioisotope scans in order to gain more information on the morphology of the lesions. The method is now being extended to include eqivocally increased areas of uptake seen on the conventional views, and lesions not seen on the conventional views but expected on clinical grounds to be present. These latter lesions usually lie in sites inaccessible to conventional isotope scanning but accessible to section scanning, such as the base of the brain, and the region underlying a bone flap in post operative cases. So far, too few cases in the latter two categories have been examined to suggest the amount by which the rate of detection of abnormalities may be improved.

8.4.1. Quality and accuracy of section scanning

The accuracy by which the section scan method delineated the morphology of a lesion could at first be assessed only by surgical exploration or by post mortem examination. In the few cases where such comparison was possible, the results correlated well.

More recently, it has been possible to correlate the results of section scanning with results obtained by a transmission transverse axial scanner (EMI Scanner). The latter machine uses a highly collimated x-ray beam as the photon source, but is otherwise very similar in concept and operation to the isotopic section scanner. The results from the EMI scanner are presented by the computer as maps of X-ray absorption defined on an arbitrary scale, with air as -500 units, water 0 units, and dense bone +500 units. Because of the very high photon flux obtained in the

EMI scanner, highly detailed pictures are obtained. Comparison of EMI scanner results with the result of isotopic section scanning confirms the accuracy of the isotopic method, but interesting differences between the results are sometimes found, suggesting that the two techniques may be complementary.

The differences found between the two methods of transverse axial scanning (ie, emission and transmission) are thought to be due to two factors. Firstly, the emission section scan demonstrates a functional distribution. In the case of examination of the brain, the function under examination is the efficiency of the blood-brain barrier, and only regions where this is impaired will demonstrate a positive uptake of isotope. The transmission section scan, by contrast, demonstrates a structural distribution in that different structures are delineated by differences in x-ray absorption coefficient. Thus, whereas a cystic lesion or a cystic structure within a lesion will be shown on a transmission scan (usually as an area of reduced x-ray absorption) it will not been shown on an emission scan. Comparing results in this way can often yield valuable information on the detailed structure of lesions.

Secondly, differences in appearance of the results obtained by the two techniques can arise because of the physical differences in the detection systems.

The in-plane resolution of the transmission scanner is about 3 mm., as shown by studies on the modulation transfer function obtained by imaging a phantom. (MacIntyre, Allidi et. al, 1976). However, the resolution in the plane perpendicular to the imaging plane (ie, the "thickness" of the "slice") is about 12 mm. The apparently sharp boundaries of lesions sometimes seen on the transmission scans can therefore be actually misleading. This is not likely to occur with the lower

resolution emission section scan, where in-plane and out of plane resolutions are the same. An example which perhaps demonstrates the latter point is shown in fig. 8.4. This lesion is a parafalx meningioma which appears to be entirely left sided on the transmission scan. The isotopic section scan suggested involvement of the right side and at operation the bone flap was fashioned well across the midline to take account of this possibility. Tumour tissue was in fact found on the right side of the falx as well as in the sinus.

The quality of the isotopic section scan was generally thought to be good, and the fact that the intensity reconstruction is not strictly quantitative is rarely a problem. One point which has been commented on is the apparently rather uneven uptake in the skull outline. This is presumably statistical in nature, as it is more noticeable in situations where the counting rate is relatively low. It is particularly noticeable in the case illustrated in fig. 8.4 (b) where the total accumulated count was only about 40,000 as compared to the usual value of about 80,000. It is possible that some of this heterogenuity can be attributed to uneven distribution of the blood supply to the scalp and dura.

8.4.2 Effect of site

The isotopic section scan will show discrete lesions in the parenchyma of the brain readily. Where the lesion is close to the edge of the skull, the peripheral uptake and the abnormality may blend into each other so that, for example, a peripheral astrocytoma cannot always be distinguished from a meningioma on the basis of skull attachment (fig 8.5). Evidence of skull attachment is, however, usually more evident in the case of meningioma.

Background activity from deeply lying highly vascular structures and activity along the sagittal sinus feature on the conventional

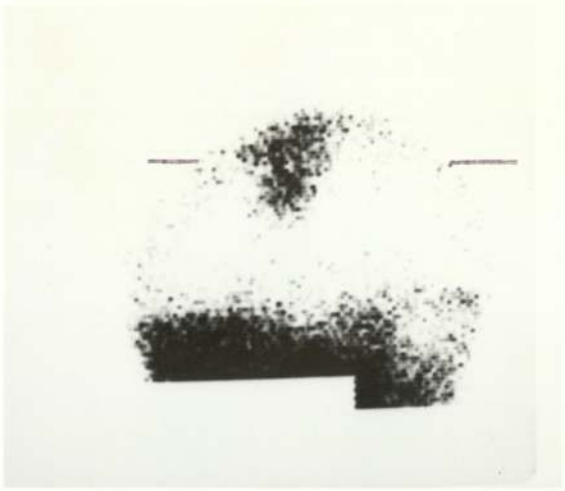

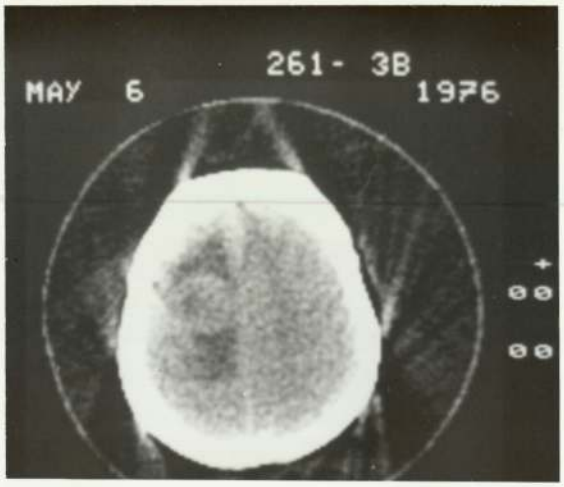

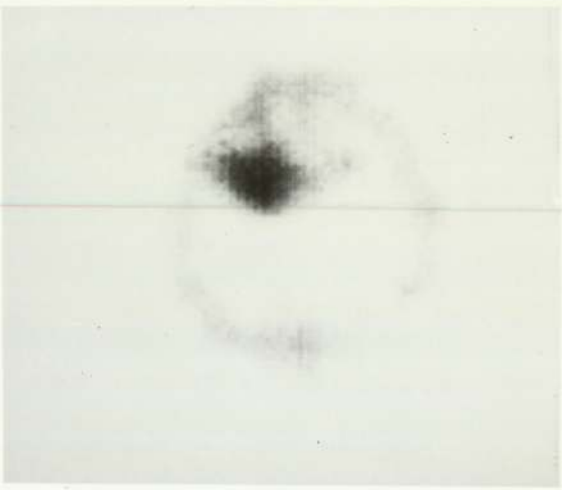

Figure 8.4 (above) A case of parafalx meningioma

(below) An acoustic neurinoma

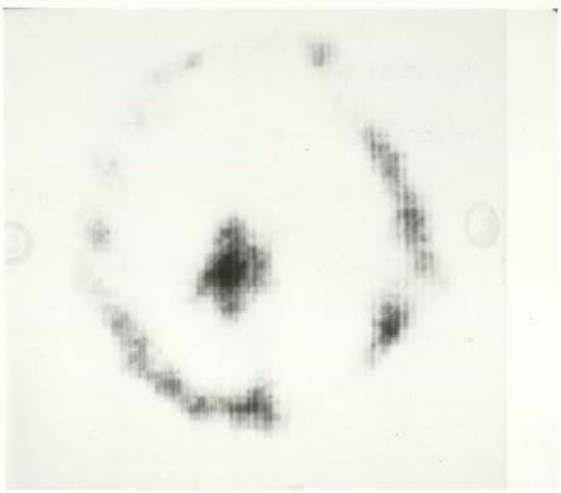

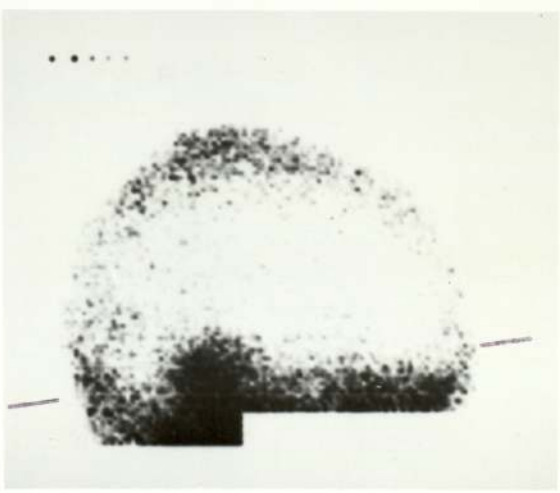

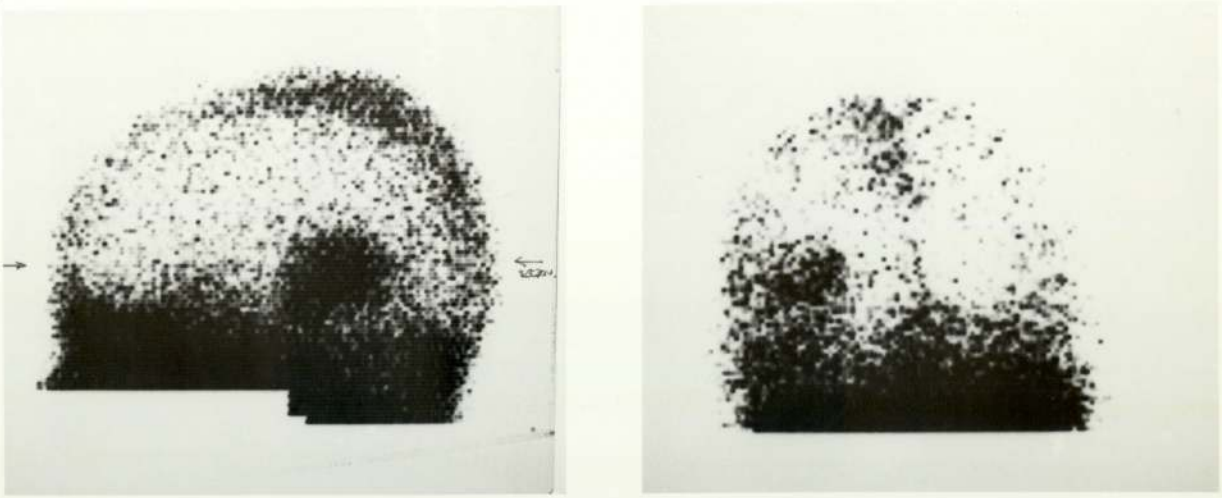

Figure 8.5 A peripheral astrocytoma

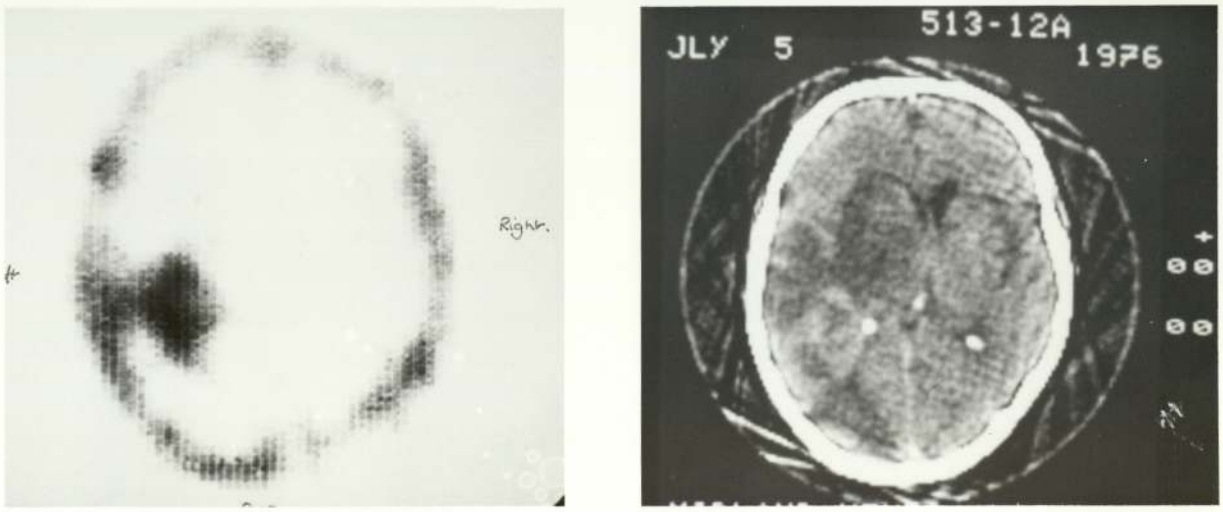

vertex view which is often employed in the localisation of parasagittal lesions. These effects can be eliminated by a section scan close to the vertex (fig 8.6). The section scan is also particularly useful in the case of basal lesions, which are often obscured by overlying peripheral activity on the conventional views. This can be well shown with basal meningioma (fig. 8.7 (a)) and also acoustic neurinomata (fig 8.4. (b)) where the true extent of the tumour can be readily appreciated. Recurrent tumour sites can also be accurately surveyed by a section scan, even though the conventional rectilinear scan may be ambiguous, due to activity concentrated in the bone flap. An example is the recurrent meningioma shown in fig 8.7 (b). The rectilinear scans show an extensive very patchy uptake, but the section scan clearly indicates an extensive sub-scalp recurrence and a smaller intracranial portion. This was verified by transmission scanning and at operation.

8.4.3. Shape of lesions as a diagnostic indicator

The shape of lesions appears to be well reproduced, an example being the recurrent meningioma discussed above (fig.8.7 (b)). It was found that cystic lesions within gliomas show reduced uptake of isotope, the increased uptake in the walls often giving a bicornuate appearance, the thickest part of the tumour being most active and the walls appearing to sprout from it like horns (fig. 8.5 and 8.7). Anaplastic or multicystic tumours often show an irregular shape and patchy uptake. The zones of increased uptake may appear to differ somewhat from the tumourous tissue demonstrated by transmission scanning, but the two methods are difficult to compare in this situation because of the problem of taking the sections in precisely the same plane. Nevertheless the added information provided by the isotopic section scan may make the diagnosis virtually certain in these cases.

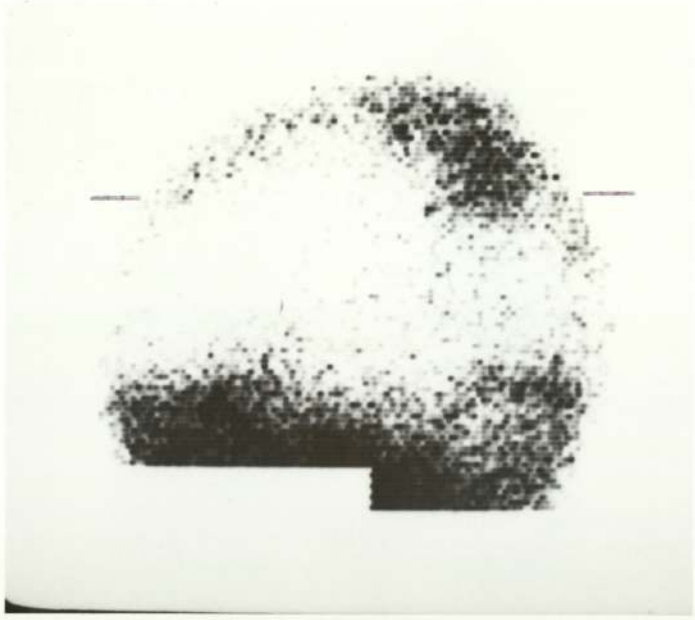

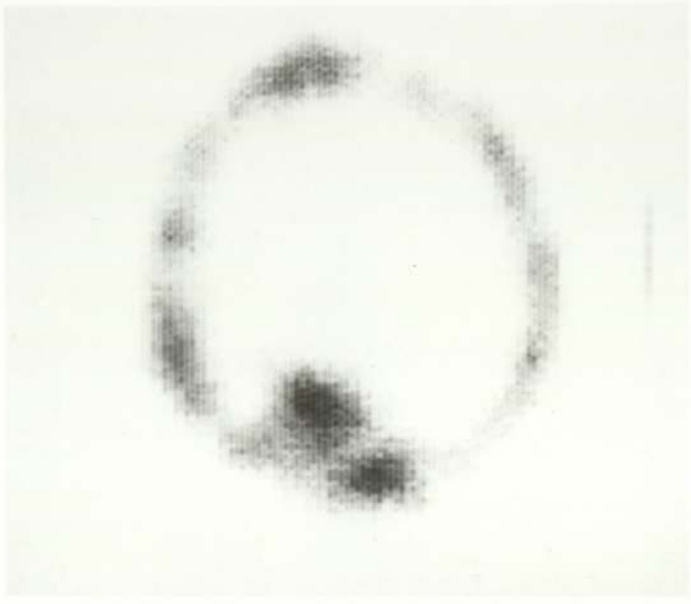

Figure 8.6

Parasagittal angioma

(comparison of vertex

and section scans)

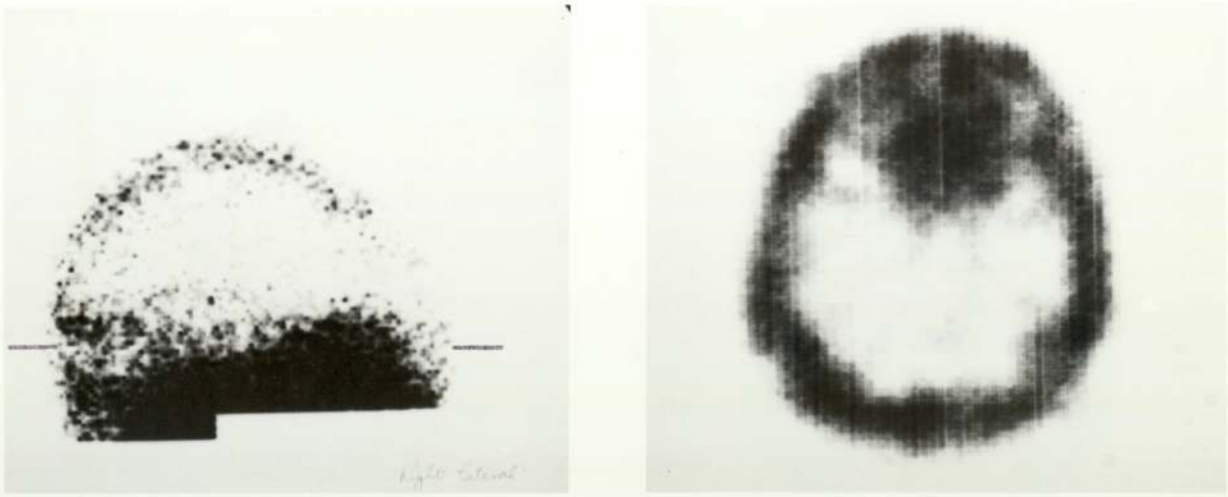

Figure 8.7 (above) a. Basal meningioma

(below) b. Recurrent meningioma

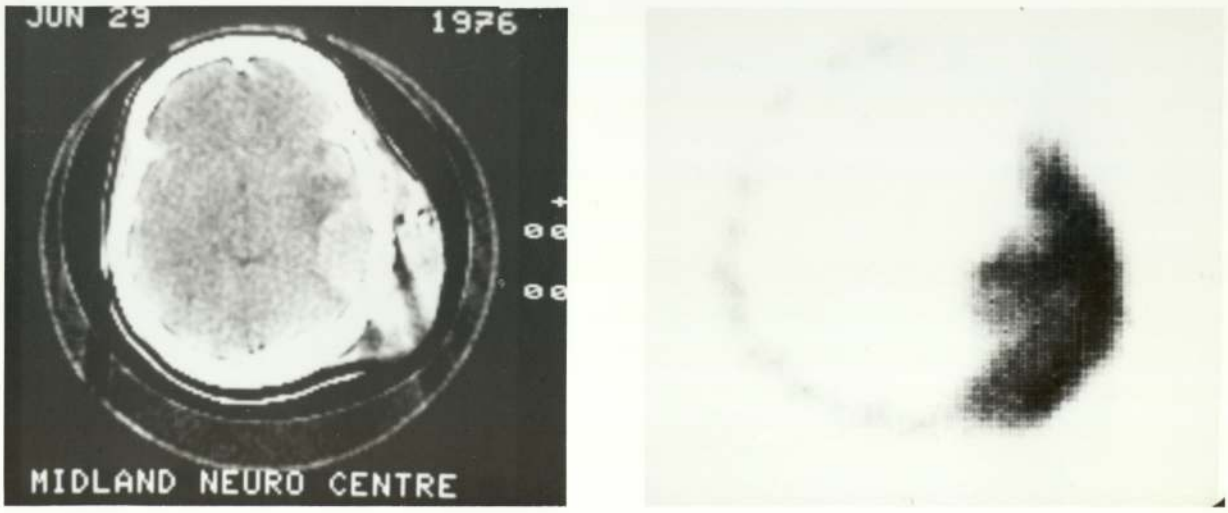

The shape of infarcts seen in transverse section is most commonly wedge shaped, as seen in fig. 8.8. Kuhl comments that in his series of section scans, 56% of the infarcts seen were clearly defined centre pointing triangles, but only 14% of tumours presented this appearance. Furthermore whilst 74% of tumours had other sharply defined shapes, only 16% of infarcts did so.

Fig. 8.9 shows two infarcts, which are also seen on the transmission scan. The foremost infarct is of the wedge shape described by Kuhl, but the rearmost infarct is of rather indeterminate shape. From Kuhl's experience which is supported by our own smaller series, the finding of a lesion which has a distinct shape other than a centre pointing triangle is a fairly strong indication that the lesion is not an infarct.

The section scan may also prove to be useful in diagnosing subdural haematoma, although here, especially with localised haematoma, the rather uneven reconstruction of the peripheral activity may present some difficulty in interpretation. The section scan was of value in the case illustrated as fig.8.10. The rectilinear scan raised the possibility of two separate lesions, but the section scan showed that they were connected and located convincingly the crescentic area of uptake.

8.5. Imaging of C.S.F. Pathways.

The brain contains a number of interconnected fluid filled spaces and is itself contained within a fluid filled bag, consisting of several layers of membrane, or dura, within the skull.The fluid (cerebrospinal fluid, or CSF) fulfils a number of functions one of which is to provide damping, to protect the brain to some extent from sharp blows to the head.

CSF is produced within the ventricles by the choroid plexi and then flows through the fluid spaces of the brain and spine and

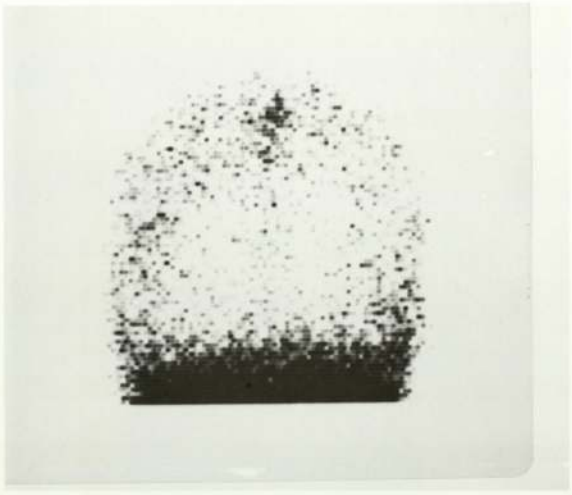

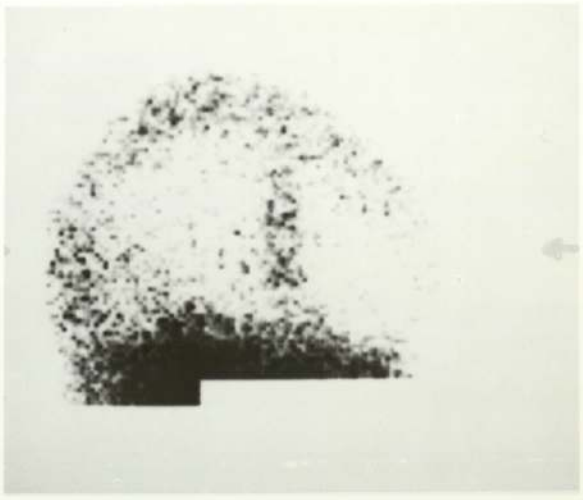

Figure 8.8 A case of infarction

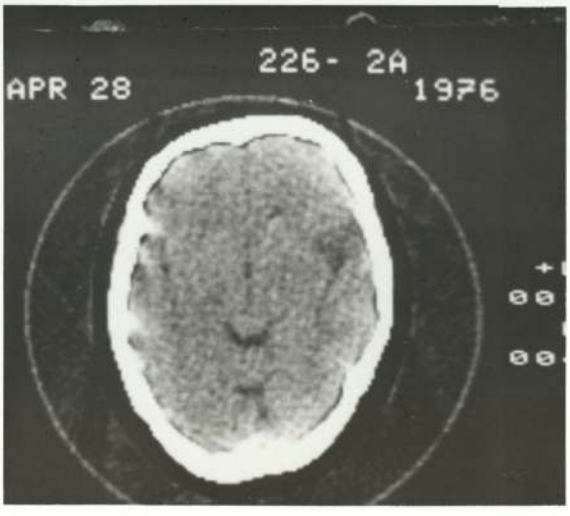

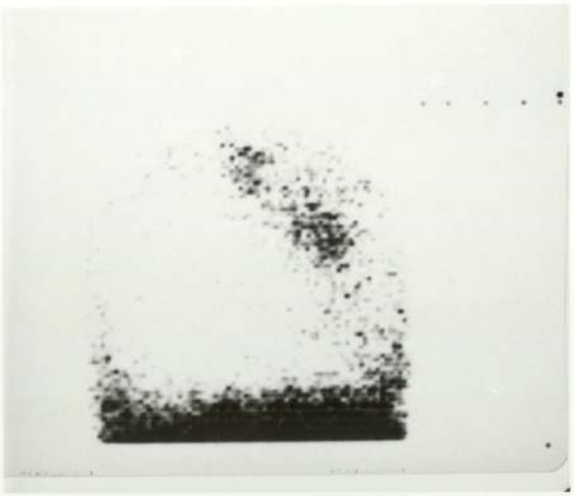

Figure 8.9 Two areas of infarction

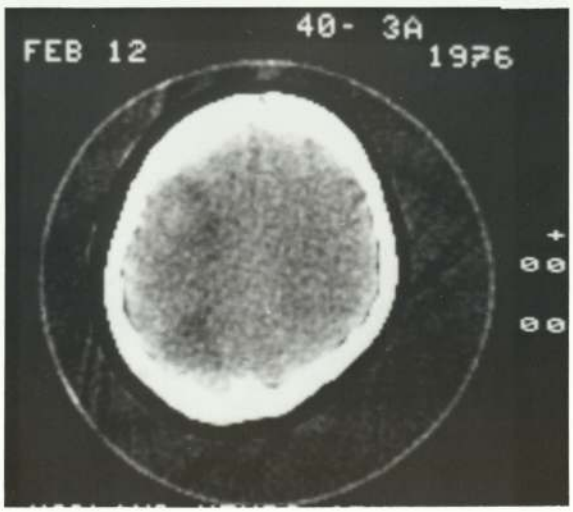

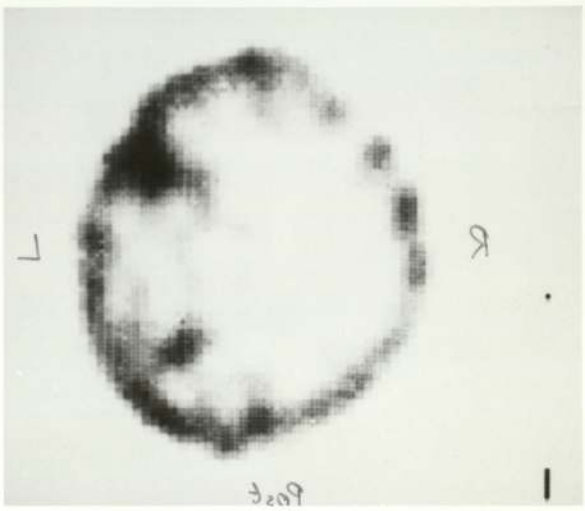

Figure 8.10

A case of subdural haematoma

finally flows over the surface of the brain where the fluid is absorbed into the bloodstream.

It is possible for injury or tumourous growth or even infection to block or partially block one of the CSF pathways. In such cases, since CSF continues to be produced, the pressure in the ventricles may rise, distorting the brain and producing the condition known as hydrocephalus. Such cases may be examined by a variety of ways, most commonly by introducing contrast medium (either air, or a water soluble medium which will mix with the CSF) into the CSF pathways, and then X-raying the patient in a number of positions to assess which pathways, allow passage of the contrast medium. These procedures often work well, but they may sometimes be misleading in that if a constriction is not total, the pathway may be too narrow to allow contrast medium to pass but yet wide enought to allow some exchange of fluid. Isotope ventriculography may be indicatedin such cases and it was found that section scanning improved considerably the information yielded by such examinations.

8.5.1. Case studies using Indium ^{111} DTPA

Case 1, A child with a mild hydrocephalus. (see fig. 8.11)

This boy had apparently suffered an infective illness and subsequently was epileptic and mentally subnormal and suffered from what appeared to be a changeable hemiparesis. The EMI scan showed, in addition to the hydrocephalus, an appearances of considerable enlargement of the sylvian fissure which was confirmed on angiography by showing a displacement of the middle cerebral group of vessels. One needed to know if the collections of CSF in the sylvian fissures were stagnant and thus likely to be largely closed off from the remainder of the CSF pathways and possibly acting as a space occupying lesion. Instillation

Figure 8.11 A child with a mild hydrocephalus

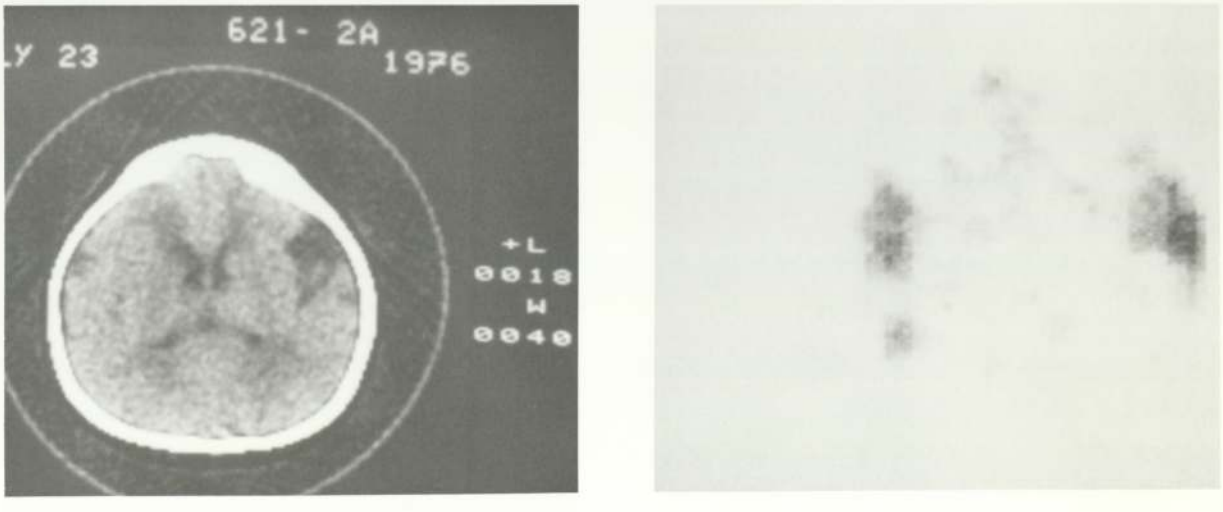

of 140 μCi In^{111} chelate into the right frontal horn via a twist drill hole was followed by rectilinear scanning and section scanning. At 24 hours the rectilinear scans show a relatively diffuse distribution of radioactivity as shown in Fig. 8.11 The concentration of the greater part of the activity in the sylvian fissures is most apparent on the section views. All activity had almost disappeared after 48 hours and this was thought to be valuable evidence that the CSF in both the sylvian fissures collections was being exchanged freely.

Case 2, A patient with raised intracranial pressure after brucella meningitis.

The EMI scan reproduced in Fig. 8.12 showed only modest hydrocephalus. The introduction of 500 μCi of In^{111} chelate into the right frontal horn via a twist drill hole showed that the isotope gradually cleared through the third ventricle but there was no detectable transfer of isotope to the left lateral ventricle. This observation seemed odd, but the use of air and Dimer X ventriculography through the same route confirmed the failure of the contrast media to pass through the left foramen of Munro presumably due to narrowing of the passageway secondary to ependymitis.

Case 3, A patient with a Dandy-Walker Cyst.

This patient had had ventriculography followed by a posterior fossa exploration fifteen years previously for a large cyst replacing the fourth ventricle. The patient had an atrophic cerebellum (Dandy-Walker malformation). He presented again with headache and blurring of the disc margins. Ventriculography with air and Dimer X (Fig. 8.13) showed an aqueduct stenosis which had not been present at previous ventriculography. The stenosis was sufficienty severe to arrest the water soluble contrast medium. The stenosis of the aqueduct under these circumstances may be due to pressure from the posterior fossa cyst. This was checked in this case and found to be indistinguishable from the pressure in the lateral ventricles. One check of pressure equality

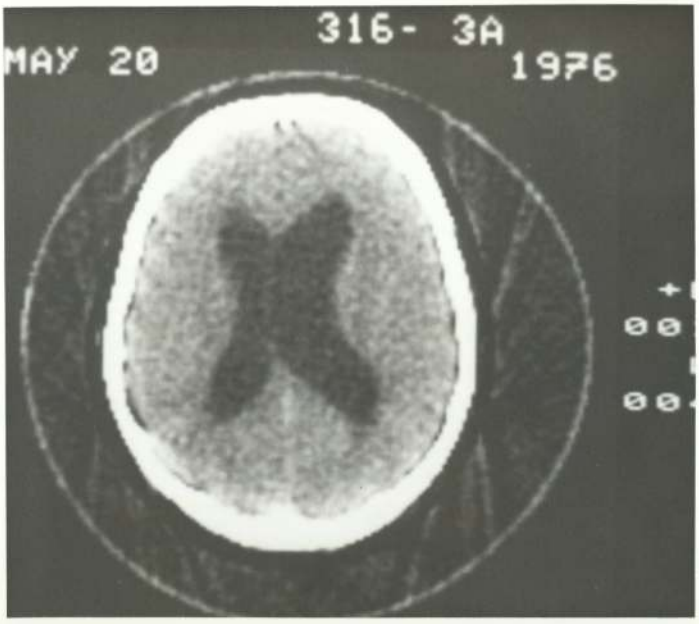

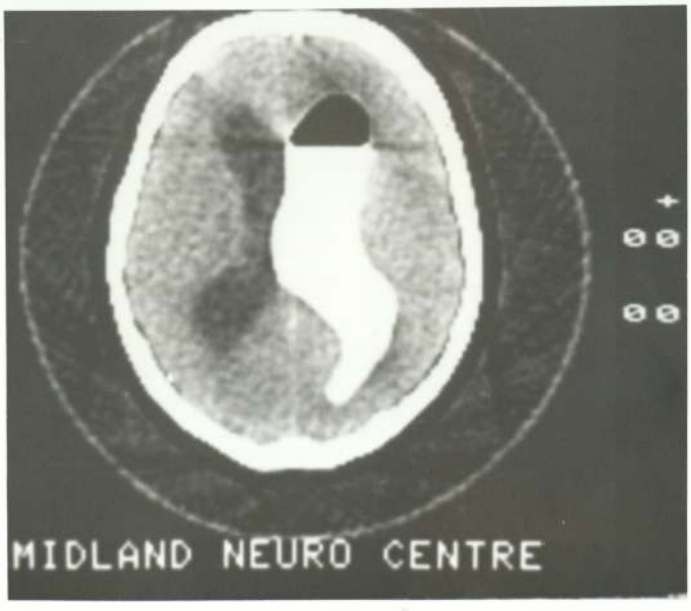

Figure 8.12

A patient with raised intracranial pressure

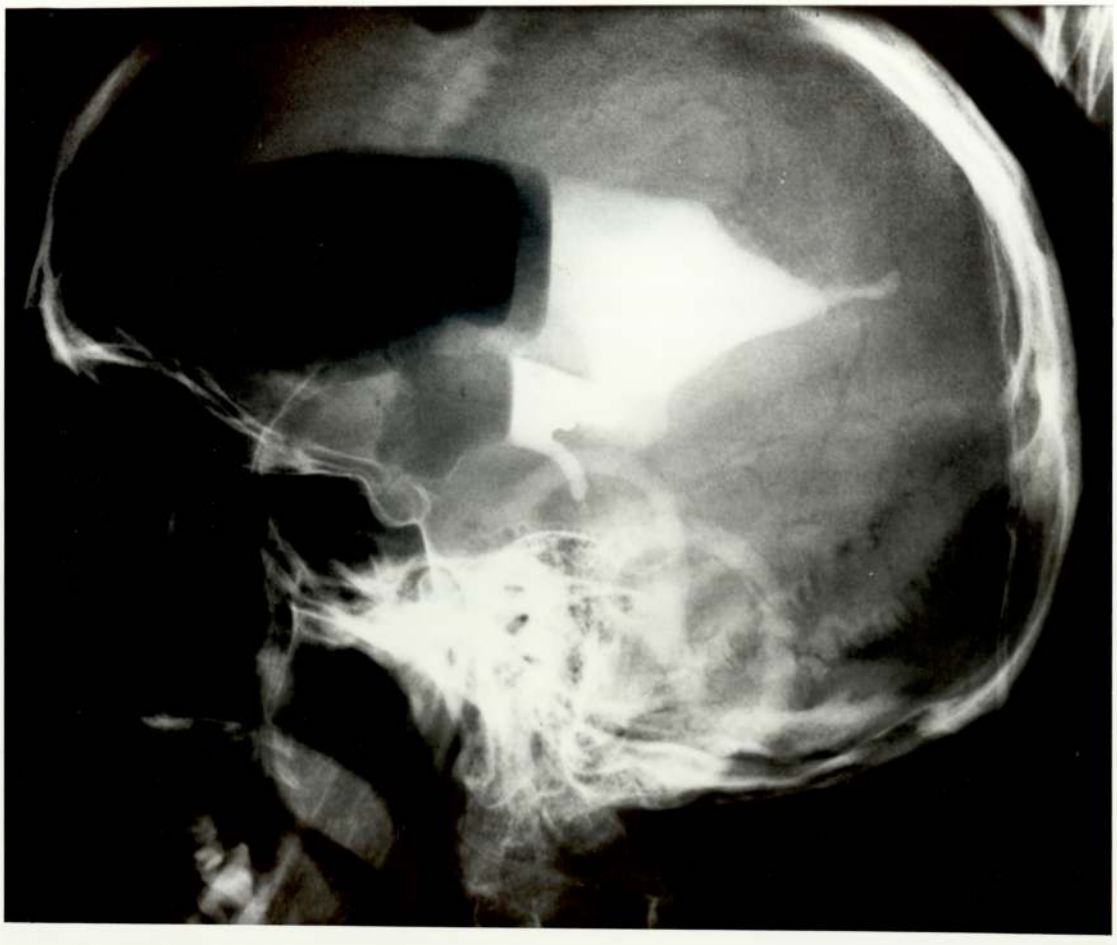

Figure 8.13 A Dandy-Walker cyst. X-ray ventriculogram

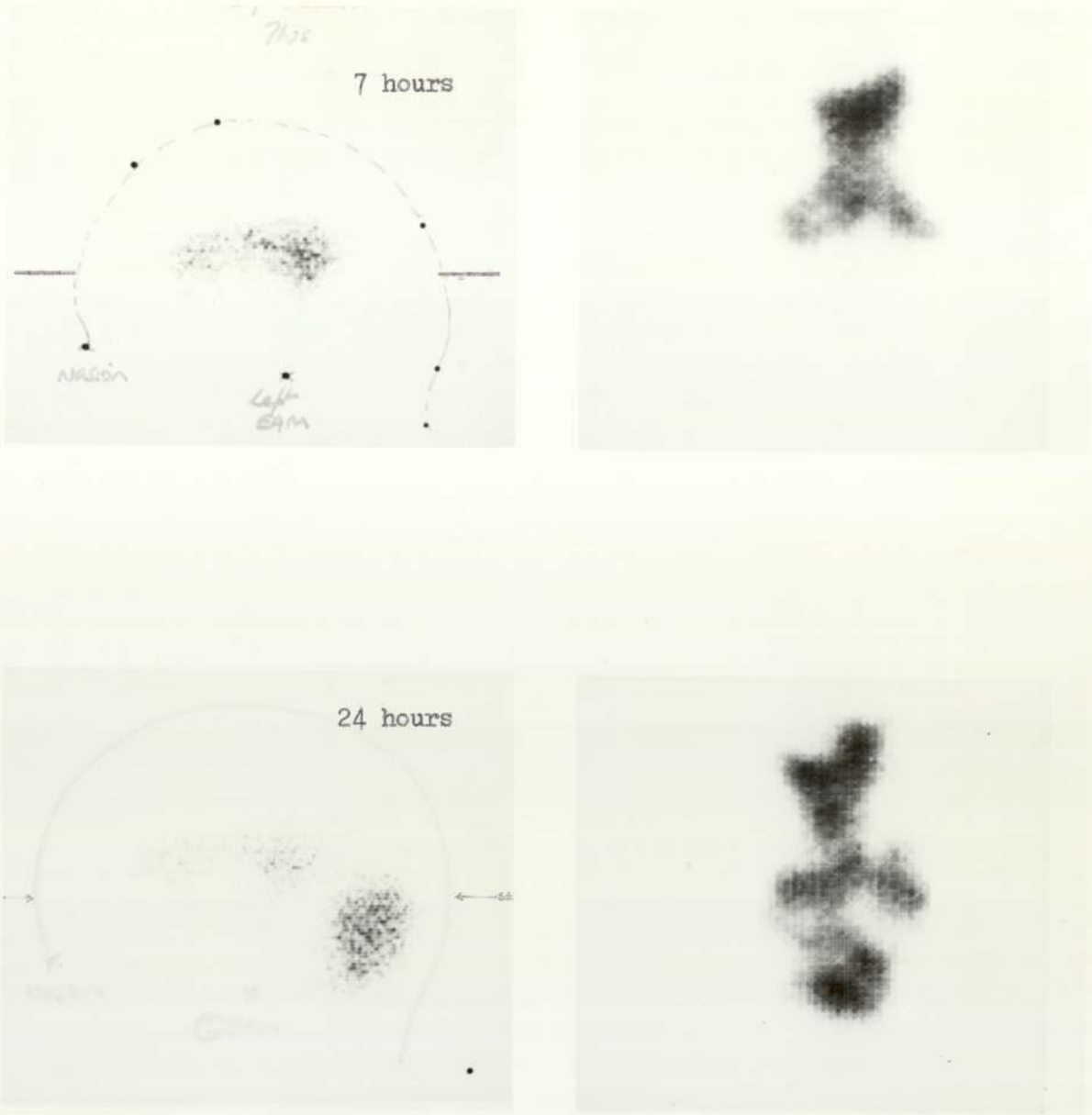

Figure 8.14 Indium 111 DTPA ventriculogram. Case of Dandy-Walker cyst

under these circumstances does not mean that aqueduct compression could not be present intermittently. A CSF diversion using a fourth ventricle to right atrium shunt and a Holter Valve was planned but the pathways of the aqueduct needed to be checked. A lateral ventricle injection of 500 μCi of Indium ^{111} chelate gave the scans shown in Fig. 8.14 the morphology of the cyst being clearly seen along with the progression of isotope from the lateral ventricles to the fourth ventricle which was interpreted as confirming that fourth ventricle CSF diversion was all that was necessary. Although the progression of the isotope can be clearly seen on the conventional lateral views, the structure of the ventricles can be seen with much greater detail in the section scan.

Sectional scanning has proved to be a valuable additional technique in elucidating the structure and flow patterns of the CSF pathways in the brain. If the method can be made more quantitative, it is possible that these results could be used to provide information on flow rates which could be most useful in planning treatment. At present with existing data processing and contrast media the EMI Scanner cannot give such information.

CHAPTER 9

Review of methods and conclusions

9.1 The changing pattern of encephalography

Encephalography, or the science of investigating the brain to detect and diagnose disease, has undergone considerable change during the past decade. In order to assess the significance of the research reported in this thesis, it is necessary to briefly review these recent developments.

9.1.1 Invasive methods of investigation

The longest established methods of investigating the brain by means of X-rays involve the use of contrast materials, as the brain itself cannot be visualised without these agents. Plain skull X-rays (i.e. those taken without use of contrast media) can reveal fractures, which might suggest the presence of blood clots following injury, and also, occasionally, bone erosion which can suggest the presence of tumours associated with bony structures. Occasionally, evidence of a shift of midline structures can also be revealed if the pineal (a structure which forms part of the midline structure of the brain) can be visualised. In a minority of patients, the pineal is calcified and can be seen on plain X-rays. A shift of the pineal away from the midline is taken as fairly reliable evidence of the presence of a space-occupying lesion (S.O.L.) on the opposite side, causing distorsion and displacement of the midline structures.

There are three main methods of contrast investigation of the brain. Cerebral angiography is a technique in which a radio-opaque dye is injected into an artery feeding the brain, and a rapid series of X-ray photographs is taken as the dye passes through the cerebral circulation. This technique can reveal abnormalities of blood vessels including newly formed vessels which usually indicate the presence of

tumours. A second technique is air encephalography in which air is introduced into the cerebrospinal fluid spaces, and X-ray films are taken with the patient in various positions to reveal the internal and external morphology of the brain by negative contrast. Ventriculography is also used which is a technique in which radio-opaque material is introduced directly into the ventricles through a cannula which is passed through a hole drilled in the skull and then through the brain itself to reach the ventricles. In this latter investigation X-rays reveal the shape of the ventricles and may reveal evidence of blockage of the normally open fluid pathways of the brain.

These three techniques, singly or in combination, reveal much detail of the anatomy of the brain, and are frequently very accurate aids to diagnosis. They are, however, very complex procedures, occasionally hazardous, and most definitely require hospitalisation of the patient. They are usually performed under general anaesthetic. They are therefore quite unsuitable as screening procedures and are only used to investigate patients in which there is a very strong possibility of a lesion, or to assist in the diagnosis of a lesion which has been demonstrated by other investigations.

9.1.2 Non-invasive methods of investigation

These methods do not necessarily require hospitalisation of the patient, and are sufficiently simple and safe to be used as screening procedures.

The longest established non-invasive method of investigating the brain is electro-encephalography (E.E.G) in which a number of electrodes are fixed to the scalp, and the potential differences between electrodes or groups of electrodes are measured and displayed using a sensitive, multi-channel chart recorder. Where the brain is diseased or damaged, the normal electrical activity of the brain may be disturbed

and the presence of a focal lesion may often be revealed by abnormal electrical activity confined to a certain region of the brain.

Ultrasound has also been used as a means of encephalography. This technique is complicated by the presence of the skull, which results in poor acoustic coupling of the transducer and produces large amplitude echos from the skull on the opposite side. Often, however, echos are also obtained from the midline structures of the brain, and may reveal evidence of a shift in these structures. This technique not infrequently gives misleading information, and the interpretation of the results has been shown by White and Hudson (1971) to be rather subjective. Ultrasound is now only rarely used.

In the mid 1960's, isotope scanning became more widely available and isotope encephalography was rapidly established as the most specific and accurate non-invasive method of encephalography. However, the accuracy and specifity of the technique still did not match those of the invasive methods of investigation, and cases shown by isotope encephalography to have focal disorders of the brain often required follow up investigations by one of the invasive methods.

In 1973, Ambrose described the results obtained from a new instrument, the EMI scanner. This is an X-ray scanner, in which the intensity of a transmitted beam of X-rays is monitored by scintillation detectors, and a transverse axial image is obtained by computer calculation as the apparatus scans and rotates around the brain in a very similar manner to the isotope section scanner described earlier in this thesis. This machine requires no injections of contrast, and is capable of revealing for the first time detail of the soft tissue anatomy of the brain.

This type of apparatus, sometimes known as TCAT (for Transmission Computed Axial Tomography) has been adopted very widely, and is

now in use at most major centres throughout the world. It's diagnostic accuracy is impressive, and it is rapidly becoming a standard against which the value of other methods of encephalography must be judged.

9.2 The accuracy of TCAT scanning as compared to Isotope scanning

A number of investigators have compared the diagnostic accuracy of TCAT scanning and isotope scanning in different types of lesion. Gawler et. al (1974) working with an early model TCAT scanner, detected 95% of a series of 75 cases with proven intracranial tumours. Radioisotope imaging was performed in 64 of these cases, and detected 75% of the tumours.

Claveria et. al. (1977) investigated a series of 71 cases of meningioma and reported an overall accuracy for TCAT scanning of 96%. Of the 40 cases in this series investigated by radioisotope imaging, 36 meningiomas were detected, an overall accuracy of 90%.

Kendall and Claveria (1976) in analysing a series of cases diagnosed as intracranial angiomas, found diagnostic changes in 66% of the 41 cases investigated with TCAT, and a focal abnormality which was frequently suggestive of the diagnosis in a further 27.5%, making an overall accuracy of 92.5%. Of the 9 cases in this series in which radioisotope imaging was performed, 8 were positive.

Results of comparisons such as these must be treated with some caution. It is not clear how the decision to perform radioisotope imaging was arrived at, but in at least a proportion of the cases, isotope imaging was probably performed because the results of the TCAT scan were inconclusive. The angioma series is a case in point. Two of the three cases in which the TCAT scan did not reveal the lesion were examined by radioisotope imaging. A positive uptake was found in both cases. There may therefore be a tendancy to underestimate the

accuracy of the isotope scan, since this may have been used mostly on the more difficult cases. On the other hand, it must be said that isotope imaging, whilst revealing the presence of a lesion, is seldom precisely informative about its pathology. TCAT scanning frequently yields quite specific information about the nature of the lesion detected.

Despite the superior lesion detection rate of the TCAT scanner, the early demise of the technique of isotope encephalography which was confidently predicted in a Lancet leading article in 1974 has not occurred. Most centres in which both methods of investigation are in use have reported a drop in the number of referrals for isotope imaging, but the pattern seems to be emerging of isotope encephalography as a useful complementary investigation to TCAT scanning. The fundamental difference between the two techniques, as pointed out by Phelps (1976) among many others, is that isotope techniques are essentially tracer techniques giving functional information as opposed to the purely morphological information provided by TCAT. Isotope imaging provides high object contrast with appropriate labelled compounds which can to a large extent off-set the poorer resolution of this technique. The point is amply demonstrated by the results discussed in chapter 8. In view of this new role for isotope imaging, a reappraisal of the conclusions reached as to the usefulness of the two techniques of analysis discussed in this thesis may be necessary.

9.3 The Value of analysing Radionuclide Scan Images by reference to Standardized Normal Patterns

The results obtained by Popham using mercury labelled compounds gave an optimistic view of the value of this technique in improving the overall detection rate. This optimism has not been bourne out by later workers using technetium labelled compounds, and

the results obtained by the author confirm the marginal nature of any improvement in the detection rate which may be expected using these methods.

It would seem that this technique of analysis has little relevance to the new situation in regard to non-invasive investigations of the brain. Any further refinement of the analysis technique would require the expenditure of a considerable amount of effort, and it seems likely, in view of the magnitude of patient to patient variation, that any improvement in accuracy would still be fairly insignificant compared with the improvement which could be obtained from the use of TCAT techniques.

It is interesting to consider the possibility of using similar numerical methods as a means of detecting abnormalities within TCAT scans. Such an approach, using purely graphical methods was attempted by Mueller et. al. (1974). It seems to the author that such an approach would be doomed to failure because of the magnitude of patient to patient variation. The resolution of the TCAT system is such that quite fine detail can be perceived, and very small variations in positioning, particularly for images obtained close to the base of the brain, can result in surprisingly large changes in the appearance of the pictures. It is, indeed, quite difficult when re-examining a patient to position in exactly the same way as on the original scan. Another factor, so far unexplained, is the slight shift in measured absorption values, of the order of the noise level (i.e. 2-3 'Hounsfield' units) which often occurs from day to day and even from hour to hour. For all these reasons, correlation of data between patients to produce some kind of 'normal' pattern would be extremely difficult. A more promising approach would be to utilise the cross sectional symmettry of

the brain, and to compare corresponding areas on each side. This has been shown in one or two cases so far examined, to be capable of revealing subdural haematomata which were not visualised on the picture data.

9.4 The value of Radionuclide Section Scanning as a complementary investigation to TCAT Scanning

In contrast to the above, the development of radionuclide section scanning seems likely to considerably enhance the usefulness of isotope imaging techniques in centres where TCAT scanners are in use. Direct correlation of TCAT images and section scans is possible and where discrepancies exist between the information yielded by TCAT imaging and contrast investigations, or where areas of doubtful significance are noted on the TCAT scan, the isotope scan and particularly the section scan will often resolve the matter. The pattern of isotope uptake does not always correspond exactly with the pattern of X-ray absorption coefficients as shown on the TCAT image, and the structure of different parts of a lesion may thus be revealed. However, in the case of solid tumours which demonstrate no internal structure, the correlation of the two images is usually good, indicating that the isotope section scan method is capable of tracing accurately the morphology of such lesions.

Work on comparing the accuracy and usefulness of the two techniques is still in progress, and so far only about 100 direct comparisons are available, rather too few for detailed analysis. Interest has recently been focussed on the role that radiopharmaceuticals other than sodium pertechnetate may play in the search for abnormalities in the brain. Indium-111 DTPA has proved to be very useful in mapping abnormal CSF pathways, and very impressive transverse sectional images of the normal basal cisterns have recently been obtained with this agent.

The use of bone scanning agents has also been explored and a recent examination on a patient suspected of having a small sphenoidal wing meningioma revealed on transverse section scan a quite unequivocal increased uptake of isotope in precisely the region suspected of harbouring the tumour. This region, because of its proximity to the bony base of the skull is often difficult to examine with the TCAT scanner, and impossible to examine with conventional radionuclide imaging techniques.

9.5 The value of Radionuclide Section Scanning in general

For those centres without access to TCAT scanning, the provision of facilities for isotope section scanning would seem to offer a useful improvement in detection rate, and a considerable improvement in diagnostically useful information when a lesion is detected. In the case of brain images, Kuhl and Sanders (1970) found that 6% of tumours were detected on the basis of section scans alone. In their series, all such tumours were located in the basal regions of the brain. The tentative results of the current work in progress has produced no evidence to contradict this finding. Kuhl's figure of 6% may in fact be conservative, because a number of small low uptake lesions close to the midline and high in the cerebral hemispheres in which the conventional images were negative have also been seen in the current series. It must be admitted, however, that without strong clinical or other evidence of the most likely location of such lesions, the probability of detection on the basis of conventional views plus one or two section scans would be low.

Transverse sectional radionuclide imaging is not, of course, confined to the examination of the brain, and it seems likely that the method will be of even greater usefulness in imaging other organs

of the body. Interest in this method of imaging now appears to be mounting rapidly, and suitable equipment and programs are becoming commercially available. It seems most unfortunate that the work of the early pioneers in the field should have had to wait so long for recognition.

It is interesting to speculate upon future developments in equipment for radionuclide section scanning. The J&P tomoscanner (a development of the machine described in this thesis) was the first system in commercial production, but two other instruments are now available. Both are essentially gamma cameras mounted in a rotating gantry. Although such systems have the advantage of greater crystal area, giving higher sensitivity and the possibility of multiple simultaneous sections, they have the disadvantage of very high cost. The ring detector systems mentioned in section 1.6 are likely to be even more costly, but could, in principle, be used for dynamic studies. It seems likely to the author that the relatively simple and cheap dual detector scanner is likely to be the instrument of choice for routine clinical work for some time to come.

REFERENCES

Ambrose, J: Computerised transverse axial scanning (tomography) Part 2 Clinical application. Brit. J. Radiol. 46: 1023-1047 (1973)

Ambrose, J Gooding, MR Uttley, D: EMIscan in the management of head injuries. Lancet, 1976(i) 847

Anger, HO: Scintillation camera. Rev. Sci. Instr. 29: 27-33 (1958)

Anger, HO: Gamma-ray and positron scintillation camera. Nucleonics 21: 56-66 (1963)

Anger, HO: Radioisotope cameras. Instrumentation in Nuclear Medicine. Hine: pp 485 (Academic Press, New York, 1967)

Anger, HO: Multiplane tomographic gamma-ray scanner. Medical Radioisotope Scintigraphy vol. 1 (Vienna IAEA): 203-216 (1969)

Atkins, HL Hauser, W Richards, P: A comparison of conventional and data blended display technics in scintiscanning. Radiology, 90: 912-920 (1968)

Baker, RG Scrimager, JW: An investigation of the parameters in scintillation camera design. Phys. Med. Biol. 12: 51-63 (1967)

Barfield, PA Holmes, RA: Pertechnitate accumulation in the choroid plexus. Amer. J. Med. Sci. 178: 542-548 (1967)

Barrett, HH DeMeester, GD Wilson, DT: Fresnel zone plate imaging with X-ray film cassettes. J. Nucl. Med. 13: 781 (1972)

Bedrossian, P Lengyel, T Torko, J: Rapid milking system for obtaining 57 min. 103mRh. Atompraxis 14: 193-195 (1968)

Bender, MA Blau, M:The autofluoroscope. Progress in Medical Radioisotope scanning.Kniseley: p.151 (Oak Ridge Institute of Nuclear Studies, Tennessee 1962)

Bender, MA: The digital autofluoroscope. Medical Radioisotope Scanning, vol. 1: 391-400 (IAEA, Vienna, 1964)

Bender, MA Blau, M Sigmund, EM: Dual memory techniques with the autofluoroscope. J.Nucl. Med. 7: 375-381 (1966)

Ben-Porath, M Imperato, AA Kaplan, E:A simple method for the improvement of scanning images. J. Nucl. Med. 7: 589-593 (1966)

du Boulay, G: Help! Brit. J. Radiol. 46: 783-796 (1973)

Bowley, AR Taylor, CG Causer, DA Barber, DC Keyes, WI Undril, PE Corfield, JH Mallard, JR: A radioisotope scanner for rectilinear, arc, transverse section, and longitudinal section scanning. Brit. J. Radiol. 46: 262-271 (1973)

Bracewell, RN Riddle, AC: Inversion of fan-beam scans in radio-astronomy. Astrophysical Journal, 150: 427-434 (1967)

Cassen, B Curtis, L Reed, C Libby, R: Instrumentation for I-131 use in medical studies. Nucleonics 9: 46-51 (1951)

Chaapel, DW Sprau, AC: Data acquisition for computer analysis and display of radionuclide scans. Int J. Appl. Radiat. 18: 723-727 (1967)

Charleston, DB Beck, RN Wood, JC Yasillo, NJ: A versatile photo-scan analysis instrument produces color display from black and white pictures. J. Nucl. Med. 8: 323-324 (1967)

Christie, JH Rodriguez-Antunez, A MacIntyre, WJ: The use of data-blending for technètium-99m brain scans. Nucl. Med. (Stuttg.) 5: 308-312 (1966)

Chu,D:Multiwire proportional counters. International Symposium on Medical Radioisotope Imaging (IAEA, Los Angeles, 1976)

Claveria, LE du Boulay, GH Moseley, IF: Intracranial infections; Investigation by computerised axial tomography. Neuroradiology 12: 59-71 (1976)

Claveria, LE Sutton, D Tress, BM: The radiological diagnosis of meningiomas; the impact of EMIscanning. Brit J. Radiol. 50: 15-22 (1977)

Clifton, JS Potehen, EJ Hill, RL: A digital data acquisition system for Nuclear Medicine. Int. J. Appl. Radiat. 19: 505-509 (1968)

Corry, PM: A simple magnetic tape recording system for medical scintiscanners. Int. J. Appl. Radiat. 17: 459-465 (1966)

Curie, M Debierne, A: Metallic radium. C. R. Acad. Sci. (Paris) 151; 523-525 (1910)

Damascelli, B Fava, G Pietrjusti, M Roncoroni, L Sichirollo, AE: Comparative evaluation of scanning methods. Tumori 53: 343-357 (1967)

Dereymaker, A De Roo, MJK Dardenne, G: Study of the realtissue concentration of radioactive tracers used for the external detection of cerebral tumours. J. Belge. Radiol. 50: 69-77 (1967)

Desgrez, A Agnely, J Dutheil, M Sejourne, C: A new system of color scintiscanning without inertia or time constant. Rev. Med. Liege 23 suppl. 1: 260-261 (1968)

Detko, J: Semiconductor diode matrix for isotope localisation. Phys. Med. Biol. 14: 245-254 (1969)

Dewey, WC Sinclair, WK: Criteria for evaluating collimators used in in-vivo distribution studies with radio isotopes. Int J. Appl. Radiat. 10: 1-16 (1961)

Dowsett, DJ Perry, BJ: A comparative statistical analysis of brain scans using a digital computer. Brit. J. Radiol. 43: 617-628 (1970)

Dowsett, DJ Ritchie, DR: An off line computer interface for a rectilinear scanner. Phys. Med. Biol. 16: 249-256 (1971)

Drukier, AK: Stimulated positron emission camera. International symposium on Medical Radionucline Imaging (IAEA, Los Angeles, 1976)

Dyer, GR McClain, WJ Satterfield, MM: A system for recording and displaying radioisotope scan data. Int. J. Appl. Radiat. 21: 93-104 (1970)

Fitzer, LF: Digital autofluoroscope. Bio-med. Engineering 2: 488-489 (1967)

Freedman, GS Wolberg, JR Johnson, PM: Comparison of the information content of data-blended and conventional photoscans. Radiology 90: 921-924 (1968)

Freedman, GS: Tomography with a gamma camera- theory. J. Nucl. Med. 11: 602-604 (1970)

Freedman, GS: Gamma camera tomography- preliminary clinical experience. Radiology 102: 365-369 (1972)

Gawler, J du Boulay, GH Bull, JWE Marshall, J: Computer assisted tomography (EMIscanner). Its place in the investigation of suspected intracranial tumours. Lancet 1974 (ii): 419-423

Gilbert, PFC: Iterative methods for the reconstruction of three dimensional objects from projections. J. Theor. Biol. 36: 105-107 (1972a)

Gilbert, PFC: The reconstruction of a three dimensional structure from projections and its application to electron microscopy. II Direct methods. Proc. Roy. Soc. Ser.B. 182: 89-102 (1972b)

Goitein, M: Three dimensional density reconstruction from a series of two dimensional projections. Nucl. Instrum. Methods 101: 509-518 (1971)

* Gordon, R Bender, R Hermann, GT:Algebraic reconstruction techniques (ART) for three dimensional electron microscopy and X-ray photography. J. Theor. Biol. 29: 471-481 (1970)

Griver, J Perry, BJ Uttley, D: The analysis of radioisotope brain scans by comparison with normal patterns of uptake Brit. J. Radiol. 49: 788-793 (1976)

* Gold, B Rader CM: in 'Digital Processing of Signals' (McGraw-Hill), 226-232 (1969)

Hardwick, AD Wilks, RJ: A paper tape interface for a Picker 500 scanner. Phys. Med. Biol. 17: 846-848 (1972)

Harris,CC Satterfield, MM Uchiyama, G Kimble, HE: A rescanner with photographic color readout. J. Nucl. Med. 7: 501-509 (1966)

Haybittle JL: The quantitative analysis of cerebral scintiscans. Phys. Med. Biol. 11; 474-475 (1966)

Heiss, WD Prosenz, P Tschabitcher, H: Evaluation of gamma camera scintigrams by multichannel store, computer and colour T.V. Fortschr. Roentgenstr. 110: 108-117 (1969)

Herman, GT Rowland, S: Three methods for reconstruction of objects from X-rays: A comparative study. Comp. Graphics Image Process. 2: 151-177 (1973)

Hindel, R Cecil, JN Sloane Jr. TE: Dynapix. Design and performance of a digital multichannel scanner. J. Nucl. Med. 8: 319-320 (1967)

Hoffer, PB Beck, RN Charleston, DB: Use of lithium drifted germanium detectors for clinical radioisotope scanning. J. Nucl. Med. 11: 326 (1970)

Holman, BL: The blood brain barrier: anatomy and physiology. Progress in Nuclear Medicine vol. 1 (S. Karger, 1972): 236-248

Horwitz, NH Lofstrom, JE Forsith, AL: The spintharicon - a new approach to radiation imaging. J. Nucl. Med. 6: 348-352 (1965)

Horwitz, NH Forsaith, AL Lofstrom, JE: Constructional details and operating parameters of the spark imaging camera. J. Nucl. Med. 8: 318-326 (1967)

Hounsfield, GN: Computerised axial scanning (tomography) part 1. Description of system. Brit. J. Radiol. 46: 1016-1022 (1973)

Husak, V: Determination of optimum gamma radiation energy for scintigraphic examinations. Radiobiol. Radiother. (Berl.) 10: 25-32 (1969)

Kaplan, SN Kaufman, L Perez Mendez, V Valentine, K: Multiwire proportional chambers for biomedical applications. Nucl. Instrum. Methods 106: 397-406 (1973)

Keeling, DH: Recent advances in brain scanning. Proceedings of the Roy. Soc. Med. 64: 340 (1971)

Kendall, BE Claveria, LE: The use of computed axial tomography (CAT) for the diagnosis and management of intracranial angiomas. Neuroradiology 12: 141-160 (1976)

Kellershohn, C Pellerin, P: Sur la possibilité d'utiliser un tube amplificateur d'image pour mettre en évidence la localisation et la distribution d'un corps radioactif. C. R. Soc. Biol. 149: 533-536 (1955)

Kellershohn, C Lansiart, A: Spark chambers and image intensifiers. Radioactive isotopes in the localisation of tumours (Heinemann,1967): 58-62

Kemplay, JR: A digital data logging technique for medical radioisotope scanners. Phys. Med. Biol. 13: 413-420 (1968)

Keyes, WI: A practical approach to transverse-section gamma-ray imaging. Brit. J. Radiol. 49: 62-70 (1976)

Kuhl, DE Chamberlain, RH Hale, J Gorson, RO: A high contrast photographic recorder for scintillation counter scanning. Radiology 66: 730-732 (1951)

Kuhl, DE Edwards, RQ: Image separation radioisotope scanning. Radiology 80: 653-662 (1963)

Kuhl, DE Edwards, RQ: Reorganising data from transverse section scans of the brain using digital processing. Radiology 91: 975-983 (1968)

Kuhl, DE Sanders, TP: Comparison of rectilinear vertex and transverse section views in brain scanning. J. Nucl. Med. 11: 2-8 (1970)

Kuhl, DE Sanders, TD Edwards, RQ Mackler, PT: Failure to improve observer performance with scan smoothing. J. Nucl. Med. 13: 752-758 (1972)

Lancet (Leading article): Computer assisted tomography of the brain. 1974 (ii): 1052-1054

Lansiart, AJ Kellershohn, C: Spark chambers in nuclear medicine. Nucleonics 24: 56-60 (1966)

Lying Tunell, V Soderborg, B: Dot counting in scintigraphy. J. Nucl. Med. 12: 269-270 (1971)

MacIntyre, WJ Allidi, RJ Haage, J Chernak, E Meany, TF: Comparative modulation transfer functions of the EMI and Delta scanners. Radiology 120: 189-191 (1976)

Mallard, JR: The performance of analogue read-out systems for scintiscanning. Nucl. Med. (Stuttg.) suppl. 6: 35-43 (1967)

Mallard, JR Corfield, JR: A statistical model for the visualisation of changes in the count density on radioisotope scanning displays. Brit. J. Radiol. 42: 530-538 (1969)

Mallard, JR Myers, MJ: The performance of a gamma camera for the visualisation of radioactive isotopes in-vivo. Phys. Med. Biol. 8: 165-182 (1963)

Mallard, JR Peachey, CJ: A quantitative automatic body scanner for the localisation of radioisotope in-vivo. Brit. J. Radiol. 32: 652 (1959)

Mallard, JR Wilks, RJ: Characteristics of display systems in scanning, and a simple phantom procedure to evaluate overall scanner performance. J. Nucl. Med. 9: 96-109 (1968)

Mallard, JR Wilks, RJ: The Abergammascope. An image intensifier gamma camera. Medical Radioisotope Scintigraphy vol. 1 (IAEA, Vienna 1969): 305

Manlio, FL Masland, WS Kuhl, DE: The prognostic significance of a deep wedge pattern in transverse section scanning of cerebral infarctions. Radiology 103: 135-137 (1972)

Mante, CM Allen, FH Verdon Jr. TA: Photoscan reversal. A valuable aid in photoscan interpretation. J. Nucl. Med. 9: 610-612 (1968)

Mantel, J Cook, KJ Ruskin, RL: A miniscan system utilising an electro-pantographic display. Radiology 89: 740-741 (1967)

Matthews, CME Mallard, JR: Distribution of Tc 99m and tumour/brain concentrations in rats. J. Nucl. Med. 6: 404-408 (1965)

Mayneord, WV Turner RC Newberry, SP Hodt, HJ:A method of making visible the distribution of activity in a source of ionising radiation. Nature 168: 761 (1951)

Mishkin, FS Reece, I Dowell, JW: Advantages of producing a minified scan image. Am. J. Roentgen. 109: 682-685 (1970)

Morgan, RH: Visual perception in fluoroscopy and radiography. Radiology 86: 403-416 (1966)

Morrison, RT Olde, G Louis, H Evans, TC: Color coding counting rate data on Ektacolor paper- a new technique. J. Nucl. Med. 9: 140-144 (1968)

Muehllehner, G: A tomographic scintillation camera. Phys. Med. Biol. 16: 87-96 (1971)

Mueller, HR Wuethrich, R Huenig, R et. al: A graphical reporting system for computerised axial X-ray tomography (EMI scanning). Eur. Neurol. (Basel) 11: 197-207 (1974)

Mueller, WC Cameron, JR Wilson, CR: A gamma camera optimum length of light pipe and evaluation of mapping errors. J. Nucl. Med. 6: 349-356 (1965)

Mulder, H Pauwels, EKJ: A new nuclear medicine scintillation camera based on image intensifier tubes. J. Nucl. Med. 17: 1008-1012 (1976)

Nagai, T Watari, K: An improved 137mBa generator. J. Nucl Med. 9: 608-609 (1968)

Oldendorf, WH Lisaka, Y: Interference of scalp and skull with external measurements of brain isotope content: part 2. Absorption by skull of gamma radiation originating in brain. J. Nucl. Med. 10: 184-187 (1969)

O'Mara, RE Subramanian, G McAfee, JG Burger, CL: Comparison of 113mIn and other short lived agents for cerebral scanning. J. Nucl. Med. 10: 18-27 (1969)

Onai, Y Tomaru, T Irifune, T Uchiada, I: A new method of producing spots for the blending photoscan and representation of isodensity patterns of the photoscans by application of the Sabattier effect. Nippon Acta. Radiol. 27: 421-428 (1967)

Patton, JA Brill, AB Erickson, JJ: A new approach to the mapping of three dimensional radionuclide distributions. J. Nucl. Med. 10: 363-370 (1969)

Peters, TM Smith, PR Gibson, RD: Computer aided body section radiography. Brit. J. Radiol. 46: 314-317 (1973)

Pexman, JHW Woolley, JL: Cerebral scintigraphy with a Nuclear Chicago 1206 high performance gamma camera. Brit. J. Radiol. 47: 417-421 (1974)

Phelps, M: Review of radionuclide reconstruction tomography. International Symposium on Medical Radionuclide Imaging (IAEA, Los Angeles, 1976)

Pizer, SM Vetter, HG: Processing radioisotope scans. J. Nucl Med. 10: 150-154 (1969)

Popham, MG Bull, JWD Emery, EW: Interpretation of brain scans by computer analysis. Brit. J. Radiol. 43: 835-847 (1970)

Radon, J: Uber die Bestimmung von Funktionen durch ihre integralwerte langs gewisser Mannigfaltiglceiten (On the determination of functions from their integrals along certain manifolds). Ber. Sacchs. Akad. Wiss. Leipzig, Math-Phys. 69: 262-277 (1917)

Ramachandran, GN Lakshminarayanan AV: Three dimensional reconstruction from radiographs and electron micrographs: application of convolutions instead of Fourier transforms. Proc. Nat. Acad. Sci. U.S. 68: 2236-2240 (1971)

Richards, P: A survey of the production at Brookhaven National Laboratory of radioisotopes for medical research. V Congresso Nucleare, Ressegna Internazionale Elettronica Nucleare and Teleradiocinematografica, Rome. Vol. 2: 225-244 (1960)

Robertson, JS Marr, RB Rosenblum, M Radeko, V Yamarto, YL: 32 crystal positron transverse section detector. Tomographic Imaging in Nuclear Medicine. Ed. GS Freedman. Society of Nuclear Medicine, New York: 142-153 (1973)

Röentgen, WC: On a new kind of rays. Sitzungsberichte der Würzurger Physik-medic. Gesellschaft 132-141 (1895), translated by A. Stanton, Nature 53:274-277 (1896)

Rose, A: Quantum effects in human vision. Advances in Biological and Medical Physics, vol 5: 211-219 (Academic Press, New York, 1957)

Rothenberg, HP Devenney, J Kuhl, DE: Transverse section radionuclide scanning in cisternography. J. Nucl. Med. 17: 924-929 (1976)

Scheer, KE: The use of short lived isotopes in medical diagnosis. Brit. J. Radiol. 42: 641-650 (1969)

Smith, FR Peters, TM Muller, HR Elke, M: Towards the assessment of the limitations on Computerised Axial Tomography. Neuroradiology, 9: 1-8 (1975)

Smith, RO Love, WD: A buffer storage interface foe use in recording individual scintillation pulses on magnetic tape. J. Nucl. Med. 8: 607-610 (1967)

Spergel, P: Automatic data processing for digital autofluoroscope and scintillation camera. J. Nucl. Med. 7: 335 (1966)

Stanbury, JB: On the use of radioisotopes in human experimentation. J. Nucl. Med. 11: 586-591 (1970)

Svedberg, JB: Image quality of a gamma camera system. Phys. Med. Biol. 13: 597-610 (1968)

Tanaka, E Hiramoto, T Nohara, N: Scintillation cameras based on new position arithmetics. J. Nucl. Med. 11: 542-547 (1970)

Teddenham, WJ: Visual physiology of Roentgen diagnosis: basic concepts. Am. J. Roentgen. 78: 116-123 (1957)

Ter-Pogossian, MM Eichling, JO: Autofluroscopy with an X-ray image amplifier. Medical Radioisotope Scanning (IAEA, Vienna, 1964) vol. 1: 411

Todd-Pokropek, A: The non-uniformity of imaging devices and its impact on quantitative studies. International Symposium on Medical Radioisotope Imaging (IAEA, Los Angeles, 1976)

Vainshtein, BK Orlov, SS: (Theory of the recovery of functions from their projections). Kristallografiya 17: 253-257 (1972)

Van Eck, JHM: Isotopen-encephalografie. Academic thesis, University of Groningen (1968)

Vernon, P: Display factors in radioisotope scanning. M. Sc. thesis, University of London, 1968.

Werff, JT van der: Gamma encephalography with radioactive bismuth 206. Acta Radiologica (Diagnosis) 4, 403-416 (1966)

Westerman, B Sharma, RR Fowler, JF: Relative importance of resolution and sensitivity in tumour detection. J. Nucl. Med. 9: 638-640 (1968)

White, DN Hudson, AC: The future of A-mode midline echoencephalography. Neurology (Minneap.) 21: 140-153 (1971)

Wolf, F Kronert, E: Scintigraphic diagnosis with short life radionuclides. Electromedical (Amst.) 37: 33-37 (1969)

Yano, Y Anger, HO: A gallium 68 positron cow for medical use. J. Nucl. Med. 5: 485-486 (1964)

APPENDIX

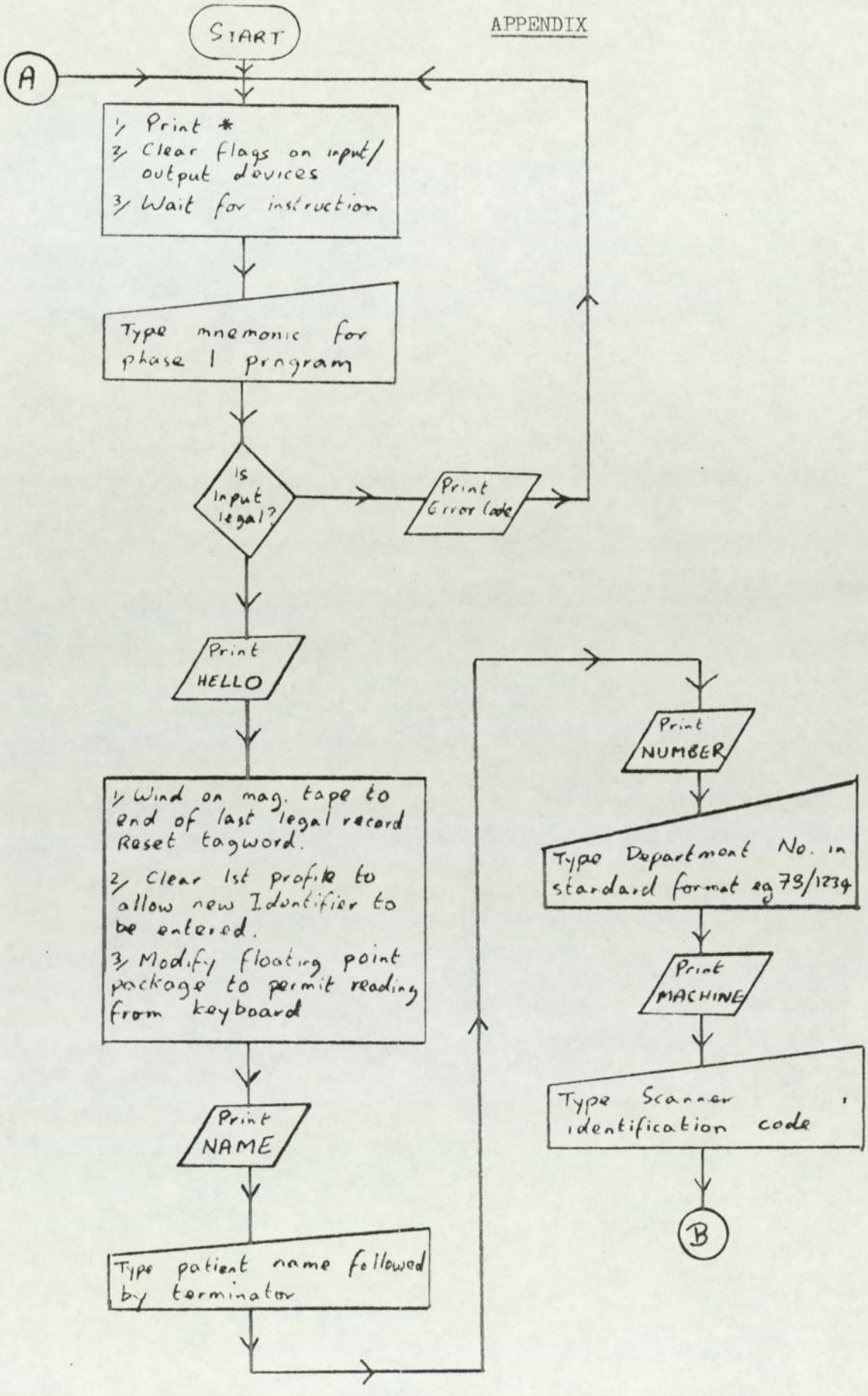
START
A
1/ Print *
2/ Clear flags on input/output devices
3/ Wait for instruction
Type mnemonic for phase 1 program
Is input legal?
Print Error code
Print HELLO
1/ Wind on mag. tape to end of last legal record Reset tagword.
2/ Clear 1st profile to allow new Identifier to be entered.
3/ Modify floating point package to permit reading from keyboard
Print NAME
Type patient name followed by terminator
Print NUMBER
Type Department No. in standard format eg 73/1234
Print MACHINE
Type Scanner identification code
B

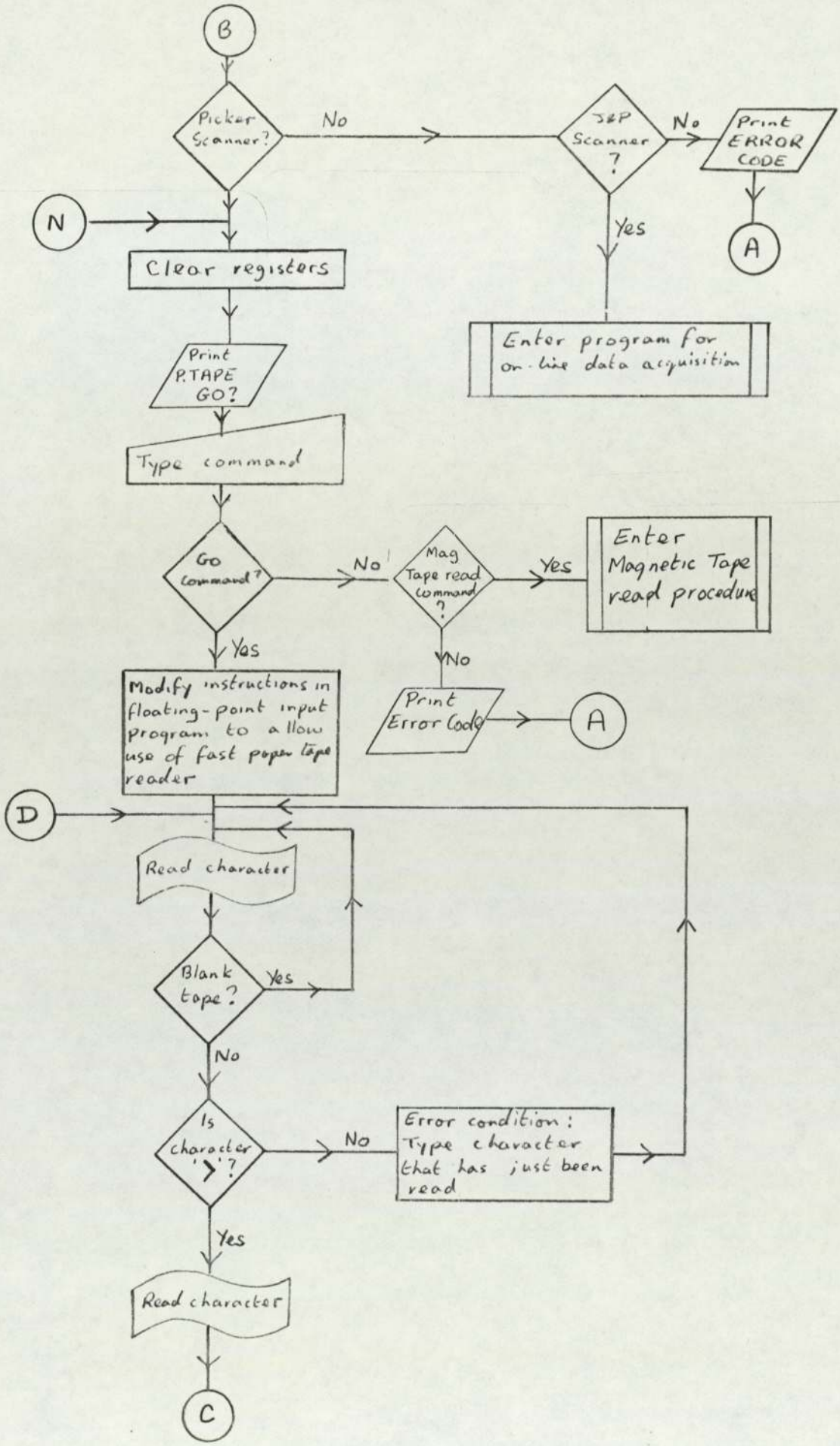
B
Picker Scanner?
No
JEP Scanner ?
No
Print ERROR CODE
A
Yes
N
Clear registers
Enter program for on-line data acquisition
Print P.TAPE GO?
Type command
GO command?
No
Mag Tape read command ?
Yes
Enter Magnetic Tape read procedure
Yes
No
Modify instructions in floating-point input program to allow use of fast paper tape reader
Print Error Code
A
D
Read character
Blank tape?
Yes
No
Is character '>'?
No
Error condition: Type character that has just been read
Yes
Read character
C

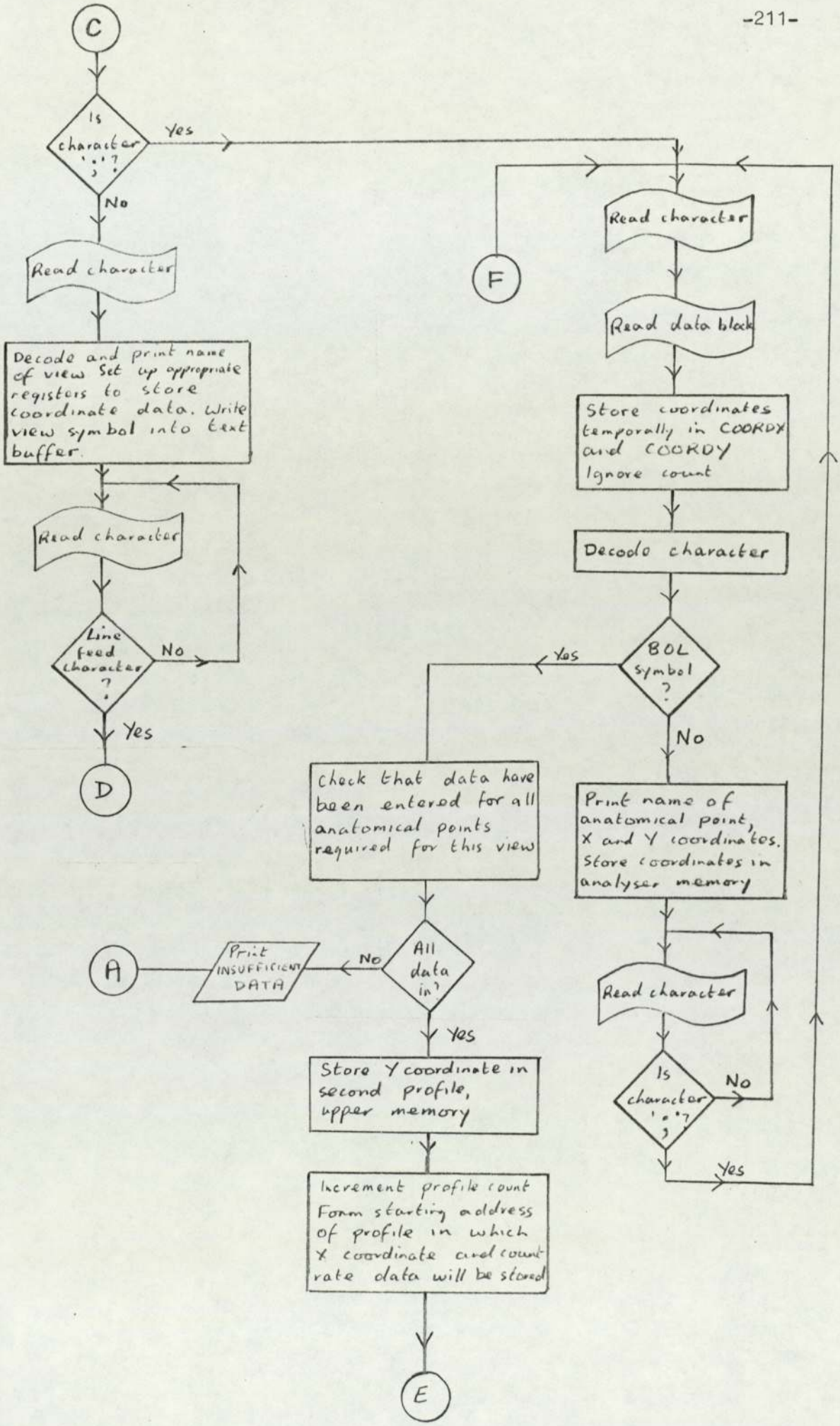
C
Is character '.' ?
Yes
No
Read character
Decode and print name of view Set up appropriate registers to store coordinate data. Write view symbol into text buffer.
Read character
Line feed character ?
No
Yes
D
F
Read character
Read data block
Store coordinates temporally in COORDX and COORDY Ignore count
Decode character
BOL symbol ?
Yes
No
Check that data have been entered for all anatomical points required for this view
Print name of anatomical point, X and Y coordinates. Store coordinates in analyser memory
All data in?
No
Print INSUFFICIENT DATA
A
Yes
Read character
Is character '.' ?
No
Yes
Store Y coordinate in second profile, upper memory
Increment profile count Form starting address of profile in which X coordinate and count rate data will be stored
E

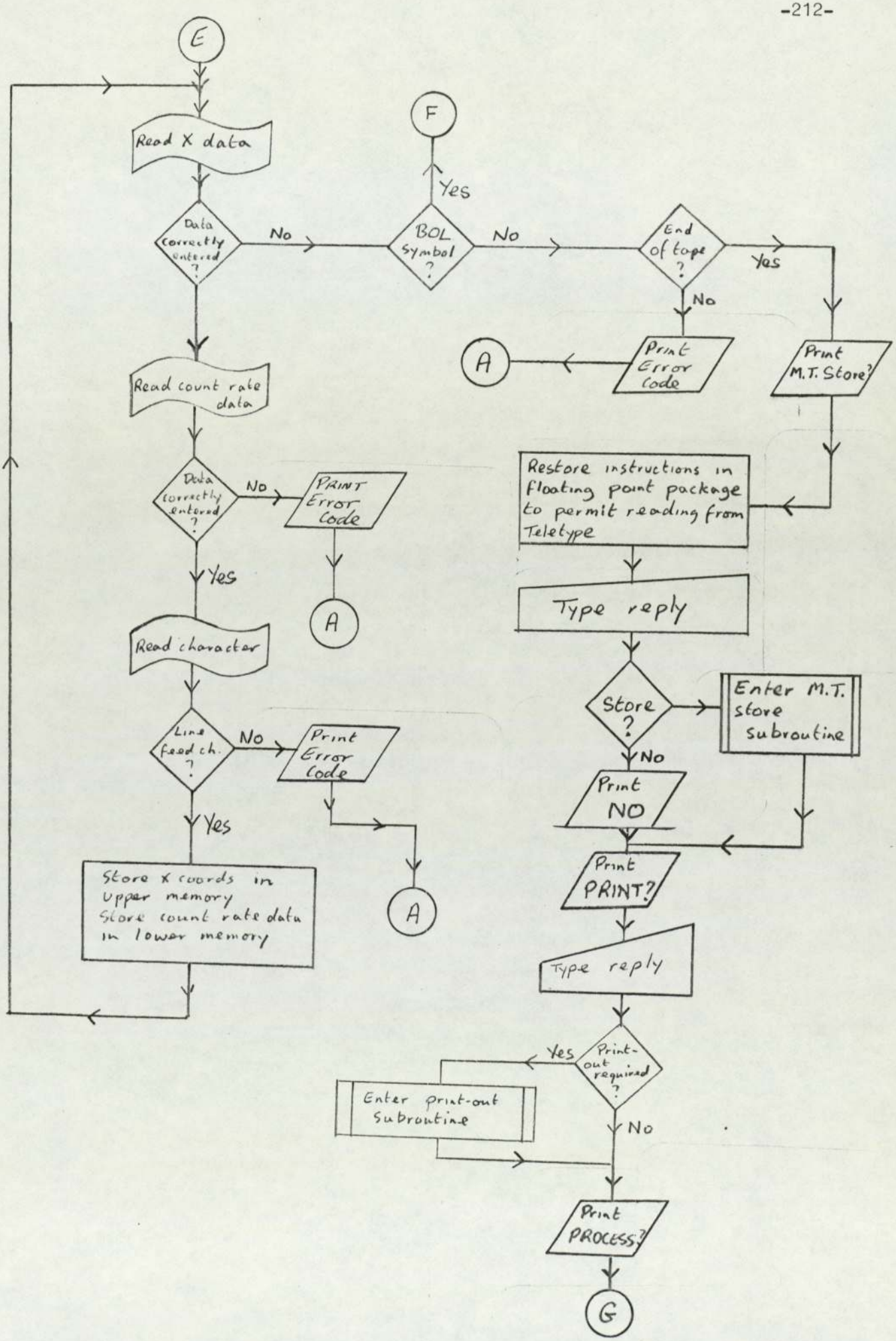
E
Read X data
Data correctly entered ?
No
F
Yes
BOL symbol ?
No
End of tape ?
Yes
No
A
Print Error Code
Print M.T. Store?
Read count rate data
Data correctly entered ?
No
PRINT Error Code
A
Yes
Read character
Line feed ch. ?
No
Print Error Code
A
Yes
Store x coords in upper memory
Store count rate data in lower memory
Restore instructions in floating point package to permit reading from Teletype
Type reply
Store ?
Enter M.T. store subroutine
No
Print NO
Print PRINT?
Type reply
Print-out required ?
Yes
Enter print-out subroutine
No
Print PROCESS?
G

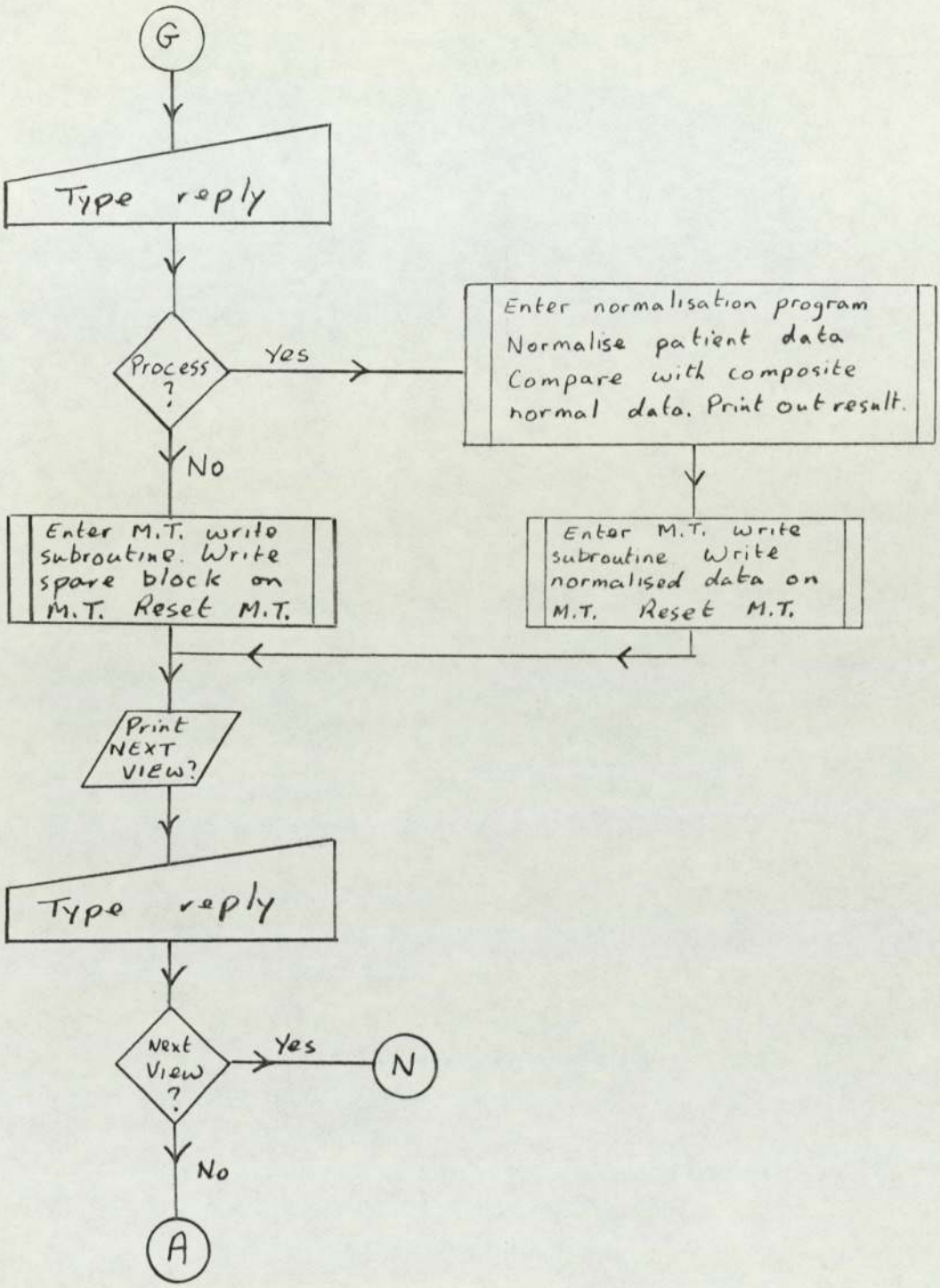
G
Type reply
Process ?
Yes
Enter normalisation program
Normalise patient data
Compare with composite normal data. Print out result.
No
Enter M.T. write subroutine. Write spare block on M.T. Reset M.T.
Enter M.T. write subroutine Write normalised data on M.T. Reset M.T.
Print NEXT VIEW?
Type reply
Next View ?
Yes
N
No
A